

Characterisation and Evaluation of the Mechanical Properties of Alternative Masonry Units

by

Johannes Fourie

*Thesis presented in fulfilment of the requirements for
the degree of Master of Engineering in Structural Engineering in
the Faculty of Engineering at Stellenbosch University*



Department of Structural Engineering,
University of Stellenbosch,
Private Bag X1, Matieland 7602, South Africa.

Supervised by:
Mrs Wibke de Villiers

March 2017

Declaration

By submitting this document, I declare that the work that is contained herein is my own original work. I know the meaning of plagiarism and declare all of the work, except for that which is properly acknowledged, is my own. I am the owner of this document and it has not been submitted for any other examination.

Johannes Fourie

Signature of Candidate

Abstract

One of the greatest challenges facing the South African government is the provision of adequate and affordable housing to the 1.1 million families still living in informal settlements. Currently, the most widely used method of constructing low income housing (LIH) in South Africa is through the use of cement based masonry units. However, it is well known that concrete and cement have a significant negative impact on the environment due to carbon dioxide emissions from the production of cement clinker, as well as the consumption of natural resources. In order to reduce the environmental impacts, alternative masonry units (AMUs) are required that are structurally viable, environmentally friendly and socially acceptable.

To properly begin implementing AMUs in practice the evaluation and characterisation of their mechanical properties are necessary. While standardised tests for conventional masonry units are widely available, it is unclear whether these tests are suitable for use on AMUs due to the large differences in the material properties between certain AMUs and conventional masonry units. Few standards exist that have been designed with AMUs in mind.

This study investigates whether the standards and guidelines available for conventional masonry units can be applied to AMUs. Three different AMUs are compared with a conventional concrete masonry unit (CMU) in a variety of tests to determine if the applicable standards are successful at classifying the mechanical properties of the AMUs. The AMUs that were chosen for this investigation are: alkali-activated concrete blocks (AACBs), compressed stabilised earth blocks (CSEBs) and adobe blocks. These materials were chosen so that the mechanical properties of each material varied notably from each other and from the CMU.

The AMUs and the benchmark CMU were tested for a large variety of mechanical properties. Not only can the results from these tests be used to determine if the standards and guidelines are applicable to both conventional and alternative masonry units, but the data acquired from the investigation can be used in future numerical modelling.

The standardised tests and mechanical properties investigated in this study include the following:

- Compressive strength of the masonry units at 7, 14, 28, 56 and 91 days. Including both bedface and headface tests at 28 days.
- Modulus of elasticity and Poisson's ratio tests conducted on masonry cylinders.
- Wedge splitting tests to determine the fracture energy of the materials.
- Constant mass density tests.

- Triplet tests to determine the shear behaviour at the interface of the masonry samples. Including both initial shear strength and internal angle of friction.
- Compressive strength tests on small scale masonry wallets to determine both the compressive strength and modulus of elasticity.

The outcomes of the study showed that the AACBs and CSEBs satisfy the minimum strength requirements for LIH in South Africa, while the adobe blocks were too weak. The weak adobe masonry units caused the most complications during the test procedures, nevertheless, the investigation found that with small adjustments to the standards, particularly the loading procedures, the tests could be successfully completed on the AMUs. Issues were however, encountered with the tests for Poisson's ratio. The tests also provided a large variety of mechanical properties for both conventional and alternative masonry units which can be used in future studies for the numerical modelling of masonry for low income housing in South Africa. The knowledge gained in this study can therefore be used to begin laying the framework for the minimum technical specifications for AMUs in South Africa.

Opsomming

Een van die grootste uitdagings vir die Suid-Afrikaanse regering is die voorsiening van voldoende en bekostigbare behuising aan die 1,1 miljoen gesinne wat steeds in informele nedersettings woon. Die mees algemene metode vir die bou van lae-inkomste behuising in Suid-Afrika is met sement gebaseerde boueenhede. Dit is bekend dat beton en sement 'n beduidende negatiewe impak het op die omgewing as gevolg van koolstofdioxiedemissies van die produksie van sement klinkers asook die verbruik van natuurlike hulpbronne. Met die doel om die omgewingsimpak te verminder, is alternatiewe eenhede nodig wat struktureel lewensvatbaar, omgewingsvriendelik en sosiaal aanvaarbaar is.

Om behoorlik te begin met die implementering van alternatiewe boueenhede in die praktyk is die evaluering en karakterisering van hul meganiese eienskappe nodig. Terwyl gestandaardiseerde toetse vir konvensionele boueenhede oral beskikbaar is, is dit nie duidelik of hierdie toetse ook geskik is vir gebruik op alternatiewe boueenhede nie as gevolg van die groot verskille in die materiaal eienskappe tussen sekere alternatiewe boueenhede en konvensionele boueenhede. Min standaarde bestaan wat ontwerp is met alternatiewe boueenhede in gedagte.

Hierdie studie ondersoek of die standaarde en riglyne wat beskikbaar is vir konvensionele boueenhede gebruik kan word op alternatiewe boueenhede. Drie verskillende alternatiewe boueenhede word vergelyk met 'n konvensionele beton bou eenheid, in 'n verskeidenheid van toetse om te bepaal of die toepaslike standaarde suksesvol is om die meganiese eienskappe van die alternatiewe boueenhede te bepaal. Die alternatiewe boueenhede wat vir hierdie studie gekies is, is: alkali-geaktiveerde betonblokke, saamgeperste gestabiliseerde grondblokke en adobeblokke. Hierdie materiale is gekies sodat die meganiese eienskappe van elke materiaal verskil van mekaar en van die konvensionele betonblokke.

Die alternatiewe boueenhede en die maatstaf beton bou eenheid word getoets vir 'n verskeidenheid van meganiese eienskappe. Die resultate van hierdie toetse kan gebruik word om te bepaal of die standaarde en riglyne van toepassing is op beide die konvensionele en alternatiewe boueenhede, en die data kan gebruik word in die toekoms om numeriese modellering to doen.

Die gestandaardiseerde toetse en meganiese eienskappe wat ondersoek word in hierdie studie sluit in die volgende:

- Druksterkte van die boueenhede op 7, 14, 28, 56 en 91 dae. Insluitend beide bedgesig en hoofgesig toetse op 28 dae.
- Elastisiteitsmodulus en Poisson se verhoudingtoetse uitgevoer op boublok silinders.

- Splyttoetse om die verbrekingsenergie van die materiaal te bepaal.
- Konstantemassadigtheids toetse.
- ‘Triplet’ toetse om die skuifgedrag by die koppelvlak van die boublok monsters te bepaal. Insluitend beide aanvanklike skuifsterkte en internehoek van wrywing.
- Druksterkte toetse op kleinskaal blok mure om beide die druksterkte en elastisiteitsmodulus te bepaal.

Die resultate van die studie het getoon dat die alkali-geaktiveerde betonblokke en saamgeperste gestabiliseerde grondblokke voldoen aan die minimum krag vereistes vir lae-inkomste behuising in Suid-Afrika, terwyl die Adobeblokke te swak was. Die baie swak Adobeblokke het die meeste komplikasies veroorsaak tydens die toets prosedures, maar die studie het bevind dat met klein aanpassings aan die standaarde, veral die laai prosedures, kan die toetse suksesvol voltooi word op die alternatiewe boueenhede. Probleme was egter ondervind met die toetse vir Poisson se verhouding. Die toetse het ook 'n groot verskeidenheid van meganiese eienskappe vir beide die konvensionele en alternatiewe boueenhede uitgewys, wat in toekomstige studies kan gebruik word vir die numeriese modellering van boublokke vir lae inkomste behuising in Suid-Afrika. Die kennis wat in hierdie studie opgedoen is, kan dus gebruik word om die raamwerk te lê vir die minimum tegniese spesifikasies van alternatiewe boueenhede in Suid-Afrika.

Acknowledgements

I would like to express my sincere gratitude to the following people for their assistance, guidance and support during this study:

- My supervisor, Mrs Wibke de Villiers for her continual guidance, advice and mentorship over the course of my research. Your patience and support is greatly appreciated.
- Oom Johan van der Merwe for his meticulous assistance with constructing and planning of tests. His influence on my work can not be overstated and I thank him for all the skills and lessons he taught me.
- The laboratory manager Stephan Zeranka for his continual assistance and patience with the many test set-ups.
- The laboratory staff, Charlton Ramat and Peter Cupido for all their help and jokes over the hundreds of hours in the laboratory.
- My office colleagues and friends for their advice and help as well as making the whole experience more memorable.
- My parents and brother for their prayer, words of encouragement and always being there for me.

Most importantly I thank my Lord and saviour for giving me the opportunity and the ability to see this project through to the end.

Contents

Declaration	i
Abstract	ii
Opsomming	iv
Acknowledgements	vi
List of Figures	xi
List of Tables	xiii
Nomenclature	xv
1 Introduction to Research	1
1.1 Introduction	1
1.2 Motivation for this Work	2
1.3 Objectives and Methodology	3
1.4 Scope	3
1.5 Thesis Layout	4
2 Literature Review	5
2.1 A Brief Overview of Bricks and Blocks	5
2.2 Low Income Housing and CMUs	6
2.3 Environmental Issues of Conventional Masonry	8
2.4 Alternative Masonry Units	10
2.5 Limestone Powder Waste Bricks	12
2.6 FaL-G	13
2.7 Adobe	14
2.7.1 Soil Characterisation	14
2.7.2 Creating Adobe Blocks	15
2.8 Compressed Stabilised Earth Blocks (CSEB)	17
2.8.1 Stabilised Soil	18
2.8.2 Production of CSEB	19
2.9 Alkali-Activated Materials	20
2.9.1 Background, Applications and Terminology	21

2.9.2	Alkali Activated Cement Chemistry	22
2.9.3	Alkali-Activated Concrete Blocks (AACB)	23
2.9.4	Health Concerns	23
2.10	Conclusion	24
3	Mechanical Characterisation of Masonry Units	25
3.1	Compressive Strength of Masonry Units	26
3.1.1	Compressive Strength of Different Masonry Materials	27
3.1.2	Compressive Strength Testing Specification	28
3.2	Modulus of Elasticity	30
3.2.1	Modulus of Elasticity Testing Specification	31
3.3	Poisson's Ratio	33
3.3.1	Poisson's Ratio Testing Specifications	33
3.4	Fracture Energy	35
3.4.1	Wedge Splitting Test Method	36
3.5	Density	39
3.5.1	Density Testing Specifications	40
3.6	Masonry Shear Strength	40
3.6.1	Triplet Test Specifications	42
3.7	Masonry Compressive Strength	45
3.7.1	Compressive Strength of Masonry Specifications	47
3.8	Conclusion	48
4	Materials and AMU Creation	49
4.1	Materials	49
4.1.1	Aggregate	49
4.1.2	Binders	51
4.1.3	Alkaline Solution	51
4.1.4	Water	51
4.2	Concrete Masonry Unit (CMU)	52
4.2.1	Mix Design	52
4.2.2	Mixing and Manufacturing Procedure	54
4.2.3	Curing	56
4.3	Alkali-Activated Concrete Block (AACB)	57
4.3.1	Mix Design	57
4.3.2	Mixing and Manufacturing Procedure	59
4.3.3	Curing	59
4.4	Compressed Stabilised Earth Block (CSEB)	60
4.4.1	Mix Design	60
4.4.2	Mixing and Manufacturing Procedure	61
4.4.3	Curing	61
4.5	Adobe Block	62
4.5.1	Mix Design	62

4.5.2	Mixing and Manufacturing Procedure	63
4.5.3	Curing	64
4.6	Mortar Design	64
4.7	Conclusion	65
5	Experimental Design	67
5.1	Masonry Units Compressive Strength Tests	67
5.2	Modulus of Elasticity Tests	68
5.3	Poisson's Ratio Tests	70
5.4	Wedge Splitting Tests	72
5.5	Density	75
5.6	Triplet Tests	75
5.7	Masonry Compressive Strength Tests	79
5.8	Conclusion	81
6	Experimental Results	83
6.1	Compressive Strength of Masonry Units Results	83
6.1.1	Strength Gain of Masonry Units	84
6.1.2	Influence of Masonry Orientation	87
6.2	Modulus of Elasticity Results	89
6.2.1	Influence of Material Type on Modulus of Elasticity	91
6.3	Poisson's Ratio Results	92
6.4	Wedge Splitting Results	93
6.5	Density Results	97
6.6	Triplet Results	98
6.7	Compressive Strength of Masonry Results	102
6.7.1	Masonry Failure Mechanisms	104
6.8	Conclusion	106
7	Comparisons and Discussions	108
7.1	Prediction Methods	108
7.1.1	Compressive Strength of Units and Wallets	109
7.1.2	Compressive Strength and Modulus of Elasticity	110
7.1.3	Concluding Remarks	112
7.2	Suitability of Test Set-ups	112
7.2.1	Compressive Strength of Masonry Units Test	113
7.2.2	Modulus of Elasticity Test	114
7.2.3	Poisson's Ratio Test	116
7.2.4	Wedge Splitting Test	118
7.2.5	Density	119
7.2.6	Triplet Test	119
7.2.7	Compressive Strength of Masonry Test	120
7.2.8	Concluding Remarks	121

8 Conclusion	122
8.1 Conclusions	123
8.1.1 Observations Made with Regards to the Mechanical Properties	123
8.1.2 Observations Made with Regards to the Test Set-ups	125
8.2 Recommendations for Future Studies	126
References	128

List of Figures

Figure 2.1	Conventional Affordable Home with Clay Bricks	7
Figure 2.2	Commonly Used CMUs for LIH	8
Figure 2.3	Creation of Adobe Blocks with Wooden Mould	17
Figure 2.4	Stages in CSEB Compaction Process	20
Figure 3.1	Behaviour of Quasi-Brittle Material in Compression	26
Figure 3.2	Orientation, Loading Direction and Casting Direction of Bedface and Headface Specimens	27
Figure 3.3	Behaviour of Concrete Under Successive Loading Cycles	31
Figure 3.4	Cycles for Determining Modulus of Elasticity	32
Figure 3.5	Combined Compressometer-Extensometer	34
Figure 3.6	Principle of the Wedge Splitting Test	36
Figure 3.7	Typical Horizontal Force versus Crack Opening Displacement	37
Figure 3.8	Front and Side View of Wedge Splitting Set-up with Indicated Forces . .	38
Figure 3.9	Single vs Double Wedge Splitting Support	38
Figure 3.10	Dilatancy Behaviour of Masonry	41
Figure 3.11	Different types of shear tests: (a) couplet test (b) van der Pluijm test and (c) triplet test	41
Figure 3.12	Triplet Test Loading	43
Figure 3.13	Triplet Test Pre-Compression	43
Figure 3.14	Triplet Test Failure Modes	44
Figure 3.15	Typical Plot from Triplet Test	45
Figure 3.16	(a) Masonry in Compression (b) Stress State for Stiffer Block and Softer Mortar, (c) Stress State for Softer Block and Stiffer Mortar	46
Figure 3.17	Representations of Common Prism and Wallet Specimens	46
Figure 3.18	Masonry Wallet Specimen	47
Figure 4.1	Grading of Materials	50
Figure 4.2	Manual Earth Block Press	55
Figure 4.3	‘Cookie Cutter’ Extrusion Frame	56
Figure 4.4	CMU Block	56
Figure 4.5	Wooden Mould for AACBs	59
Figure 4.6	Alkali-Activated Concrete Block (AACB)	60
Figure 4.7	Compressed Stabilised Earth Block (CSEB)	62
Figure 4.8	Adobe Block	65

Figure 5.1	Compressive Strength Bedface Test Set-up	68
Figure 5.2	Compressive Strength Headface Test Set-up	68
Figure 5.3	Cylinders for Elastic Modulus Tests	69
Figure 5.4	Elastic Modulus Tests Set-up	69
Figure 5.5	Ring method for Poisson Tests	71
Figure 5.6	Poisson's Ratio with Circumferential Wire Set-up	71
Figure 5.7	Poisson's Ratio Set-up with Longitudinal (Long.) and Transverse (Trans.) LVDTs	72
Figure 5.8	Dimensions of Wedge Splitting units	73
Figure 5.9	Close up of Wedge Splitting Set-up	73
Figure 5.10	Total Wedge Splitting Set-up	74
Figure 5.11	CSEB Triplet Specimen	76
Figure 5.12	Triplet Set-up for Zero Pre-Compression	77
Figure 5.13	Close up of Triplet Set-up for Pre-Compression	78
Figure 5.14	Full Triplet Set-up for Pre-Compression	79
Figure 5.15	AACB Wallet	80
Figure 5.16	Masonry Compressive Strength Set-up	81
Figure 6.1	Compressive Strength Values for 7, 14, 28, 56 and 91 day strength for CMU, AACB, CSEB and Adobe	84
Figure 6.2	Compressive Strength Values of CMU, AACB, CSEB and Adobe Bedface and Headface Units	88
Figure 6.3	Mean Modulus of Elasticity Measured at 28 Days for CMU, AACB, CSEB and Adobe Specimens	90
Figure 6.4	Typical Splitting Force-COD Curve for the CMU, AACB, CSEB and Adobe materials	93
Figure 6.5	Fracture Energy of CMU, AACB, CSEB and Adobe Specimens	94
Figure 6.6	Cracked Wedge Splitting Specimens	96
Figure 6.7	Mean Dry Density of CMU, AACB, CSEB and Adobe Specimens	97
Figure 6.8	Shear Stress versus Pre-compressive Stress from Triplet Tests	100
Figure 6.9	Regression Lines from Triplet Results for CMU, AACB, CSEB and Adobe	100
Figure 6.10	Shear Failure Types from Triplet Tests	102
Figure 6.11	Compressive Strength of Masonry Wallets	103
Figure 6.12	Modulus of Elasticity of Masonry Wallets	103
Figure 6.13	Vertical Crack on Head Face of Masonry Wallet	105
Figure 6.14	Crack Pattern on Side Face of Masonry Wallet	106
Figure 7.1	Comparison Between Characteristic Compressive Strength and the Sim- plified Characteristic Compressive Strength	110
Figure 7.2	Comparison Between Experimental Results and Prediction Methods of the Modulus of Elasticity	111
Figure 7.3	Comparison Between Block and Cylinder Compressive Strength	115
Figure 7.4	Typical Stress/Strain Curve from Poisson Tests	117

List of Tables

Table 2.1	Compressive Strength Requirements for CMUs	9
Table 3.1	Shape Factor (d) for Normalising Compressive Strength	30
Table 4.1	Aggregate Characteristics	50
Table 4.2	Chemical Composition of Fly Ash (FA) and Ground Granulated Corex Slag (GGCS)	51
Table 4.3	CMU Mix Proportions	54
Table 4.4	Factors that lower AAC strength	58
Table 4.5	AAC Mix Proportions from Barnard (2014) and Mix Proportions Used in this Study	58
Table 4.6	CSEB Mix Proportions	61
Table 4.7	Adobe Mix Proportions	63
Table 4.8	Mortar Mix Proportions	65
Table 4.9	Masonry Units Mix Proportions	66
Table 5.1	Loading Rates of Wedge Splitting Units	75
Table 6.1	Average Compressive Strength Values (f_c) presented in Figure 6.1 and the Coefficient of Variation (COV)	85
Table 6.2	Average Compressive Strength Values Presented in Figure 6.2 and the Coefficient of Variation (COV)	89
Table 6.3	Normalised Bedface and Headface Strength at 28 Days Age	89
Table 6.4	Modulus of Elasticity Values Presented in Figure 6.3 and the Coefficient of Variation (COV)	90
Table 6.5	Modulus of Elasticity of Common Masonry Construction Materials	91
Table 6.6	Results from Poisson's Ratio Tests	92
Table 6.7	Results from Wedge Splitting Tests	94
Table 6.8	Comparison of Fracture Energy from the Equation by Wittmann (2002) to the Experimental Results	96
Table 6.9	Density Values Presented in Figure 6.7 and the Coefficient of Variation (COV)	98
Table 6.10	Triplet Test Results	101
Table 6.11	Compressive Strength, Modulus of Elasticity and COV Results from Masonry Wallets	104
Table 6.12	Main Results from All Tests Conducted in this Study	107

Table 7.1	Percentage Change in Pre-Compression During Triplet Tests	120
-----------	---	-----

Nomenclature

Symbols

Latin Letters	Units	Description
A_i	mm ²	Cross-sectional area parallel to bed joint
A_m	mm ²	Gross contact area
A'_m	mm ²	Net contact area
d	mm	Width of wedge splitting specimens
E	GPa	Modulus of elasticity
E_{wy}	GPa	Modulus of elasticity of masonry
f_b	MPa	Normalised compressive strength
f_c	MPa	Compressive strength
f_i	MPa	Compressive strength of masonry specimen
f_k	MPa	Characteristic compressive strength
$f_{k,s}$	MPa	Simplified characteristic compressive strength
f_m	N	Mortar compressive strength
f_p	MPa	Pre-compressive stress of individual sample
f_v	MPa	Shear strength of individual sample
$F_{i,\max}$	MPa	Maximum load of masonry specimen
F_{\max}	N	Maximum shear load
F_p	N	Pre-compressive force
F_s	N	Splitting force for wedge splitting tests
F_v	N	Vertical force for wedge splitting tests
G_f	N m	Fracture energy

h	mm	Ligament length of wedge splitting specimens
K_E	—	Constant for determining simplified modulus of elasticity
m_{dry}	kg	Constant mass of a specimen
R^2	—	Coefficient of determination
t	s	Time
ν	—	Poisson
V_n	mm ³	Volume of a specimen
Greek Letters	Units	Description
α	degrees	Wedge angle of wedge splitting tests
γ_e	—	Mortar elasticity reduction factor
Δu	mm	Normal displacement
Δv	mm	Shear displacement
ϵ	mm/mm	Strain
ϵ_p	mm/mm	Strain parallel to applied stress
ϵ_n	mm/mm	Strain perpendicular to applied stress
μ	—	Friction coefficient
ρ	kg/mm ³	Dry density
σ	MPa	Compressive stress
σ_D	MPa	Normal stress
σ_h	MPa	Notch tensile strength
τ_a	MPa	Shear stress
τ_o	MPa	Initial shear stress
ϕ	mm	Maximum aggregate diameter
ϕ_f	degrees	Internal angle of friction
ψ	degrees	Dilatancy angle

Acronyms

Acronym	Description
AAC	Alkali-activated concrete
AACB	Alkali-activated concrete block
AACBB	Alkali-activated cement-based binders
AMU	Alternative masonry unit
CMU	Concrete masonry unit
COD	Crack opening displacement
COV	Coefficient of variation
FM	Fineness modulus
GGBS	Ground granulated blast-furnace slag
GHG	Greenhouse gases
HCP	Hardened cement paste
OPC	Ordinary Portland cement
LIH	Low income housing
LPW	Limestone powder waste
LVDT	Linear variable differential transducers
RD	Relative Density
SCM	Supplementary cementitious materials

Chapter 1

Introduction to Research

1.1 Introduction

Cement based masonry units are one of the most widely used methods of construction for low income housing (LIH) in South Africa. However, their use has a significant negative impact on the environment due to carbon dioxide emissions from the production of cement and the consumption of non-renewable natural resources. To reduce these environmental impacts structurally viable alternative masonry units (AMUs) are needed that are not only more environmentally friendly but are also economical and socially acceptable.

To allow for the further development and acceptance of AMUs the characterisation and evaluation of their mechanical properties are necessary. Standardised tests are widely available for conventional masonry units, however it must be determined if these tests are suitable for use on AMUs due to the difference in material properties between AMUs and conventional masonry units.

This study focusses on three different AMUs that are used to develop and/or select appropriate benchmark tests for the determination of conventional masonry properties as well as properties that are not normally tested for, such as tensile strength and fracture energy. The criteria used for selecting these AMUs are: a low environmental impact, economic advantages and most importantly, to ensure that they would display a range of different mechanical properties.

The AMUs that are investigated in this study include alkali-activated concrete blocks, compressed stabilised earth blocks and adobe blocks. Laboratory tests are conducted on these AMUs as well as on conventional concrete masonry units which are then used as a benchmark. Parameters that are tested for include compressive strength, modulus of elasticity, Poisson's ratio, fracture energy and density. Interface tests are also conducted for each AMU to determine the mechanical properties of the masonry unit/mortar interface.

This thesis documents the tests that were used to determine the mechanical properties of the different AMUs as well as the results from these tests. These results can then be used in further studies for the modelling of the mechanical behaviour of masonry.

1.2 Motivation for this Work

International human rights law recognizes everyone's right to adequate housing as part of their right to an adequate standard of living. Even though this right has a central place in international legal systems, there are still nearly a billion people who are inadequately housed. Slums and informal settlements house millions around the world in life or health threatening conditions (UN Habitat and Ohchr, 2014).

Due to the Millennium Development Goals and a concerted effort from countries around the world the percentage of slum dwellers has been reduced. However, a continuous population growth and movement from rural to urban areas has caused an increase in the actual number of slum dwellers (United Nations, 2015). This lack of adequate housing is felt most severely by those with low income.

In order for states or organisations to be able to address the lack of adequate housing, a durable and low cost housing solution must be found. At the same time the solution must be socially and environmentally acceptable. An important aspect that must be kept in mind when choosing a housing solution is the marketability of the house. A previously impoverished family that has been living in informal settlements or slums will aspire to live in 'modern' houses made of concrete, steel and glass (Hall, 2012). Therefore, the house must not only perform well but also be aesthetically pleasing to its occupants.

Cement based masonry units, also called concrete masonry units (CMUs), are the most widely used building material for LIH in South Africa (Laing, 2011). Not only are they more socially acceptable than other alternative housing systems, but the skills required to build with them are also readily available (Boshoff et al., 2013). However, CMUs have an adverse impact on the environment, mainly due to the large amount of cement used in their creation. For this reason masonry units made from alternative construction materials are needed that are not only economically and socially acceptable but also more environmentally friendly.

If an AMU is found that meets the above requirements then the next step is to create applicable standards for use with its construction and to introduce it to the housing market. However, in order to do this it is necessary to determine the minimum mechanical specifications. While standards and tests for use on conventional masonry units are widely available and in use, it is inappropriate to apply these to AMUs due to the material differences between them. One of the focuses of this study is therefore to develop and/or select appropriate benchmark tests for the determination of the mechanical characterisations of AMUs.

A further motivation for the research and characterisation of the mechanical properties of the AMUs is for numerical modelling. To accurately create non-linear finite element models of masonry walls, many mechanical properties of the masonry are required. These include density, modulus of elasticity, Poisson's ratio, compressive strength, tensile strength, and fracture energy among others. Literature often does not contain all the parameters that are necessary for numerical modelling and therefore experimental tests are required to determine them.

1.3 Objectives and Methodology

The purpose of this study can be split into two main objectives:

- The first objective is to determine if standards for testing the mechanical properties of conventional masonry units can be successfully applied on alternative units.
- The second objective is to determine reliable mechanical properties from a variety of alternative masonry materials.

With regards to the first objective, if it is found that certain aspects of the standards or tests investigated are not appropriate for the alternative masonry units then adjustments are made in an effort to acquire reliable results from the materials. In order to thoroughly analyse whether the standards or tests are applicable, a range of alternative masonry materials are investigated. These materials are chosen so that their mechanical properties differ as widely as possible from each other.

To ensure that the tests are conducted properly, a conventional concrete masonry unit is tested in addition to the alternative units. The results from the conventional material act as a benchmark and can be compared with recognised values from literature to ensure the tests are functioning properly. The tests that are investigated include: tests on the compressive strength of individual units over a range of ages from 7 to 91 days, tests for the modulus of elasticity and Poisson's ratio, tests for the fracture energy, density tests, tests of the shear behaviour of the unit/mortar interface, and compressive strength tests on masonry wallets.

The second objective is possible due to the wide range of materials and mechanical properties investigated in this study, presenting an opportunity to provide data for in depth numerical modelling. Models such as these show the structural demands on masonry walls and units, which could then be translated into minimum technical specifications. In order to further research into affordable, environmentally friendly low income housing in South Africa, the masonry materials investigated are chosen so that they would be suitable for low income housing.

1.4 Scope

The scope of the study is limited in the following regards. Firstly, the numerical modelling discussed above is not conducted in this study but can be accomplished in future research. Secondly, the focus of this study was not on creating masonry materials that are optimised with regards to their mix design. Rather, a mix is created that properly represents a masonry material type, but it can still be optimised in terms of its mechanical properties in future studies. Thirdly, the study focuses on solid masonry blocks and not on hollow blocks.

1.5 Thesis Layout

The layout of this report is as follows. Chapter 2 consists of a literature study into masonry materials. The state of low income housing in South Africa and the environmental influences of conventional masonry are briefly discussed. The chapter then focuses on alternative masonry materials, specifically the adobe, compressed stabilised earth blocks and alkali-activated concrete blocks investigated in this study.

Chapter 3 is a literature study into the mechanical properties of masonry, both of individual units and of the unit/mortar interface. Available international standards and practices are also given for each of the mechanical materials discussed. The compressive strength, modulus of elasticity, and fracture energy of individual masonry units were investigated as well as the compressive strength and modulus of elasticity of masonry wallets. The shear strength between the masonry units and mortar was also studied through the use of triplet tests.

Chapter 4 discusses the materials used in the creation of the conventional concrete blocks, compressed stabilised earth blocks, alkali-activated concrete blocks and adobe blocks. The mix design, mixing procedure and curing of the various masonry materials are also explained.

Chapter 5 applies the experimental tests covered in Chapter 3 on the masonry units created in Chapter 4. The creation and execution of each test set-up is documented along with any relevant concerns.

Chapter 6 documents the results from the experimental tests. The results are compared between the various alternative materials as well as with the benchmark material. Results from other researchers are also compared with that found in this study to determine if the values fall within recognised ranges.

Chapter 7 first considers prediction methods given in literature or international standards that are used to determine mechanical properties of masonry. The chapter then discusses whether the test set-ups were successful on both the conventional and alternative materials.

The research is concluded in Chapter 8. Recommendations for future work are made based on observations and knowledge gained from this study.

Chapter 2

Literature Review

The aim of this chapter is to give an overview of the current knowledge of alternative masonry units (AMUs) in literature as well as a theoretical base for the work done in this study. First a brief overview is given of the main masonry units used in practice. Low income housing (LIH) is discussed next as well as the materials currently used for their construction. This is followed by a review of the negative environmental issues that these conventional masonry units have. An examination of AMUs in literature is then covered, followed by a look at the particular AMUs used in this study.

2.1 A Brief Overview of Bricks and Blocks

Masonry units have been used for thousands of years by mankind, with the first units being made from dried mud in Mesopotamia. Earthen masonry has continued to be used since then with estimates of up to 50 % of the worlds population living in houses with earth based construction (Avrami et al., 2008). The history of the fired clay bricks starts around 3000 BC with their use continuing to today (Malherbe, 2016). Their strength, ease of construction, low maintenance and cost effectiveness has made them a popular choice worldwide.

The most common method for the creation of fired clay bricks is to start with raw clay and mix in 25 to 30 % sand to reduce shrinkage. The clay mixture is ground and mixed with water to the desired consistency. Next, the clay is pressed into moulds with a hydraulic or mechanical press. Finally, the bricks are dried to remove excess water before being fired at 900°C to 1000°C to achieve their final strength.

With the invention of Portland cement in the 19th century came the use of concrete masonry units (CMUs). While CMUs are widely used in LIH and many other applications, fired clay bricks are still predominately used throughout the world. However, fired clay bricks have an energy consumption that is nearly 300 % that of CMUs (Venkatarama Reddy and Jagadish, 2003). Due to the recent popularity of eco-friendly materials it is expected that CMUs will become more prevalent in the future. However, CMUs still have a negative impact on the environment due to the use of cement in their creation.

The general method for creating CMUs begins with mixing of sand, gravel, cement and water.

The mixture is then fed into a block machine which compresses the mixture into moulds and ejects them onto a flat pallet. The units are then cured, with the more common methods being low-pressure steam curing and high-pressure steam curing.

In this study fired clay bricks and CMUs are called conventional masonry units, while other units such as compressed stabilised earth blocks, alkali-activated concrete blocks, adobe blocks, etc. are considered to be AMUs.

2.2 Low Income Housing and CMUs

The provision of adequate and affordable housing is one of the greatest challenges facing the South African government. According to Deputy Minister of Human Settlements Zou Kota-Fredericks, the government has provided over 3 millions houses since 1994 (Kota-Fredericks, 2013). However, there is a backlog of 2.1 million units with over 1.1 million households still living in informal settlements (Centre for Affordable Housing Finance in Africa, 2013). This number is steadily increasing due to population growth and rural-urban migration. Ms Kota-Fredericks goes on to say that despite an increase in housing subsidies the actual delivery of housing has decreased as a result of building costs, lack of suitable well-located land and rising land prices (Kota-Fredericks, 2013).

In an effort to increase the delivery of LIH, the Application of the National Building Regulation (SANS 10400, 1990) has introduced a new category of housing, Category 1 Buildings, aimed at making buildings affordable to poorer communities. These Category 1 Buildings have comparable safety standards with other categories but have different resistances on items such as: water penetration, deflection limits, maintenance requirements, etc. The main differences between a Category 1 Building and non-Category 1 Buildings can be found in Table C.1 in SANS 10400-A (2010). The introduction of the Category 1 Buildings allows for different performance requirements for materials used in LIH which may help reduce building costs.

In order to further reduce the building and material costs and accelerate delivery of LIH, numerous studies have been conducted with alternative housing systems. The foundations of these LIH systems are dependent on the local geotechnical conditions, while the roofs are considered to be standard and are designed according to specification set out by the National Building Regulations. One of the main focuses for improving LIH systems is therefore the walling systems. The main walling systems used in South Africa are the massive wall system, the frame wall system, and the core wall system (Theart, 2014).

The frame wall system and the core wall system contribute to only a small percentage of all LIH systems in South Africa and are often referred to as alternative systems. The massive wall system is the conventional construction method and therefore the most common (Theart, 2014). The minimal implementation of the alternative LIH systems is mainly due to a lack of social acceptance, limitations with regards to additions to the structure, and limited skills for construction with these systems (Boshoff et al., 2013).

As the massive walling system is the most popular it is the focus of this study. The main characteristic of such a system is that the walls are constructed from only one material. This base material can be burnt clay bricks, concrete blocks and bricks, timber or reinforced concrete (Theart, 2014). Figure 2.1 shows an example of such a system.



Figure 2.1: Conventional Home with Clay Bricks (The Clay Brick Association of SA, 2016)

While both clay bricks and CMUs are used for LIH in South Africa, the most common building block of the massive walling system is the CMU. A number of advantages for using the massive wall systems with CMUs are as follows (Theart, 2014):

- Economical
- Socially acceptable
- Information for design, construction and maintenance locally available
- Reduced number of materials and components
- Thermal and sound resistance
- Moderate construction speed

The two main CMUs used for subsidy housing in South Africa are the ‘Maxi’ block and the hollow concrete block (Laing, 2011). The ‘Maxi’ block is mainly used in Gauteng and inland provinces. This block is 290 mm long, 140 mm wide and 90 mm high (Laing, 2011). The ‘Maxi’ block is sometimes referred to as the ‘Maxi’ brick, however, SANS 10400 (1990) defines a block as a masonry unit with a length of more than 300 mm or a width of more than 130 mm while a brick is defined as any masonry unit that is not a block. For this reason the unit is referred to as the ‘Maxi’ block in this study.

Hollow concrete blocks are used in coastal provinces due to their superior thermal properties and resistance against wet climates. The air voids provided by the hollow sections of the block provide excellent protection against water penetration and increase the thermal performance. The block is 390 mm long, 140 mm wide and 190 mm high (Laing, 2011). Figure 2.2 shows a

‘Maxi’ block and a hollow concrete block.

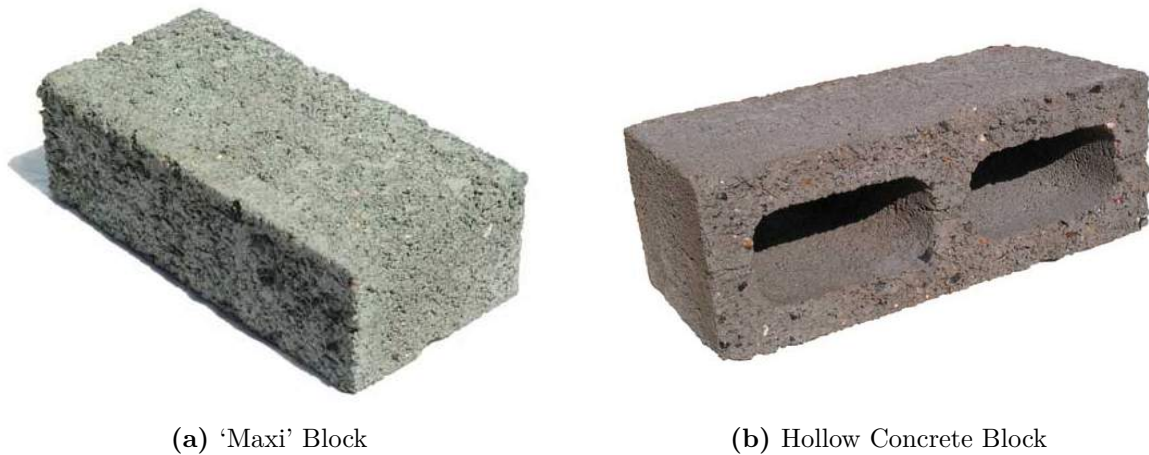


Figure 2.2: Commonly Used CMUs for LIH (Malherbe, 2016)

Table 1, found in SANS 10400 (1990), shows that for single-storey buildings or the upper storey of double-storey buildings, hollow and solid masonry units require a gross compressive strength of 3.5 MPa and 7 MPa, respectively. The lower storey of double-storey buildings require a gross compressive strength of 7 MPa for hollow concrete blocks and 10.5 MPa for solid blocks. However, the newer SANS 10400-K (2011) Section 4.2.2.1, states that single-storey buildings or the upper storey of double-storey buildings shall have an average compressive strength for hollow and solid masonry units not less than 3.0 MPa and 4.0 MPa, respectively. While the lower storey in a double-storey building shall have an average compressive strength for hollow and solid masonry units not less than 7.0 MPa and 10.0 MPa, respectively. The single-storey specifications are more relevant to LIH, and it can be seen that the required strengths have had a reduction in their requirements, thereby reducing the expected costs.

The requirements of both hollow and solid CMUs are given by SANS 1215 (2008). It covers inspections and methods of test as well as aspects such as shape, appearance, surface texture, dimensions, etc. SANS 1215 also gives the strength requirements of the CMUs which are shown in Table 2.1. The structural use of unreinforced masonry walling is governed by SANS 10164-1 (1980).

2.3 Environmental Issues of Conventional Masonry

While conventional masonry units are the most widely used material for LIH in South Africa, they still have disadvantages, of which the most significant is their environmental impact. Due to the growing concerns of the impact that the construction industry has on the environment, steps need to be taken to rectify this situation. Few papers have thus far looked at the eco-efficiency and environmental impact of masonry units (Pacheco-Torgal, 2015a); this lack of research into environmentally friendly masonry units must be addressed with more studies in order to lower the construction industries impact on the environment.

The manufacturing of fired clay bricks results in excessive extraction of clay and top soils. Not

Table 2.1: Compressive Strength Requirements for CMUs (Table 2 in SANS 1215 (2008))

Nominal compressive strength [MPa]	Minimum compressive strength [MPa]	
	Average (for 5* units)	Individual units
3.5	4	3
7	8	5.5
10.5	11.5	8.5
14	15.5	11
21	23.5	17
*In the case of units having an overall length of 290 mm or less, an average of 12 units is taken		

only does this use large amounts of non-renewable resources but the use of these resources results in a decrease in area available for the conservation of biodiversity. Fired clay bricks are also an energy intensive material with high temperatures necessary for their production. Natural gas, propane, coal or firewood is generally used as the fuel source (Venkatarama Reddy and Jagadish, 2003). This leads to the release of many greenhouse gases (GHG) into the atmosphere as well as creating waste materials.

While fired clay bricks have a higher energy consumption than CMUs, the CMUs still have severe negative environmental impacts. In the United States of America the largest source of carbon dioxide emission other than fossil fuel consumption is cement manufacture, specifically the production of clinker (US Energy Information Administration (EIA), 2009). According to Dahmen and Muñoz (2014) 91 % of the GHG released during the manufacturing of CMUs is attributable to the creation of the ordinary Portland Cement (OPC) constituents. Therefore, one of the most effective ways to reduce the environmental impact of the CMU is to reduce the cement content in the mix.

One of the most common methods for reducing the cement content is through the use of supplementary cementitious materials (SCMs). Common SCMs used in practice include fly ash and ground granulated blast furnace slag, due to their low cost and wide spread availability. These SCMs can reduce the cement content and thereby the GHG produced with only a minor reduction in strength and durability of the concrete. However, there are limitations to the use of SCMs (Dahmen and Muñoz, 2014).

While the SCMs mentioned above are wide spread, if they are not located near enough to the building or mixing site, then their effectiveness is reduced. The cost and environmental impact of transporting SCMs long distances can be exorbitant and negate any possible advantages they may have had. Another serious consideration is the potential toxicity of SCMs. Due to their derivation from industrial byproducts certain SCMs have been shown to contain highly toxic elements such as arsenic, beryllium, cadmium, chromium and lead, among others. It is

not clear yet whether the hydration reaction of the SCMs are capable of immobilising these toxins (Dahmen and Muñoz, 2014). Further research is therefore necessary to ascertain whether they should be used in large quantities.

Due to the negative environmental effects of conventional masonry units and the urgent need for mass LIH, a construction material is necessary that is economical, environmentally friendly and socially acceptable. One method that can be looked at is AMUs.

2.4 Alternative Masonry Units

While the most popular masonry blocks are fired clay bricks and CMUs, they are not considered to be environmentally sustainable. Hence it is necessary to research and develop AMUs that can replace the conventional masonry units while still maintaining their advantages. This section considers AMUs found in literature and in practice. To help understand why certain AMUs are focused on while others are just briefly touched, the thought process behind choosing AMUs for this study is first given.

One of the objectives of this study is to develop tests that can be used on a wide variety of AMUs with very different material properties. For this reason one of the first characteristics looked at in potential AMUs is the difference in material properties compared with other AMUs. Therefore, AMUs considered also needed to have different material properties from the CMUs that would be used as a benchmark. The second aspect that is looked at is the environmental benefits of an AMU. AMUs with less embodied energy, GHG emissions or use of non-renewable natural resources were prioritised. The third aspect looked at is cost. As the AMUs investigated are to be used for LIH they have to be more, or at least as, economical as CMUs. The final consideration and arguably the most limiting is the availability of manufacturing equipment. For instance, large mechanical pressures or high temperatures could not be achieved with the currently available laboratory equipment.

Many AMUs have been investigated by other researchers to try and find a viable sustainable masonry unit. This section briefly considers some of the AMU's that are discussed in literature followed by an in depth look at the units chosen for this study. Shakir and Mohammed (2013) give a comprehensive list of research done to create more sustainable masonry units. The research they looked at can be broadly organised into the following categories:

- Enhancing clay brick quality through the introduction of various recycled wastes into the mix. These wastes include foundry sand, granite sawing waste, harbour sediments, perlite, sugar-cane baggase ash, clay waste and fine waste of boron, sewage sludge, waste glass from structural walls and other wastes.
- Developing bricks with only waste materials with few to no natural resources such as sand or gravel. Materials that were used to create these bricks include waste treatment residual, granite waste, paper sludge, straw fibres, waste treatment sludge, fly ash and other wastes.

The first category of research focuses on reducing the excessive extraction of clay and top soils as

well as reducing the contamination of the environment from other wastes. While these methods do increase the sustainability of the bricks they do not focus on reducing the creation of GHG and the burning of fossil fuels in the firing stages of the bricks (Shakir and Mohammed, 2013). Due to this and the fact that CMU's are used more commonly in LIH than clay bricks in South Africa, this category of sustainable bricks is not investigated in detail.

Due to the increasing population and thereby the need for infrastructure and housing, the demand for construction materials may soon outstrip the supply. For this reason researchers have been looking to design and develop sustainable alternative construction materials which consist mainly or wholly out of waste materials. The second category of research from Shakir and Mohammed (2013) covers a wide range of these waste masonry units.

Raut et al. (2011) also give a list of researchers who have looked at alternative methods to create sustainable masonry units. Once again the main focus is the addition of wastes to the masonry mix. These additions serve different purposes, such as reducing usage of non-renewable resources, consuming waste materials, reducing thermal conductivity, and creating light weight bricks. Wastes that were used in these studies include paper processing residues, cigarette butts, fly ash, textile effluent treatment plant sludge, polystyrene foam, plastic fiber, straw, polystyrene fabric, cotton waste, dried sludge collected from an industrial wastewater treatment plant, rice husk ash, granulated blast furnace slag, rubber, kraft pulp production residue, limestone dust and wood sawdust, processed waste tea, petroleum effluent treatment plant sludge, welding flux slag and waste paper pulp. Many of the researchers listed by Raut et al. (2011) are also covered by Shakir and Mohammed (2013). However while Shakir and Mohammed (2013) focused on the environmental aspects of the masonry units, Raut et al. (2011) focused on the strength, water absorption and governing codes of the masonry units.

These researchers looked at a comprehensive list of research into alternative materials used for masonry, however, it was seen that the vast majority of this research consisted of adding waste to clay bricks and thus still requires firing at high temperature. Most of the second category of research from Shakir and Mohammed (2013) and a few of the researchers from Raut et al. (2011) provided a means of creating alternative masonry units without firing, however, these units were created from specific wastes with often limited availability. The only units that were seen to be applicable as AMUs for mass use and creation in South Africa were bricks with waste limestone powder and the FaL-G brick, so called because of its binder content of fly ash, lime, and gypsum. These are looked at in more detail in Sections 2.5 and 2.6 respectively.

The alternative units discussed so far focussed heavily on the addition of wastes partly or wholly into the masonry mix. One AMU that also uses waste material that Shakir and Mohammed (2013) and Raut et al. (2011) failed to mention was the alkali-activated concrete block (sometimes referred to as the geopolymers block). It is considered to be a new family of masonry unit whose production can consume large quantities of waste materials including: fly-ash, blast furnace slag, mine-tailings, red-mud, silica fume, and metakaolins (Pacheco-Torgal et al., 2015). Alkali-activated concrete blocks are discussed in detail in Section 2.9.

While there are undoubtedly many other AMU's created from waste materials, an in depth

study found the above mentioned units to be the most prevalent in literature. However AMUs do not only need to be created from waste materials. The variety of these AMUs are much more limited, especially for large scale use in South Africa, and the main types that were found to be studied or used in any great depth are only adobe blocks and compressed earth blocks or some variation of earth based blocks. These units are examined in detail in Section 2.7 and 2.8 respectively.

2.5 Limestone Powder Waste Bricks

Limestone is an easily accessible sedimentary rock that has numerous uses including: building material, aggregate for the base of roads, white pigment or filler for products such as toothpaste and paints, and chemical feedstock for the production of lime. Limestone powder is created as a by product of the extraction and cutting of limestone, which is currently done with chain saw, diamond wire and diamond saws from quarries (Murat Algin and Turgut, 2008). The estimated production of limestone powder during extraction from quarries is approximately 20 % of the total limestone produced (Manning and Vetterlein, 2004).

There are limited studies on the utilisation of limestone powder waste (LPW) in the construction industry. Galetakis and Raka (2004) investigated cylindrical specimens made with LPW and cement, however, these units were not in standard masonry forms. LPW masonry units were studied in depth by Paki Turgut in Turkey. He investigated multiple combinations of LPW with other wastes, including LPW combined with wood sawdust waste (Turgut, 2007; Turgut and Murat Algin, 2007), LPW combined with cotton waste (Murat Algin and Turgut, 2008), LPW combined with waste glass powder (Turgut, 2008), and LPW combined with fly ash and/or silica fume to create masonry units with no cement (Turgut, 2010; Turgut, 2012).

The masonry units studied by Turgut consisting of LPW mixed with wood sawdust, cotton waste, or glass powder all gave promising results. The samples showed that the new brick materials are capable of producing economical and light weight masonry units. The results further showed that the obtained compressive strength, flexural strength and ultrasonic pulse velocity (UPV) satisfied the relevant international standards. UPV is a technique used as a means of quality control for the production of masonry blocks which are made of a similar mixture. Compaction and ratio of waste material can be detected with this technique (Turgut, 2008). Turgut also investigated masonry units created without the addition of Portland cement. These include studies with only fly ash as well as fly ash and silica fume. Both studies gave rewarding results, with the compressive strength and flexural strength satisfying the relevant standards.

The focus of these units was to create materials from waste products to combat the accumulation of waste materials which may cause environmental and health concerns. However, the mixes with wood sawdust waste, cotton waste and waste glass powder still used cement and therefore the negative environmental aspects coupled with cement production were not addressed. Two of Turgut's studies replaced cement with fly ash and silica fume, using compression as the method of forming the bricks. This greatly reduced the environmental impacts of the units as they were

created with only waste materials and without high temperatures.

LPW masonry units were not chosen to be researched in this study due to the limited literature available which in turn led to limited information on their mix design. As the focus of this study is not designing AMU's but rather testing them, it was decided that other AMU's with more information on their mix design would be used. However, LPW blocks can be a suitable AMU for LIH in South Africa if more research is conducted.

2.6 FaL-G

FaL-G has potential for use as an alternative masonry material for LIH in South Africa. Named due to its constituents of fly ash, lime and gypsum, the material finds extensive application in producing bricks, hollow bricks and structural concrete (Raut et al., 2011). Its usage of waste materials and little to no OPC, results in a material that is cheap and environmentally friendly.

All three main constituents of FaL-G can be taken from industries as waste materials. This not only helps reduce the negative environmental effects of disposing of waste, but also helps reduce the negative environmental aspects coupled with cement production. FaL-G has also been researched as a material that can be used with no aggregate, thereby acting as a possible solution to future generations that may face a shortage of sand and stone (INSWAREB, 2011).

Another advantage of FaL-G is that its reaction does not depend on the application of external heat, reducing the energy required to create the units. FaL-G blocks can also be created without heavy-duty press and autoclave, thereby making the process practically energy free (Bhanumathidas and Kalidas, 2005).

Kumar (2003) has undertaken extensive research into using FaL-G as bricks for LIH (Kumar, 2000; Kumar, 2002). His research concluded that FaL-G blocks have sufficient strength and have potential as a replacement for conventional burnt clay and concrete blocks. Jayasudha et al. (2013) also conducted a study into FaL-G masonry blocks and found that FaL-G blocks could effectively replace burnt clay bricks, with the added advantage of large scale utilisation of fly ash.

The research done by others shows that FaL-G can be suitable for LIH and could find application in South Africa. However, this study did not choose FaL-G as one of the materials investigated due to the requirement that the materials characteristics be as diverse as possible. A decision was made to include adobe blocks rather than FaL-G due to the possibility of FaL-G's mechanical characteristics being similar to that of alkali-activated concrete block, while adobe would be vastly different. If however, the time frame allowed for a fourth alternative material to be investigated, then FaL-G would be the logical choice.

2.7 Adobe

Earthen materials have been used for thousands of years across the globe and remain one of the most used forms of habitation. Recently the material has undergone a revival in interest due to the focus on low-energy and sustainable building materials. These earthen materials have multiple advantageous characteristics, including low cost, local availability, recyclability, good thermal and acoustic properties and reduced energy when transformed into a building material (De Almeida, 2012). However, there are certain disadvantages as well, namely, the need to protect the stored material before construction and before a roof is installed, shrinkage during the drying phase, low tensile and flexural strength, low resistance to water erosion and often lower social acceptance due to it being seen as the poor man's masonry (Aymerich et al., 2012).

Due to the low strength of earth in tension and bending, earth buildings are designed so that all the compressive forces pass down within the thickness of the structure. The moderate compressive strength of earthen walls also means that load bearing walls are generally massive. The thickness of the walls can be reduced slightly with the addition of stabilisers to the soil or with more compaction effort. Another key element of designing with earth is to protect the material from contact with water, due to the loss of compressive strength when wet (Norton, 1986).

The main forms of earthen construction can be categorised into four categories: wattle and daub, rammed earth, adobe and compressed earth blocks, with many variations in each category. Adobe and compressed earth blocks are both formed into blocks in a mould, whereas the rammed earth is compacted directly into walls. Wattle and daub involves pressing earth into a woven lattice of wooden strips (Torgal and Jalali, 2011). Due to this study's focus on masonry blocks, the adobe and compressed earth blocks are investigated. This section discusses the adobe material and Section 2.8 looks at compressed earth blocks.

Adobe is a very basic form of block, consisting of earth and water, with straws or other fibres occasionally added. The mixture is generally placed into wooden moulds, which are often immediately demoulded and the units are left to dry (De Almeida, 2012). Due to the requirement of proper drying for the production process, as well as the general weakness to water erosion, adobe is most successful in hot regions with limited rainfall.

Due to the ease of creation, an adobe block is a building material that can be created by anyone with some research and hard work. For this reason many of the mixing procedures and material tests are very simple.

2.7.1 Soil Characterisation

The main method of designing adobe mixes is by looking at the soil gradation. Soils are generally split into four grades of particle sizes: gravel, sand, silt and clay. The British standard soil grading is given as (BS 5930:2015, 2015):

Gravel	60.00 mm to 2.00 mm
Sand	2.00 mm to 0.06 mm
Silt	0.06 mm to 0.002 mm
Clay	less than 0.002 mm

The clay content in the earth used for adobe creation is crucial as it is the principal agent of formation. Adobe uses the shrinking characteristics of the clay and earth materials to give form and stability to the blocks. The clay becomes a compact and resistant mass upon drying due to the electrostatic forces between the clay particles (Velde, 2008). Balancing the clay with gravel, sand and silt is crucial to build successfully with earth. To accomplish this a soil analysis must be conducted (Norton, 1986).

Various methods exist for classifying soil, from more complicated methods to lower accuracy but very simple methods. These begin with detailed laboratory tests, to field laboratory tests and finally simple fields tests. Due to the sheer number of tests they will not be given here. The more detailed laboratory tests are given by Parts 1 through 9 of BS 1377:1990 (1990), while many of the more simple tests are explained by Norton (1986) and Horn (2006). Rigassi (1985) and Torgal and Jalali (2011) give a brief overview of both the laboratory and field tests.

From the soil analysis tests there are three main characteristics that are important for designing adobe blocks. First, there is the composition of the soil, which indicates the basic characteristics and gives an indication of its potential for block making. Secondly, the plasticity of the soil, which is important when considering soil stabilisation. Lastly, there is the optimum water content of the soil. This indicates the level of water that is necessary to ensure maximum density when compacted, and thereby the maximum strength (Norton, 1986).

2.7.2 Creating Adobe Blocks

Using the soil tests a suitable soil can be selected. Top soil should not be used to avoid the inclusion of organic matter. Rotting of the organic matter will leave cavities in the blocks, reducing the overall strength (Horn, 2006). The soil's grading is generally used to identify a suitable soil, however, due to the extremely varied nature of soils found across the globe and the lack of standardisation, different sources recommend different grading proportions for a mix. Norton (1986) recommended the following particle distribution:

Sand	40 to 75 %
Silt	10 to 30 %
Clay	15 to 30 %

There is a great deal of variability in the clay content of naturally occurring soils used for adobe, therefore additional materials are sometimes added to the clay to achieve gradings similar to

the recommended values. A soil that has a high sand content will lower moisture absorption and increase resistance to abrasion, however, it may not have enough cohesive strength to avoid crumbling. Conversely, a soil with a high clay content will provide more cohesive strength but is more vulnerable to water; swelling when wet and shrinking when dry (Norton, 1986). Extra sand may be added if the mix does not have enough clay, conversely extra clay may be added to a soil with too much sand. However, adjusting a mix in such a manner typically requires a large amount of extra work and therefore it is sometimes easier to settle for a soil that is not adjusted to exact values but still gives a good enough block (Horn, 2006). This must be carefully considered by looking at what the final goal of the project is and that the final product dries into a homogeneous, compact mass without cracks forming within it (Velde, 2008).

Straw is not essential to adobe mixes, however, when utilised correctly it provides certain advantages. The straw helps to reduce shrinkage and cracking during the curing process. It also improves the tensile strength of the blocks. Due to its light weight it also reduces the final weight of the block and provides improved insulation (Horn, 2006).

Due to the great difference in grading and material composition between soils, the optimum water content varies greatly as well. However, determining the optimum water content at time of moulding is important due to the direct influence it has on the strength of the units. The optimum water content allows the greatest dry density which in turn provides the highest compressive strength. Various methods are used to determine the optimum water content including: the proctor test, compaction test, bar test and drop test (Horn, 2006; Norton, 1986).

Once a soil and water mixture has been created it is placed into a mould and compacted by hand to reduce the air voids and compress the material. The mould is generally removed immediately and the block left to dry. The size and shape of the blocks are not standardised and are chosen based on what is required for the structure. Adobe is almost always made solid as the material is not suited for hollow blocks.

The moulds used for the creation process are generally created from wood or metal, occasionally having metal sheeting placed inside wooden moulds to aid with demoulding. These moulds are created to form either one block at a time, or a 'ladder' mould is created that can produce multiple blocks at once. These moulds commonly have no bottom to allow immediate demoulding of the blocks. Figure 2.3 shows a 'ladder' mould in use, illustrating how adobe blocks are commonly demoulded.

After demoulding the blocks are very weak and are generally left where they are to dry for a few days. Even though adobe blocks are sometimes known as 'sun-dried bricks', direct sunlight in their fresh state may result in the water evaporating too quickly and causing cracks. It is therefore better to let them dry in shade or under a layer of loose dirt or straw (Norton, 1986). The bricks are dried for one to three days and then lifted to rest on their side for approximately a month before being used for construction.

Very few international standards exist for testing and constructing with adobe or earth in general. However, New Zealand developed the first set of standards for the engineering design of earth



Figure 2.3: Creation of Adobe Blocks with Wooden Mould (Horn, 2006)

buildings, including (EBANZ, 2015):

- NZS 4297:1998 Engineering Design of Earth Buildings (Specific Design)
- NZS 4298:1998 (Including Amendment#1) Materials & Workmanship for Earth Buildings
- NZS 4299:1998 (Including Amendment#1) Earth Buildings Not Requiring Specific Designs

2.8 Compressed Stabilised Earth Blocks (CSEB)

The compressed earth block is a modern descendent of the adobe block. With technological advancement came the mechanisation of the adobe block with pressure being applied to the block, through manual or mechanical means. This was further advanced with the addition of stabilisers to the mix design, creating the compressed stabilised earth block (CSEB). CSEBs are sometimes known as stabilised mud blocks or stabilised soil blocks (Torgal and Jalali, 2011). CSEBs have many of the same advantages of adobe while negating some of the disadvantages. Some of the advantages over conventional adobe blocks include (Rigassi, 1985):

- The use of mechanical compaction results in an increased consistency of quality in the products obtained, and the regular shape and sharp edges are appreciated by builders. This increase in quality and visual aesthetic also improves the social acceptance of the earthen materials.
- The higher density due to the compaction increases the compressive strength of the blocks as well as their resistance to damage and erosion from water.
- CSEB units can be consistently created in a variety of shapes and sizes, allowing easy assimilation into areas that make heavy use of small masonry elements. The wide range of geometry available allows widely differing needs and requirements in both rural and urban environments.

- CSEB production can be linked to quality control procedures that meet requirements for building product standards.

Just as with adobe, soil is the fundamental material for CSEBs, with clay being a key component. It is therefore essential to understand the properties of the soil. Soil classification systems (briefly discussed in Section 2.7.1) are used to help understand the properties and behaviour of the soil to be employed for engineering purposes.

A large variety of clay minerals exist in nature, with the most common being kaolinite, illite and montmorillonite. For the purposes of stabilised earth, these can be classified into two categories, expansive (montmorillonite) and less expansive soils (kaolinite and illite). As the name suggests, expansive soils swell and shrink more when they come into contact with water or dry out. Less expansive soils are better suited for soil stabilisation. The type and percentage of clay dictates the type and amount of stabiliser added to CSEBs (Venkatarama Reddy, 2012).

The important characteristics of CSEBs are strength, durability, water absorption, mortar/unit bond, and the stress-strain relationship. The main factors that influence these characteristics are: the composition of the soil mixture, the density of the block, and the type and quantity of stabiliser (Venkatarama Reddy, 2012).

2.8.1 Stabilised Soil

Naturally occurring soil has specific characteristics such as strength, plasticity, swelling and shrinkage. The grain size and clay content generally control these characteristics, however, for certain applications these properties need to be altered to make the natural soil more suitable. The alteration of the existing soil properties is termed ‘soil stabilisation’ (Venkatarama Reddy, 2012). There are three main forms of stabilisation, namely mechanical, physical and chemical stabilisation (Rigassi, 1985). For CSEBs all three forms of stabilisation are generally used.

Mechanical stabilisation is the best known method of stabilisation where the properties of the soil are modified by compaction. The compaction of the soil modifies the density, strength, porosity and permeability (Rigassi, 1985). Two types of mechanical stabilisation exist: static and dynamic (Venkatarama Reddy, 2012).

Physical stabilisation is an inexpensive method of stabilisation where the grading of the soil is changed through the addition of another soil, sand or clay. Often used to control the clay and sand content of a soil due to their influence on the final product (Venkatarama Reddy, 2012).

Chemical stabilisation is when other materials or chemicals are added to the soil to adjust its properties (Rigassi, 1985). Types of additive includes: cement, lime, bitumen, polymers, certain salts, organic binders, organic and inorganic fibres. The type of additive is chosen based on which soil property needs to be adjusted and the required state of the final product. The most common form of chemical additive for CSEBs is cement and lime.

When using cement stabilisation, sand and gravelly soil is recommended; therefore, it is best to limit the clay content of the soil ($< 20\%$) (Rigassi, 1985; Venkatarama Reddy, 2012). It

is also recommended that the presence of organic matter be reduced as it may inhibit the cementing action and cause undesirable outcomes to the stabilisation (Torgal and Jalali, 2011). Addition of cement to a soil improves the compressive strength, resistance against rain erosion and mechanical damage to the unit. Morel et al. (2007) states that the soil is often combined with 4 to 10 % cement stabilisation.

2.8.2 Production of CSEB

CSEBs are produced in a process involving four main steps: soil selection, soil processing, compacting the block and curing. The characteristics of these blocks are strongly influenced by the clay fraction in the soil, stabiliser content and final block density (Torgal and Jalali, 2011).

Due to soil being the predominant constituent of CSEBs the selection of soil is a fundamental step in earth block production. Similarly to adobe, the soil gradation (gravel, sand, silt and clay) is an important indicator of the suitability of a soil. When a soil gradation is not suitable for CSEBs, physical stabilisation is applied to produce a proper soil grading. Rigassi (1985) recommends the following grading for CSEBs:

Gravel	0 to 40 %
Sand	25 to 80 %
Silt	10 to 25 %
Clay	8 to 30 %

It can be seen that CSEBs have a coarser recommended grading than that of adobe. However, the gravel particle size should not exceed 6 mm as it results in a poor surface finish of the final product. As stated, when chemical stabilisation with cement is applied to a mix the recommended grading has even less clay ($< 20\%$). Soils with less expansive soils (koalinite and illite clays) are also required for use with cement stabilisation. If clay content is optimised then the maximum strength and durability of the CSEBs is maximised. Venkatarama Reddy et al. (2007) found that the optimum clay content for CSEBs with cement stabilisation is 12 to 15 %.

The soil processing step involves a number of activities such as the crushing and sieving of the excavated soil, mixing in other soils (such as extra sand or clay) and stabilisers, and finally mixing with water. The excavated soil often contains lumps that must be crushed as well as larger gravel that must be removed by sieving. The soil is generally sieved through a 4 to 5 mm sieve in order to blend it more easily with sand and stabilisers. The soils, sand and stabilisers are generally mixed in their dry state, thereafter water is added to the mix. As with adobe, the optimum water content is added to the mix. Generally the water content in these mixes is in the range of 10 to 14 % (Venkatarama Reddy, 2012).

The partially saturated soil then undergoes a static compaction process which involves confined compaction, generally with a piston from either one or two sides. The compaction energy applied

depends on the soil composition, moisture content, and target density. Figure 2.4 shows the steps in a static compaction of CSEBs with a single piston, where T is the final block height.

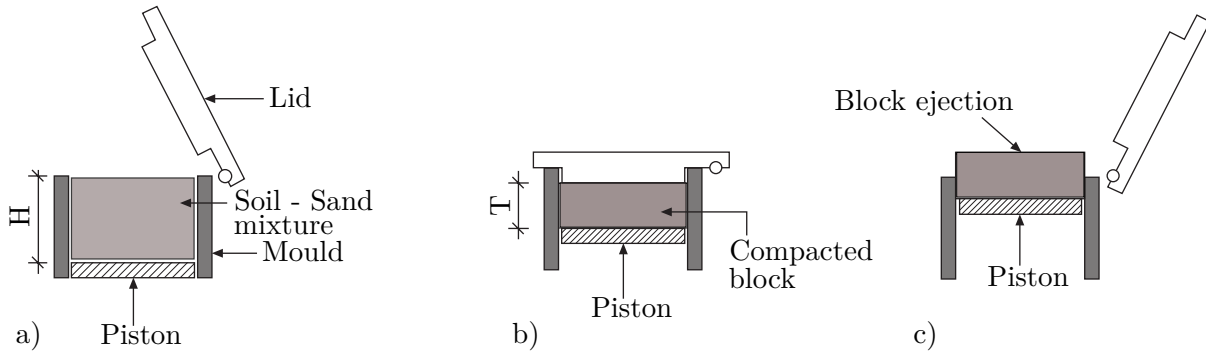


Figure 2.4: Stages in CSEB Compaction Process. From left to right: a) mould filled with soil mix b) compacted by lid and piston c) ejection of blocks (Venkatarama Reddy, 2012)

Similarly to conventional concrete, cement stabilised CSEBs require careful curing. The blocks must be kept humid for the first 7 days to allow proper hydration of the cement particles. The surface must also not dry out too quickly to avoid shrinkage cracks, therefore direct sunlight and wind must be avoided. Although not necessary for CSEB production, high temperature during curing will cause an increase in compressive strength (Rigassi, 1985).

2.9 Alkali-Activated Materials

As mentioned previously, the high demand for concrete coupled with the high CO_2 emissions from the production of OPC has caused the construction industry to become one of the largest contributors to GHG emissions. This has led to extensive research into concrete that can be created without OPC. One of the most promising results of this research is alkali-activated concrete (AAC), also known as geopolymer concrete.

This section is organised as follows. First a background is given on alkali-activated binders, including its history, applications and the terminology used in this field. This is followed by a brief explanation of the chemistry of the material. The method to develop a mix design is discussed next as well as the applications of alkali-activated concrete blocks (AACB). Finally, the health and safety issues of AAC are covered as well as relevant concerns for its use in industry.

It is important to note that alkali-activated binders are a very broad grouping of materials. This means that almost all properties of these materials can fall anywhere within the range from 'high' to 'low' for most criterion they could be measured against. This makes it nearly impossible to provide a list of properties that are 'characteristic' of the material. It is therefore recommended that a detailed molecular level understanding of the chemical and physical characteristic be understood for this material (Provis, 2014). However, such an understanding is an entire investigation of its own and this is not the focus of this study. Therefore, this section just briefly covers the basics of alkali-activated systems and does not go into any great depth.

2.9.1 Background, Applications and Terminology

The accepted first mention of alkali-activated binders as an alternative to OPC can be traced back to a patent by Kühl in 1908 (Kühl, 1908). This was followed by research and commercial work by Purdon in Belgium from the 1930s-1950s and then Glukhovsky in the Ukraine from the 1950s onwards (Provis, 2014). However, the term ‘geopolymer’ was first introduced in the 1970s by Davidovits. The original scope of his research was for the development of fire-resistant materials after a series of fires in Europe. For this reason geopolymers are still used in applications relating to this work, yet it was soon seen that a major application of geopolymers was in the construction industry (Provis and van Deventer, 2009). During the 1980s and 1990s the research into alkali-activators continued at a modest pace, but it was not until the 21st century when this research begun expanding tremendously due to the possibility of a material with low energy cost, high strength and good durability compared to OPC. Pacheco-Torgal (2015b) gives a detailed list of important historical events in the field of alkali-activated cement-based binders (AACBB).

While the interest in AACBB has only spiked recently, the material has been used in a few countries in the last 40 years, in particular the former Soviet Union and China. Much of the knowledge gained in these countries was not shared internationally as the documents were published in the countries’ respective languages and only recently has some of that knowledge been shared. Most notably, the book by Shi et al. (2006) claims to be the first book in English that attempts to summarise the progress of AACBB in the past. The main applications and products that were used in these countries, among others, include (Shi et al., 2006; Pacheco-Torgal, 2015b):

- Structural concrete
- Masonry blocks
- Concrete pavement
- Concrete pipes
- Utility holes
- Concrete sinks and trenches
- Autoclaved aerated concrete
- Refractory concrete
- Oil-well cement
- Stabilisation and solidification of hazardous and radioactive wastes

With the research and application of AACBB being spread over so many years and languages, an important aspect in its study is the various terminologies used by the scientific community. Names that have been given to geopolymers and alkali-activated materials include mineral polymers, inorganic polymers, inorganic polymer glasses, alkali-activated ceramics, alkali ash mater-

ials, soil cements, hydroceramics, zeocements, zeoceramics and others (Pacheco-Torgal, 2015b; Provis and van Deventer, 2009). This wide range of names used by different authors has caused negative impacts on both the research and commercial aspects of this material. Research has been influenced by increasing the difficulty for new researchers in the field to orientate themselves with the material and also cause them to miss important work done on the subject if a key word search is done on an academic search engine (Provis and van Deventer, 2009). Commercially the wide range of terms used has made it more difficult to present AACBB as a viable alternative to OPC (Pacheco-Torgal, 2015b). This is due to the challenge involved in raising awareness of the material as well as proper branding, which is necessary for commercial success.

The main terms used in literature are geopolymers and alkali-activated materials, with geopolymer being the more popular one. However, these two terms do not have the same meaning. Alkali-activated binders is a wide range of materials of which one is the material known as geopolymer. The production of alkali-activated binders is accomplished through the reaction of aluminosilicate with an alkaline activator. The aluminosilicates are generally an industrial by-product or inexpensive material, while the alkaline activators are supplied as a concentrated aqueous solution of alkali hydroxide, silicate, carbonate or sulphate (Provis, 2014). The term geopolymer can then be more specifically defined as an alkali-activated binder with a low calcium alkali-activated system (Pacheco-Torgal, 2015b) with an alkali aluminosilicate gel, whereas other alkali-activated systems have a calcium silicate hydrate type gel (Provis, 2014).

2.9.2 Alkali Activated Cement Chemistry

Alkaline cements are materials formed as a result of an alkaline attack on the amorphous or vitreous aluminosilicates (Garcia-Lodeiro et al., 2015). The aluminosilicates are generally from materials such as fly ash and metakaolin, while the alkaline solution is usually sodium hydroxide or sodium silicate (Ahmari and Zhang, 2015). The alkaline activators allow the material to set and harden. There are three main categories of alkaline cements (Garcia-Lodeiro et al., 2015):

- The first category consists of a low calcium alkali-activated systems. Calcium and silicon rich materials, such as blast furnace slag, are activated under moderate alkaline conditions. These result in a calcium silicate hydrate type gel.
- The second category is comprised of primarily aluminium and silicon. Low calcium materials, such as metakaolin and fly ash, are activated in aggressive alkaline conditions with higher curing temperature (60 to 200 °C). These result in an alkali aluminosilicate hydrate gel. As mentioned, these are often referred to as a geopolymer among other terms.
- The third category is a combination of the first and second categories and is known as blended or hybrid alkaline cement. This binder is formed due to the alkaline activation of materials with calcium, aluminium and silicon contents. There are two main groups that this material can be divided into. The first group contains materials having a low OPC clinker content and high proportion of mineral additions, while the second group has no OPC clinker. The first group is comprised of OPC combined with slag and/or fly

ash, while the second group generally consists of a combination of just fly ash and slag. The reaction products from this category are very complex and are comprised of a mix of cementitious gels.

Garcia-Lodeiro et al. (2015) discuss the chemistry of the three categories of alkaline cements in greater depth. The properties of alkali-activated binder are influenced by the reactivity of the initial materials, silicon/aluminium and sodium/aluminium ratios, type and concentration of alkali activator, and curing condition (Ahmari and Zhang, 2015).

2.9.3 Alkali-Activated Concrete Blocks (AACB)

AACs can be created at both higher temperatures as well as ambient temperatures. While heating is not always feasible in the field, it can be used on pre-cast members where controlled conditions can be applied (Ahmari and Zhang, 2015). Its high corrosive properties can also be handled in a safer manner in controlled conditions.

Alkali-activated materials are therefore well suited to block production due to its ability to be pre-cast. Many studies have been conducted on the material for use as masonry and it was found that it can provide an eco-friendly masonry unit (Ahmari and Zhang, 2015; Cheah et al., 2015; Abdullah et al., 2015).

AACBs can be produced from a number of materials, including fly ash, metakaolin, blast furnace slag and red mud. Whatever the materials are, the general production process is as follows (Ahmari and Zhang, 2015):

- Processing and screening of materials
- Mixing and forming of blocks
- Drying at ambient temperature for one or two days
- Heating to higher curing temperatures
- Packing and transportation

Certain AACBs can be created without Step 4 if high reactive materials are employed. It can be seen that AACBs are more sustainable than conventional masonry as a result of natural resource conservation as well as lowering energy usage due to lower firing temperatures than fired clay bricks (Ahmari and Zhang, 2015). The negative environmental effects from cement clinker creation is also avoided.

2.9.4 Health Concerns

Developing countries such as South Africa have large labour forces in the construction industry, and it is essential that health and safety is taken seriously. While alkali activated materials show

promise for use in the construction industry, they are often dangerous and this causes concerns for the labour force when working with fresh AAC.

Alkali activated materials often employ sodium silicate and sodium hydroxide as the alkaline solution. Sodium hydroxide is classified as a highly corrosive substance that can cause damage to the skin and eyes, and ingesting large quantities can be fatal. However, it is not classified as carcinogenic or mutagenic. Solutions containing a low concentration of sodium hydroxide ($< 0.5\%$ in water) has no adverse effects on human health. Solutions with higher concentrations ($> 2\%$ in water) should be prevented from coming into direct contact with skin due to the corrosive effects (Evonik Industries, 2010). There are however, various types of alkali activated materials, some of which contain little to no sodium hydroxide, and are therefore much safer. The addition of lime and sodium carbonate into a mixture is one method that reduces the corrosive nature of the material.

Alkaline products have been classified in two categories: corrosive products (hostile) and irritant products (friendly). The corrosive products must be handled with the appropriate safety precautions, i.e. gloves, glasses and masks. While studies in literature often look at alkali-activated cement that is classified as corrosive (especially those based on fly ash), AACs used in practice are mostly classified as an irritant (Davidovits, 2013). However, it is still important to conduct tests on the materials and implement the appropriate safety precautions.

2.10 Conclusion

This chapter gave an overview of masonry units and in particular AMUs. A short background on conventional masonry units and the state of LIH in South Africa is discussed. This is followed by a look at the negative environmental effects of conventional masonry units. The types of AMUs available in literature are briefly covered, followed by a more in depth look at some of the AMUs suitable for use in South Africa.

AMUs that are concluded to be suitable for LIH in South Africa include: limestone powder waste blocks, FaL-G blocks, adobe blocks, CSEBs, and AACBs. These decisions are based mainly on the availability of materials for creation in South Africa, low cost and low environmental impact.

From these AMUs the adobe blocks, CSEBs, and AACBs are chosen to be further investigated in this study. These are chosen from among the other AMUs due to more information being readily available about their mix designs and even more importantly, their mechanical properties are expected to differ widely from each other. This study is limited to these three AMUs due to time constraints, however, there is no reason the other AMUs could not also be investigated in future studies.

This study does not focus excessively on the materials and mix designs of the AMUs due to the wide range of materials investigated, rather the testing of the AMUs is a greater focus. Therefore, the various AMUs are only briefly covered in this chapter. The mechanical characterisation of masonry units is discussed in the next chapter.

Chapter 3

Mechanical Characterisation of Masonry Units

The advancement of numerical methods and programs of structural analysis over the previous decades has been enormous. This has given engineers the capability to analyse larger and more complex structures with a degree of accuracy not possible before. However, to accomplish this the material sciences cannot be neglected. In order to effectively apply numerical methods to a structure, the mechanical properties of the material must be known. To accomplish this there has been a diffusion of laboratory equipment and experimentation on the mechanical characterisation of materials.

Generally, the mechanical properties of masonry that are investigated are compressive strength, shear strength, and modulus of elasticity. Research into the tensile strength and fracture energy of masonry is much more limited. Studies in this field generally focus on the individual masonry unit or on the interface between the mortar and the units and only rarely on a combination of the two.

For this investigation an experimental study is conducted on a wide array of mechanical characterisations. The compressive strength, modulus of elasticity, Poisson's ratio, and fracture energy of individual masonry units is investigated as well as the compressive strength and modulus of elasticity of masonry wallets. The shear strength between the masonry units and mortar is also studied through the use of triplet tests. This chapter considers the relevant previous research conducted with regards to these mechanical tests as well as how international codes recommend the tests be carried out. While there are many mechanical characterisation used to classify masonry materials, this chapter focuses only on those that were investigated in this study; other characteristics such as masonry flexural strength and bond strength were not investigated.

For this study the European standards are generally used for testing, rather than the American or South African standards. This is due to the fact that the European standards will likely be adopted in South Africa in the near future. Other applicable standards are still mentioned for each test type.

The fact that a large range of materials with vastly different properties are examined in this study must also be recognised. The differences between a conventional concrete material and an earthen material influence the manner in which the materials react to the tests. Another

important distinction is between the definitions of masonry and masonry units. While the terms seem similar, BS EN 1052-1 (1999) gives the definition of masonry as an assemblage of masonry units laid in a specified bonding pattern and jointed together with mortar.

3.1 Compressive Strength of Masonry Units

Compressive strength is one of the most studied properties of brittle and quasi-brittle materials (De Almeida, 2012). This is due to the fact that the compressive strength of most building materials is a parameter that many use to judge the quality of the material. It is also one of the fundamental characteristics used to design masonry walls, although factors such as mortar strength, bonding patterns, density, frost resistance and water absorption are also related to the wall's strength (Morel et al., 2007). Generally however, if the strength of the masonry units is known then the load that a masonry wall will be able to carry can be determined.

Compressive failure of a brittle or quasi-brittle material is accomplished through the softening behaviour of the material. Softening is defined by Lourenço (1998) as a gradual decrease of mechanical resistance under a continuous increase of deformation forced upon a material unit. This is attributed to the heterogeneity of the material, mostly due to flaws and voids in the blocks. This heterogeneity has micro cracks that are stable and only grow as the load is increased. However, as the load approaches the peak strength, the cracks begin to accelerate to macro cracks that are no longer stable, eventually leading to failure. The stress-displacement diagrams for a quasi-brittle material in compression can be seen in Figure 3.1 with generalised micro and macro cracking patterns.

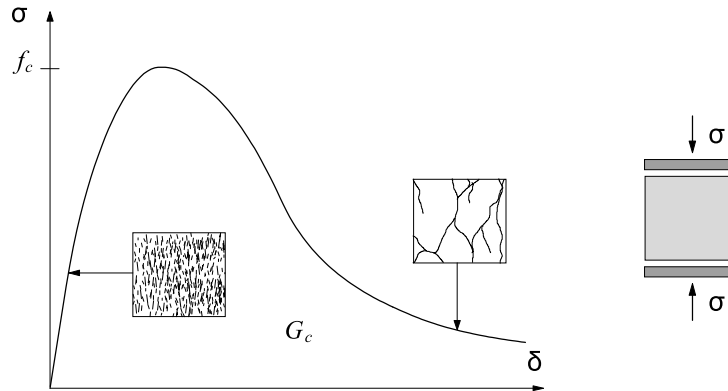


Figure 3.1: Behaviour of Quasi-Brittle Material in Compression (Lourenço, 1998)

When testing compressive strength of materials such as concrete, stone, or various masonry types, the load is normally applied uniformly through two stiff and flat hardened steel plates. As the material is compressed it expands laterally, causing friction between the steel plates and the test specimen. This friction applies restraint to the specimen which increases the apparent strength of the specimens through confinement. The distance between the steel plates relative to the thickness of the specimen (aspect ratio) therefore influences the final strength that the unit will achieve (Morel et al., 2007). As the aspect ratio increases the restraint effect decreases.

Chapter 3. Mechanical Characterisation of Masonry Units

With materials that can be cast, such as concrete and mortar, a standard size and shape, generally a cube or cylinder, can be specified. While these are not truly unconfined they can be used with specified requirements for design. Masonry units, on the other hand, are not cast and therefore have varying specimen geometry. To counter this, international standards generally normalise the compressive strength of the masonry units with a shape factor, which seeks to remove the restraint factor by converting the results to unconfined strengths (Morel et al., 2007).

Masonry units are generally tested in the same orientation as used for wall construction. This allows the strengths from the compressive tests to be directly relatable to the strength of the blocks in situ. For this study units in this orientation are referred to as being tested on their bedface. When units are tested parallel to their bedface, their compressive strength is weaker. Units tested parallel to their bedface are referred to as being tested on their headface. Figure 3.2 shows the orientation, casting direction and loading direction of specimens on their bedface and headface.

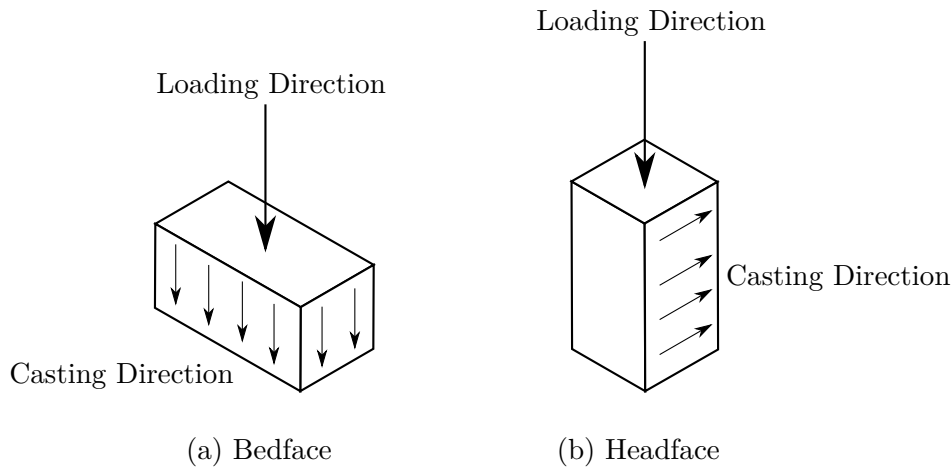


Figure 3.2: Orientation, Loading Direction and Casting Direction of Bedface and Headface Specimens

3.1.1 Compressive Strength of Different Masonry Materials

Another aspect that influences the compressive strength of masonry units is the material itself. The compressive strength of the concrete, alkali-activated, and earthen materials varies greatly due to the material properties and their respective mechanism of strength gain.

Concrete has been rigorously studied with regards to its strength due to its prolific use around the globe. Concrete masonry units have the same constituents and therefore the same strength characteristics as conventional concrete with only a few minor differences. Concrete masonry units (CMUs) are generally slightly less dense than conventional concrete due to the manufacturing process employed. This results in a material that has a lower strength. Nevertheless, good quality CMUs can still attain adequate strength for normal use. The low density also creates a unit with a rough exterior surface allowing a good bond with mortar (Owens, 2009). SANS 1215 (2008) gives the required strength of CMUs.

Concrete units are available in a wide range of strengths, ranging from hollow units of 3.5 MPa

Chapter 3. Mechanical Characterisation of Masonry Units

strength to solid units with 7 to 21 MPa strengths. Units above 10.5 MPa are generally solid units (Owens, 2009). These strength are the unit strengths and not the material strengths.

Alkali-activated concrete block (AACB) strength is not nearly as widely studied as CMUs. However, unlike concrete there is almost no difference between alkali-activated concrete (AAC) and AACBs as both are cast in the same manner. AAC shows excellent strength and appearance similar to conventional concrete. The compressive strength of fly ash based AAC relies on the strength of the alkali-activated binder and the bonding between the binder and aggregate (Manjunath et al., 2011).

Most research focuses on AAC cured at elevated temperatures, with AAC cured at ambient temperature being more scarce. However, it has been shown that both can produce a material strong enough for masonry units (Manjunath et al., 2011; Barnard, 2014; Abdullah et al., 2015).

The compressive strength of CSEBs is related to the soil types, density, and stabiliser content of the blocks. Wet or dry conditions of CSEBs also greatly affect the strength of the unit, a problem that concrete and AAC do not have. The wet compressive strength of CSEBs is generally much lower than the dry compressive strength. International standards have not achieved a consensus on whether CSEBs should be tested wet or dry (Morel et al., 2007). The low strength of saturated CSEBs can be attributed to the development of pore water pressure and the liquefaction of unstabilised clay particles (Riza and Rahman, 2015).

The optimum cement content of CSEBs is between 5 to 10 %, with a value of more than 10 % causing a reduction of the strength. An increase in the compacting pressure and thereby the density of the units will also cause an increase in the compressive strength by up to 70 % (Riza and Rahman, 2015).

Unstabilised adobe blocks are the furthest from concrete in terms of strength gain and compressive strength. However, research into the compressive strength of adobe has seen an increase as environmentally friendly building practises gain popularity. Nevertheless, there is little consensus on test procedure, curing methods, or how the aspect ratio should be taken into account (Quagliarini et al., 2015).

The strength of adobe blocks does not reach that of concrete masonry blocks or fired clay bricks. Values reported in literature vary from 0.5 to 8.3 MPa, with the most common values ranging between 0.8 to 3.5 MPa (Quagliarini et al., 2015; De Almeida, 2012). Compressive strength tests are normally conducted in the same manner as those implemented for fired clay or concrete blocks, however extensive studies have not been conducted that validate this method of testing.

3.1.2 Compressive Strength Testing Specification

The European standard BS EN 772-1 (2011) is used as a guideline for the determination of compressive strength of individual masonry units in this study and this section considers the relevant specifications from the standard with regards to testing solid masonry blocks. ASTM C1716M-

Chapter 3. Mechanical Characterisation of Masonry Units

16 (2016) and SANS 1215 (2008) both give similar guidelines for determining the compressive strength of individual masonry units.

The standard specifies that a minimum of six samples be tested and that the sample have plane and parallel faces through which the load will be applied. Capping or grinding can be used to ensure these faces fall within the tolerances. The conditioning (or curing) of the specimens shall be done according to a prescribed regime moisture conditions.

The relevant conditioning regimes are either conditioning to the air dry condition or by immersion. Specimens that are air dried must be stored in a laboratory for at least 14 days at a temperature greater than 15 °C and a relative humidity less than 65 %. Free air circulation around each specimen must also be ensured. Specimens conditioned by immersion must be placed in water at a temperature of 20 ± 5 °C for at least 15 h. After removal from water they are allowed to drain for 15 to 20 min.

The gross loaded area shall be calculated in square millimetres using the width and height or length and height as appropriate. These dimensions shall be determined in accordance to BS EN 772-16 (2011). For the testing procedure the rate of loading shall be adjusted so that the maximum load is not reached in less than approximately 1 min. The maximum load is then recorded.

The strength is calculated for each specimen by dividing the maximum load achieved by its loaded area (this includes all holes and cavities), which is its gross area. The final compressive strength shall be given as the mean value of the strength of the individual specimens to the nearest 0.1 N/mm².

BS EN 772-1 (2011) also gives an informative annex that allows the conversion of the compressive strength of the masonry units to the normalised compressive strength. This is to take into account the confinement of the units in the test setup due to the aspect ratio. First the compressive strength is converted to an equivalent strength relevant to the air dry conditioning regime. The values to be used as multipliers for the conversion is 1.0 for air dry conditioning and 1.2 for conditioning by immersion.

To obtain the normalised compressive strength the air dry compressive strength of the masonry units is multiplied by a shape factor (d). This shape factor is shown in Table 3.1 which was adapted from BS EN 772-1 (2011). Linear interpolation between adjacent values of the shape factors is allowed. The height is that of the unit after surface preparation.

Table 3.1: Shape Factor (d) for Normalising Compressive Strength

Width (mm)	50	100	150	200	250
Height (mm)					
40	0.80	0.70	-	-	-
50	0.85	0.75	0.70	-	-
65	0.95	0.85	0.75	0.70	0.65
100	1.15	1.00	0.90	0.80	0.75
150	1.30	1.20	1.10	1.00	0.95
200	1.45	1.35	1.25	1.15	1.10
250	1.55	1.45	1.35	1.25	1.15

3.2 Modulus of Elasticity

The modulus of elasticity is a value that is related to the stiffness of a material. It is an important value for calculating the stresses that result due to strains. These strains typically arise due to loads, concentrated loads, and constrained movement. The modulus of elasticity can also be used for calculating the required area of reinforcing and post-stressing bars. Young's modulus (E) is another term commonly used for modulus of elasticity. Poisson's ratio (ν) is also required for structural design, theoretical calculations and numerical modelling (Domone and Illston, 2010).

Neither concrete nor conventional masonry are ideal elastic materials. The non-homogeneous nature of concrete as well as the transition zone between the hardened cement paste (HCP) and the aggregate results in a non-linear stress-strain curve. Masonry's microcracks and imperfections as well as the varying stiffness at the mortar interface also results in a non-linear stress-strain curve. Successive loading and unloading stress cycles below the ultimate strength causes diminishing hysteresis loops, as seen in Figure 3.3. These hysteresis loops are due to cracks forming in the material in increasing size and number, resulting in an increase in the overall strain and thereby causing non-linear behaviour. As the loading cycles are repeated these cracks generally reduce in number after the first loading, provided the stress levels of previous loading cycles are not exceeded. This causes the diminishing of the size of the hysteresis loops as shown in Figure 3.3 (Domone and Illston, 2010).

Two different elastic modulus values can be defined from the non-linear stress-strain curve of the masonry. These include the tangent modulus (shown as Line A or B in Figure 3.3) and the secant modulus (shown as Line C in Figure 3.3). The tangent modulus is measured as the slope of the tangent to the curve at any point, while the secant modulus is the slope of the line

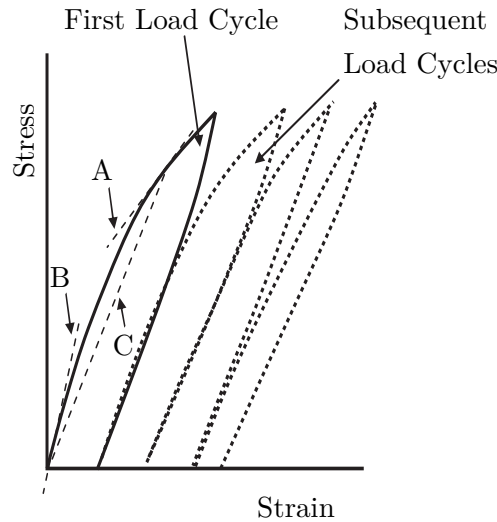


Figure 3.3: Behaviour of Concrete Under Successive Loading Cycles (Domone and Illston, 2010)

between the origin and a point on the curve (Domone and Illston, 2010); generally the point is at 33 to 40% of the ultimate strength. International standards generally give provisions for the secant modulus as it is more commonly used.

For concrete, an increase in age and water to cement ratio contributes to an increase in the elastic modulus. This means that an increase in strength causes an increase in the elastic modulus, however, there is no simple relationship between the two and it is therefore recommended that the elastic modulus be determined by experimentation if accuracy is required. Certain codes do give estimates that relate the strength of the material to the elastic modulus, generally to be used in initial design stages (Domone and Illston, 2010).

3.2.1 Modulus of Elasticity Testing Specification

International standards have been developed that provide guidelines on how to determine the modulus of elasticity of concrete. Both the European standard BS EN 12390-13 (2013) and the American standard ASTM C469/C469M (2010) provide similar methods for the determination of the secant modulus of elasticity. As stated before, due to the likelihood of South Africa adopting the European standards, this study uses BS EN 12390-13 (2013).

As with the compressive strength testing given in Section 3.1.2 only the aspects of the standard that are relevant for tests carried out in this study are given here. More information can be obtained from the standard directly. For this experiment a test specimen is loaded under axial compression and the stresses and strains are recorded. The slope of the secant to the stress-strain curve is then determined after three loading cycles. The standard also provides provision for only a single loading cycle.

The apparatus required includes a test machine suitable for the execution of programmable loading cycles and capable of remaining within the specified tolerances. Instrumentation capable of measuring strain or length change of the specimen are also required. The gauge length of the

Chapter 3. Mechanical Characterisation of Masonry Units

instrumentation must be within two-thirds of the specimen diameter and one-half of the specimen length and not less than three times the coarse aggregates diameter. The test specimens shall be a cast cylinder or prism with a diameter of at least 3.5 times the max aggregate size. The ratio between the specimen length and diameter shall be in the range of $2 \leq L/d \leq 4$.

The compressive strength (f_c) of the material must be determined before the tests on specimens of the same shape and size, or if the specimens do not have the same geometry then the difference in compressive strength shall be taken into account (generally with the use of shape factors). Once the compressive strength of the specimens are determined, it can be used to define the stress levels for the test cycles used to determine the modulus of elasticity.

Two methods are given by BS EN 12390-13 (2013). Method A involves the determination of initial and stabilised secant modulus of elasticity, while Method B covers just the determination of the stabilised secant modulus of elasticity. For this study Method B is employed.

Three loading cycles are carried out on the specimen with the secant modulus of elasticity being determined on the final cycle; this is to minimise the hysteresis effects and properly position the specimen. Figure 3.4 shows the test cycles for the determination of the modulus of elasticity.

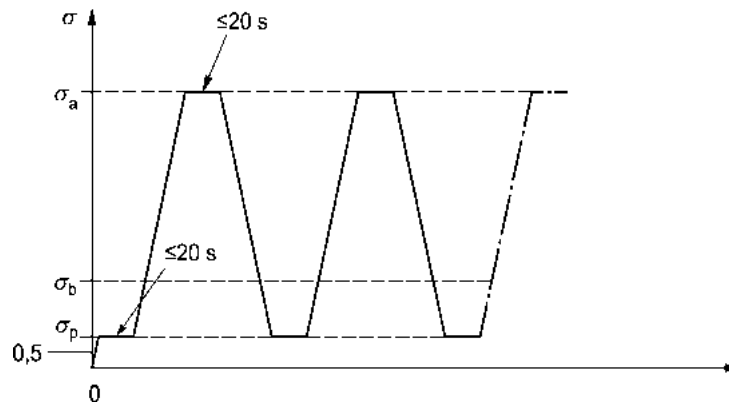


Figure 3.4: Cycles for Determining Modulus of Elasticity (BS EN 12390-13, 2013)

σ applied stress in MPa

σ_a upper stress - $f_c/3$

σ_b lower stress - $0.1 \times f_c \leq \sigma_b \leq 0.15 \times f_c$

σ_p preload stress - $0.5 \text{ MPa} \leq \sigma_p \leq \sigma_b$

t time in s

The specimen is placed, with the measuring equipment already attached, centrally in the testing machine. A preload stress (σ_p) is applied and held for 20 s. This is then increased to an upper stress (σ_a) at a rate of $0.6 \pm 0.2 \text{ MPa/s}$ and held for 20 s. The upper stress is then reduced to the preload at the same loading rate and held for another 20 s. This process is repeated 3 times as seen in Figure 3.4. At the end of the second cycle the strain (ε_p) shall be measured at the preload stress. On the third cycle the strain (ε_a) shall be measured at the upper stress.

Chapter 3. Mechanical Characterisation of Masonry Units

The stabilised secant modulus of elasticity (E_C) is then defined as:

$$E_C = \frac{\Delta\sigma}{\Delta\varepsilon_S} = \frac{\sigma_a - \sigma_p}{\varepsilon_a - \varepsilon_p} \quad (3.1)$$

3.3 Poisson's Ratio

Poisson's ratio (ν) is defined as the ratio of lateral to axial strain of a masonry specimen subjected to loading in the vertical direction (Brooks, 2015). This mechanical property is used in the structural design of masonry buildings in similar purposes as the modulus of elasticity. Literature focusing on Poisson's ratio of masonry units is limited, with most focusing on masonry walls.

Due to the similarities between Poisson's ratio and the modulus of elasticity, many of the principles discussed in Section 3.2 apply here as well. When testing the modulus of elasticity a compressive force is applied while simultaneously measuring the strain (ε_p) parallel to the applied stress (σ), giving:

$$E = \frac{\sigma}{\varepsilon_p} \quad (3.2)$$

Poisson's ratio can then be determined by also measuring the strain (ε_n) perpendicular to the applied stress, whereupon (Domone and Illston, 2010):

$$\nu = -\frac{\varepsilon_n}{\varepsilon_p} \quad (3.3)$$

This allows both Poisson's ratio and the modulus of elasticity to be determined from one test set-up if both the vertical and horizontal strains are recorded during the application of the stress.

3.3.1 Poisson's Ratio Testing Specifications

European or American standards could not be found that specifies test methods for determining the Poisson's ratio of masonry units, instead the method used on concrete cylinders is applied. While both the European standard BS EN 12390-13 (2013) and the American standard ASTM C469/C469M (2010) give guidelines for the determination of the modulus of elasticity, only ASTM C469/C469M (2010) provides information on how to determine Poisson's ratio and is thus used in this study.

The method for determining the modulus of elasticity as given by ASTM C469/C469M (2010) is very similar to the method given by BS EN 12390-13 (2013). It was therefore decided to keep the loading rates and method of load application from BS EN 12390-13 (2013) and simply add the method for obtaining Poisson's ratio from ASTM C469/C469M (2010). This addition is discussed next.

Chapter 3. Mechanical Characterisation of Masonry Units

ASTM C469/C469M (2010) specifies that if Poisson's ratio is required, the transverse strain is to be measured with either an unbonded extensometer or two bonded strain gauges. The unbonded extensometer measures the change in diameter at the mid-height of the specimen. The two bonded strain gauges are mounted at diametrically opposite points at mid-height of the specimen.

A convenient unbonded device, recommended by ASTM C469/C469M (2010), is a combined compressometer and extensometer. This device is capable of measuring both the transverse and longitudinal strain of the specimen. Figure 3.5 shows such a device on a cylindrical specimen.

Two yokes are attached to the specimen (D and C in Figure 3.5) which holds the longitudinal gauge (A). This acts as the compressometer in the test set-up. A central yoke (E) consisting of two equal segments and located halfway between the two longitudinal yokes is used to hold the transverse gauge (B). This yoke is attached to the specimen at two diametrically opposite points, and makes use of a pivot rod (F) to maintain a constant distance between the two longitudinal yokes.

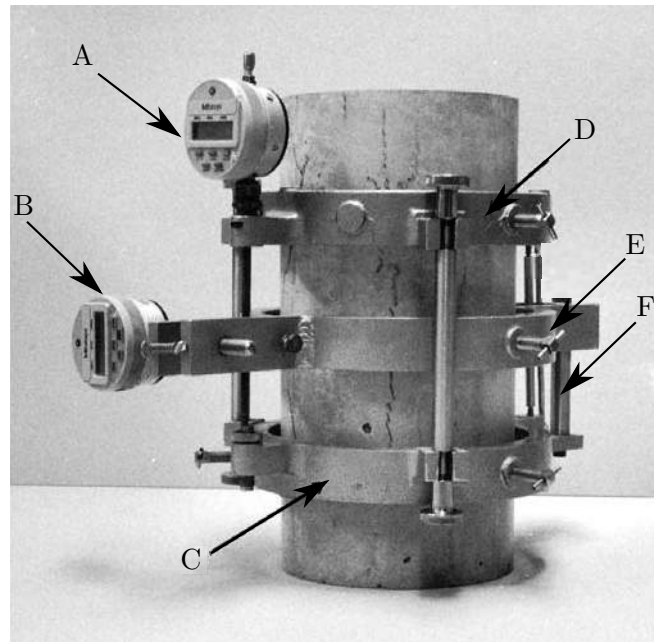


Figure 3.5: Combined Compressometer-Extensometer (adapted from ASTM C469/C469M (2010))

The equation to calculate Poisson's ratio was adjusted slightly to fit the loading procedure from BS EN 12390-13 (2013). Similar to BS EN 12390-13 (2013), ASTM C469/C469M (2010) also applies multiple loading cycles and takes the measurements used for calculations in the final cycle. However, instead of measuring the stress and strain at the upper stress (σ_a) and preload stress (σ_p) (defined in Section 3.2.1), ASTM C469/C469M (2010) takes the measurements at a stress corresponding to 40 % of the ultimate loading and at a stress corresponding to a longitudinal strain of 50 millionths. The only adjustments to the equation was therefore the stress at which the strain is measured. The adjusted equation for Poisson's ratio is:

$$v = \frac{(\varepsilon_{t1} - \varepsilon_{t2})}{(\varepsilon_{L1} - \varepsilon_{L2})} \quad (3.4)$$

where:

ε_{t1} transverse strain at mid-height of the specimen produced by the upper stress σ_a

ε_{t2} transverse strain at mid-height of the specimen produced by the preload stress σ_p

ε_{L1} longitudinal strain at mid-height of the specimen produced by the upper stress σ_a

ε_{L2} longitudinal strain at mid-height of the specimen produced by the preload stress σ_p

3.4 Fracture Energy

The fracture energy of brittle and quasi-brittle materials, such as concrete, represents the crack-ing resistance and fracture toughness of the material (Zhao et al., 2008). The nonlinear fracture energy concept was developed in the 1980s by Hillerborg et al. (1976). These properties are generally represented by fracture mechanics such as the specific fracture energy (G_f) and the strain softening diagram. To determine these properties, stable fracture mechanics tests are required, which means a stable descending branch in the load vs deformation diagram (Brühwiler and Wittmann, 1990).

There are four test methods that are used to perform stable fracture mechanics tests on concrete and materials similar to concrete. These include the uniaxial tensile test, the notched three point bending test, the compact tension test and the wedge splitting test. Of these tests the uniaxial tensile test provides the most direct method for determining the fracture properties, however the small deformations at rupture and the extreme stiffness of concrete makes it a very difficult test to perform (Brühwiler and Wittmann, 1990).

Both the notched three point bending test and the compact tension test have disadvantages for fracture mechanics. The self weight of the beams used in the three point bending test can influence the total fracture energy by 40 to 60 %. The wedge splitting test does not have this drawback due to the compact nature of the specimens. Wedge splitting specimens are also simpler than both the three point bending test and the compact tension test and can therefore be created either in the laboratory or drilled on site (Brühwiler and Wittmann, 1990; Wittmann et al., 1988).

Brühwiler and Wittmann (1990) found that all four test methods give the same G_f value if the ligament length and concrete mix are the same. However, the disadvantages of the uniaxial tensile test, the notched three point bending test and the compact tension test coupled with the fact that the wedge splitting tests has a large fracture area compared to the specimen weight and can be used to produce stable fracture tests at high deformation rates, means that it is the chosen test method for this study.

Chapter 3. Mechanical Characterisation of Masonry Units

One important aspect of fracture mechanics that influences all four tests is the size effect of the specimens. This is the phenomenon in the fracture of concrete materials where the nominal strength of the concrete is decreased as the size of geometrically similar test specimens increases (Barr et al., 1998). While the phenomenon is generally accepted, there is not always consensus in literature on whether the fracture energy is a material property and the size effect is just experimental error or if the fracture energy cannot be identified as a material property (Zhao et al., 2008).

Wedge splitting tests have also been used to investigate the fracture mechanics of masonry materials as well as the mortar to brick interface (Schneemayer et al., 2014). These tests are necessary to determine the mechanical characterisations for the material description in order to numerically model masonry.

3.4.1 Wedge Splitting Test Method

The wedge splitting test method is selected to determine the specific fracture energy of the masonry materials in this study. There are currently no standards available for the use of this test method, rather the guideline laid out by Brühwiler and Wittmann (1990) is followed.

The wedge splitting test set-up, as described by Brühwiler and Wittmann (1990), is shown in Figure 3.6. A specimen is first prepared by sawing or casting a groove and a notch, where the specimen can be either cubical or cylindrical. The specimen is then placed on a linear support. Two loading devices which have rollers attached to them are then placed on the specimen. A steel profile that has two identical wedges attached to it is then lowered in between the rollers. This steel profile is attached to the testing machine and used to apply the load.

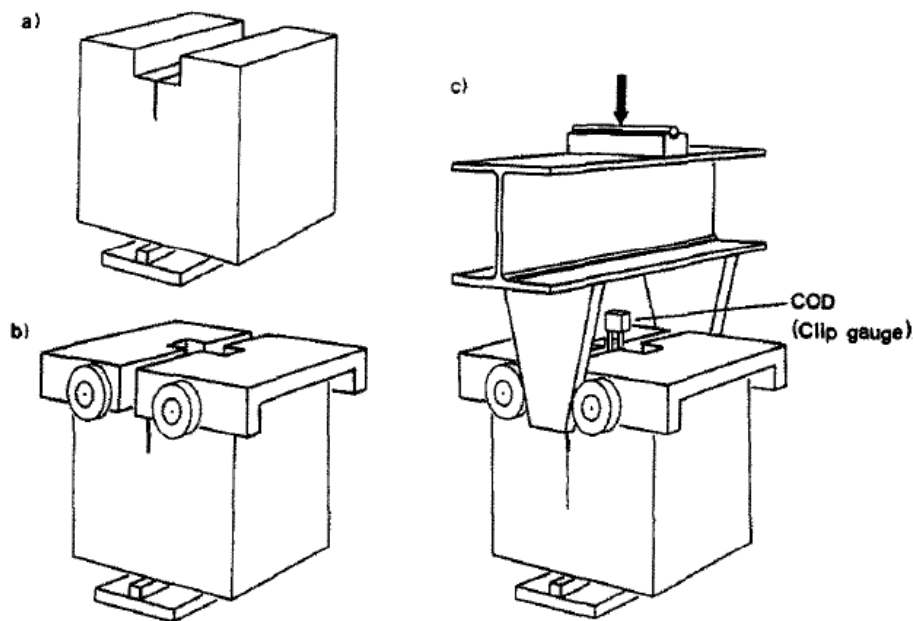


Figure 3.6: Principle of the Wedge Splitting Test (Brühwiler and Wittmann, 1990)

The reason for the notch and groove in the specimen is to ensure that a crack propagates in the

Chapter 3. Mechanical Characterisation of Masonry Units

vertical direction, thereby splitting the specimen in two. Due to the rollers and wedges on the set-up the vertical force (F_v) applied by the testing machine causes a horizontal splitting force (F_s). This force is calculated by taking the wedge angle (α) into consideration as shown in the following equation:

$$F_s = F_v / (2 \tan(\alpha)) \quad (3.5)$$

where the applied load (F_v) and the crack opening displacement (COD), are the values measured during the test. Brühwiler and Wittmann (1990) recommend using a clip gauge or transducer to measure the COD, however other researchers have also successfully used linear variable differential transducers (LVDT) (Trunk et al., 1999; Schneemayer et al., 2014; Zhao et al., 2008). The most effective way to achieve a stable wedge splitting test is with the use of a closed-loop servo-hydraulic testing machine, where the test is controlled through the COD. A stable fracture is accomplished if the test does not cause a sudden load reduction in the load-deformation curve.

With the wedge splitting method the aim of the test is to determine the amount of energy needed to split the specimen vertically in two. This energy is calculated by the area under the F_s -COD curve. Figure 3.7 shows a typical force versus COD curve. The area under the curve used to determine the fracture energy is only taken after $F_{s,max}$, i.e. the part of the curve defined as ‘fracture’.

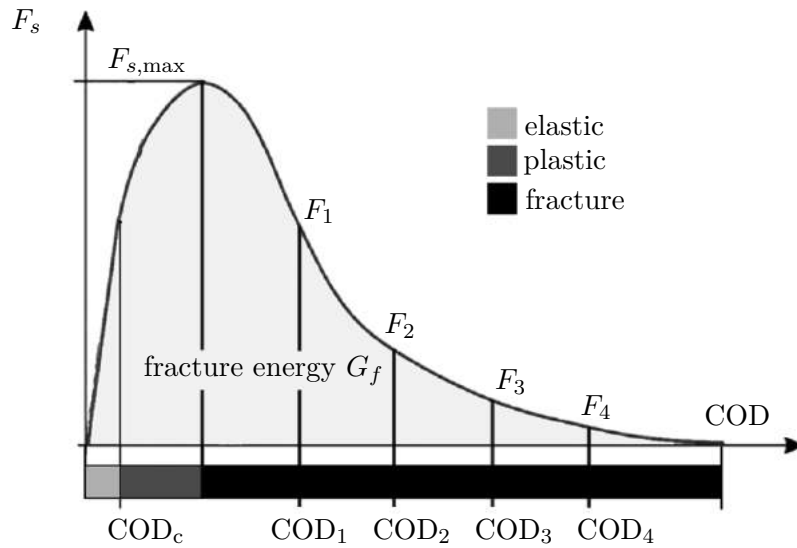


Figure 3.7: Typical Horizontal Force versus Crack Opening Displacement (adapted from Schneemayer et al. (2014))

To determine the specific fracture energy, the area under the curve is divided by the fracture area. The fracture area is the ligament length (h) multiplied with the specimen width (d) (Brühwiler and Wittmann, 1990). The resulting notch tensile strength (σ_h) can be determined by dividing F_s with the fracture area. Figure 3.8 shows a front and side view representation of the wedge splitting set-up with the forces and dimensions necessary for the calculations indicated on the drawings.

Chapter 3. Mechanical Characterisation of Masonry Units

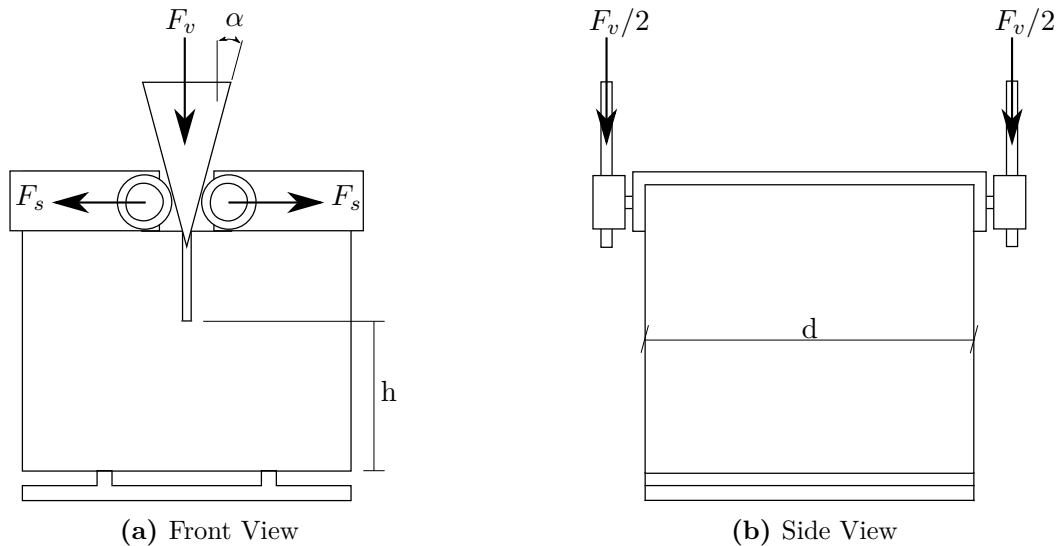


Figure 3.8: Front and Side View of Wedge Splitting Set-up with Indicated Forces

Brühwiler and Wittmann (1990) used a single linear support in the centre of the specimen, however, Trunk et al. (1999) recommends that the specimen instead be placed on two line supports. The advantage of this method is that the supports are directly under the mass concentration points of each halve of the specimen. This prevents a multiaxial stress distribution at the end of the crack path. It also prevents the crack path from moving through damaged material at the linear support, which would influence the measured specific fracture energy (Trunk et al., 1999). Figure 3.9 shows a comparison of the single support (a) and the double support (b). This study implemented the double support in the test set-ups due to its advantages.

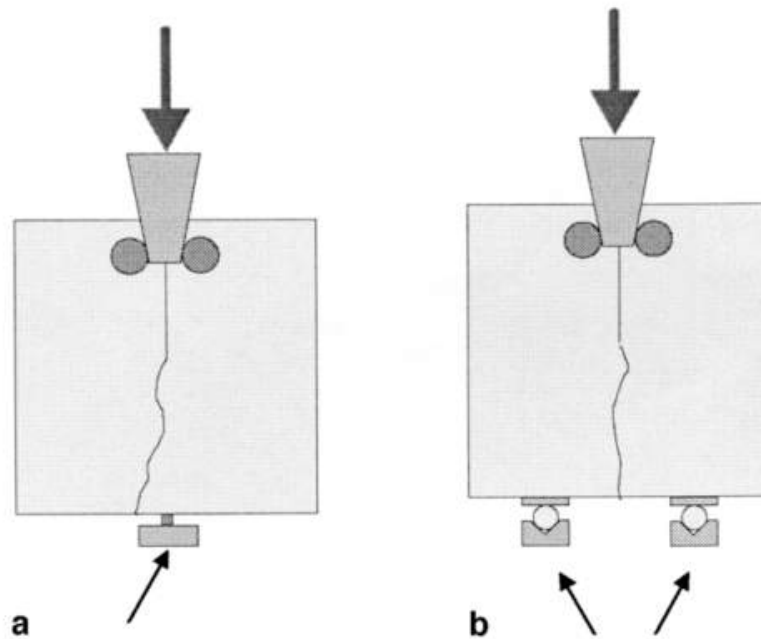


Figure 3.9: Single vs Double Wedge Splitting Support (Trunk et al., 1999)

3.5 Density

While density is not a mechanical characteristic of masonry, it is still included here with the other mechanical properties as it is also used for numerical modelling and can be used as a quality control for the mechanical characterisation tests.

The density of masonry units is influenced by the materials and manufacturing process. Density affects not only the weight of the walls (which influences the structural design) but also affects compressive strength and thermal properties of the blocks. Generally, the higher the density of a block the stronger the block is. The disadvantage of higher density is an increase in transportation costs over long distances and a decrease in the thermal resistance. However, if the blocks are produced near the construction site then this is not an issue. Monitoring the density of blocks during production is also an easy method of quality control.

Concrete masonry blocks generally have lower density than conventional cast concrete. This is due to the dryness of concrete masonry mixes, which leaves voids in the material even with the compaction involved in the manufacturing process. However, this lower density still behaves in a similar method to conventional concrete, namely as it ages the density increases due to the hydration process of the concrete, creating a more compact and denser material structure.

The various types of concrete masonry are generally classified by their density. These include dense concrete blocks (1700 to 2200 kg/m³), lightweight concrete blocks (600 to 1600 kg/m³), and aerated concrete blocks (400 to 950 kg/m³) (Deboucha and Hashim, 2011).

Similar to concrete blocks, the density of AACBs also increases with age due to the geopolymerisation reaction. As this reaction completes the material structure becomes compact and denser, thereby providing higher density (Abdullah et al., 2015). The density of AACBs in literature varies between 1800 to 2300 kg/m³, thereby placing it in a similar category to dense concrete blocks. The high density is probably due to the fact that alkali-activated concrete mixes are not very dry and are generally close to self compacting levels of workability (Abdullah et al., 2015; Barnard, 2014).

The density of CSEBs and adobe blocks are affected by similar factors. The dry density of both are related to the constituent materials characteristics, the moisture content during compaction of the units and the compaction effort applied (Riza and Rahman, 2015; Walker, 2004). The erosion of both earthen materials also decreases with an increase in the blocks density.

The density of CSEBs generally falls within 1700 to 2200 kg/m³ which is the same as that found for dense concrete (Deboucha and Hashim, 2011). It is important to remember that CSEBs are sometimes tested in their wet condition and that the wet density of CSEBs will differ from the dry density. Therefore, the dry density should be related to dry compressive strength tests and wet density to the wet tests. Adobe density values are reported at 1570 to 2000 kg/m³ (Brown and Clifton, 1978). The density of the adobe blocks has been shown to increase with increasing sand.

3.5.1 Density Testing Specifications

The European standard BS EN 772-13 (2000) gives the specifications for determining the net and gross dry density of masonry units. For this test the units are first dried to a constant mass (m_{dry}) in a ventilated oven at a temperature of $70 \pm 5^\circ\text{C}$. The constant mass of the units is reached when the loss in mass between two subsequent weighing sessions within a 24 h interval is less than 0.2% of the total mass.

A minimum of six units are to be tested in this manner. The volume (V_n) of the units is then determined by measuring the length \times width \times height of the unit, and subtracting the volume of any recesses or indentations. The dry density (ρ) can then be determined with the following equation:

$$\rho = \frac{m_{dry}}{V_n} \times 10^6 \quad (3.6)$$

3.6 Masonry Shear Strength

The bond between masonry units and mortar is often the weakest point of masonry walls. The non-linear response at this interface is an important aspect of masonry behaviour and is often the location of the shear failure phenomena (also known as mode II failure) (Lourenço, 1998). Shear failure may occur at the interface if the masonry wall is subjected to an in-plane loading, such as the case of an earthquake.

Shear behaviour of masonry joints is strongly influenced by the relation between normal (σ_D) and shear stress (τ_a). When the shear failure of a masonry specimen at the interface is characterised by slipping of the units along the joint, then a higher normal compressive force parallel to the bed joint causes an increase in the shear strength (De Vasconcelos, 2005). This case generally occurs with a moderate normal stress being applied to the masonry. Under this condition the non-linear behaviour of the mortar is negligible. Instead the friction resistance of the material plays a large role and the linear relationship represented by Coulombs friction law can be used to characterise the shear failure (De Almeida, 2012). This equation is given below:

$$\tau_a = \tau_o + \mu\sigma_D \quad (3.7)$$

where τ_o is the cohesion of the material (the shear strength at zero vertical load stress) and μ is the friction coefficient. It must be noted that this equation only describes local failure and cannot be applied for shear failure of masonry walls due to in-plane horizontal loads (De Vasconcelos, 2005). When a high normal stress is applied to the masonry then Coulombs failure mechanism no longer holds and instead a new failure mechanism occurs due to crushing and shearing of the material. A cap model can be adopted to represent this combined interface and unit failure (Lourenço et al., 2004).

Chapter 3. Mechanical Characterisation of Masonry Units

Another important aspect of the shear behaviour of masonry joints is the dilatancy angle (ψ). This value is categorised as the difference between the normal displacement (Δu) of the unit as a result of the shear displacement (Δv), see Figure 3.10. Positive values of ψ indicate an opening of the joint whereas negative values indicate a compaction of the joint (De Vasconcelos, 2005).

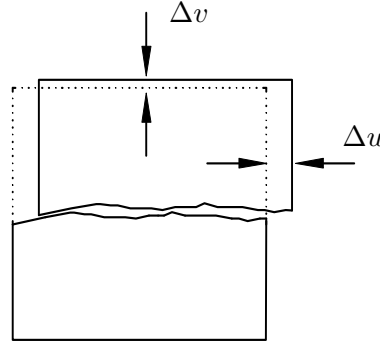


Figure 3.10: Dilatancy Behaviour of Masonry (De Vasconcelos, 2005)

Multiple testing set-ups exist for the characterisation of the interface shear behaviour. Figure 3.11 shows the three most common test set-ups used in literature, the couplet test (or Hoffmann/Stöckl test), the van der Pluijm test, and the triplet test. However, none of the test set-ups achieves an absolutely uniform distribution of normal and shear stresses (Lourenço et al., 2004). This is due to the fact that the equilibrium constraints introduce non-uniform normal stresses in the interface (Lourenço, 1998).

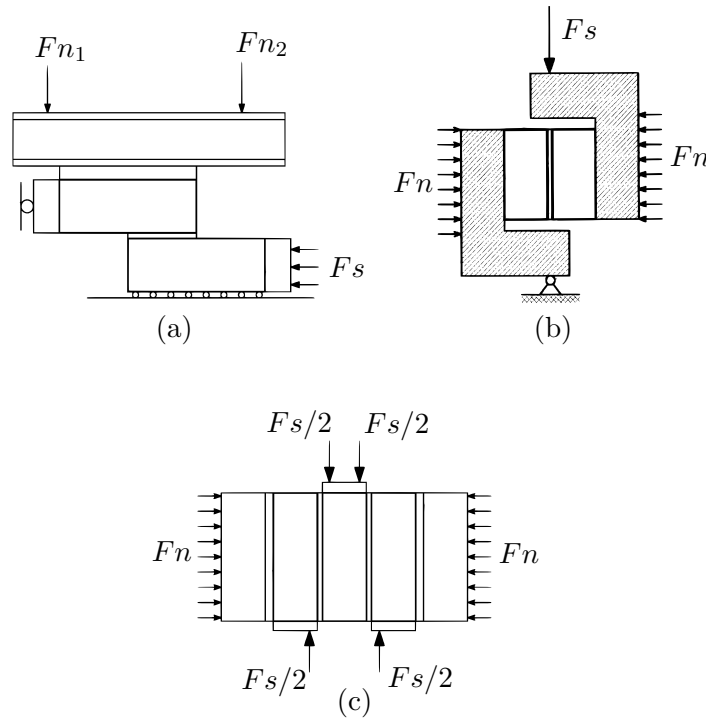


Figure 3.11: Different types of shear tests: (a) couplet test (b) van der Pluijm test and (c) triplet test (Lourenço et al., 2004)

Chapter 3. Mechanical Characterisation of Masonry Units

The couplet test leads to the most uniform normal and shear stress distribution when compared to the other tests (it does, however, still introduce a moment, so the stress distribution on the failure plane is non-uniform). While the couplet test has a more uniform stress distribution than the other tests, the testing set-up is much more complex and is therefore generally not considered suitable for use as a standard test method. Numerical analysis of the van der Pluijm test has shown a very uniform shear stress distribution but an uneven normal stress distribution. For the triplet test set-up, if the bending is minimised then a relatively uniform shear stress can be attained. This is accomplished by reducing the eccentricity of the reactions near the unit-mortar interface (De Vasconcelos, 2005). The European standard BS EN 1052-3 (2002) ensures this happens with a recommended loading arrangement.

3.6.1 Triplet Test Specifications

For this study the experimental analysis of the shear behaviour of masonry is conducted through the use of the triplet test set-up as laid out in BS EN 1052-3 (2002). The test specified by the standard determines the initial shear strength of masonry through the use of small masonry specimens tested to destruction. Two procedures are given; Procedure A tests the specimens at different pre-compressions, and the initial shear strength is then defined by a linear regression curve to zero pre-stress. Procedure B involves testing the specimen at zero pre-compression and determining the characteristic initial shear strength using a statistical analysis. However, with Procedure B the friction angle cannot be determined, therefore Procedure A is implemented for this study.

The masonry specimens tested in the triplet test set-up consists of three masonry blocks mortared on top of each other along the bed joint. The mortar joint thickness must be 8 to 15 mm and the finished sample must have been checked for linear alignment using a set square or spirit level. Immediately after building the specimens, a pre-compression vertical stress of between $2.0 \times 10^{-3} \text{ N/mm}^2$ and $5.0 \times 10^{-3} \text{ N/mm}^2$ must be applied to the units. The specimens are then tested at 28 day strength and the mortar strength is determined at the same age.

The specimens are then be placed in the test apparatus as shown in Figure 3.12. To support the ends, steel plates of at least 12 mm thick must be used, supported by roller bearings with a diameter of 12 mm and a length equal to the width of the unit. A pre-compression stress is also applied to the unit as shown if Figure 3.13.

For Procedure A, at least three specimens are tested at each of the three pre-compression loads. Units with compressive strengths over 10 N/mm^2 , use pre-compression loads of 0.2 N/mm^2 , 0.6 N/mm^2 and 1.0 N/mm^2 . Units with compressive strengths less than 10 N/mm^2 , use pre-compression loads of 0.1 N/mm^2 , 0.3 N/mm^2 and 0.5 N/mm^2 . The pre-compression load must be kept within $\pm 2\%$ of the initial value. For Procedure B six specimens are tested at zero pre-compression.

The following important measurements and observations from the test must be recorded. The age of the masonry units, the cross sectional area of the specimens parallel to the shear force,

Chapter 3. Mechanical Characterisation of Masonry Units

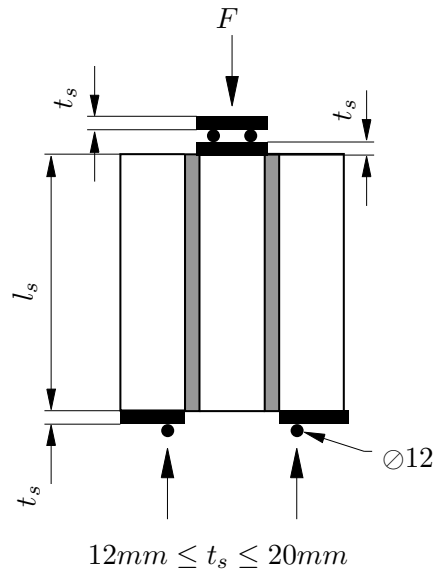
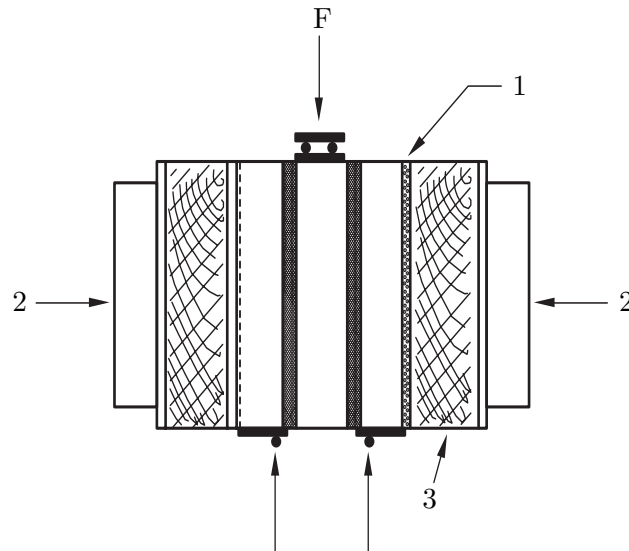


Figure 3.12: Triplet Test Loading (adapted from BS EN 1052-3 (2002))



Key

- 1 Softboard/gypsum plaster
- 2 Precompression
- 3 Loading beam

Figure 3.13: Triplet Test Pre-Compression (adapted from BS EN 1052-3 (2002))

Chapter 3. Mechanical Characterisation of Masonry Units

the maximum load applied, the pre-compression load, and the type of failure. The applicable failure types are shown in Figure 3.14. Shear failure in the unit-mortar joint (failure Types A1/1 and A1/2 in Figure 3.14) or shear failure only in the mortar (failure Type A2 in Figure 3.14) are acceptable. If failure occurs by shear failure in the unit parallel to the joint (failure Type A3) or by crushing or splitting of the unit (failure Type A4), then further tests must be conducted until failure according to Type A1 or A2 occurs. If failure Type A1 or A2 are not achieved then the results may be used as a lower bound to the shear strength for each pre-compression level.

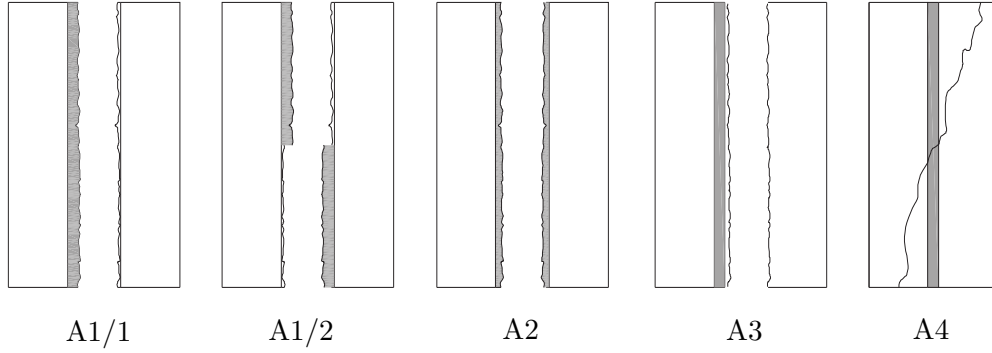


Figure 3.14: Triplet Test Failure Modes (adapted from Alecci et al. (2013))

The shear strength and pre-compression stress are calculated according to the following equations:

$$f_v = F_{max}/2A_i \quad (3.8)$$

$$f_p = F_p/A_i \quad (3.9)$$

where:

f_v shear strength of an individual sample [N/mm^2]

f_p pre-compressive stress of an individual sample [N/mm^2]

F_{max} maximum shear force [N]

F_p pre-compressive force [N]

A_i cross sectional area of a specimen parallel to the bed joints [mm^2]

Using Coulombs friction law the initial shear strength and the angle of internal friction can be determined. This is accomplished by plotting a graph of the individual shear strength against the normal compressive stress and then plotting a line using linear regression of the points. Figure 3.15 shows an example of such a graph with the important points.

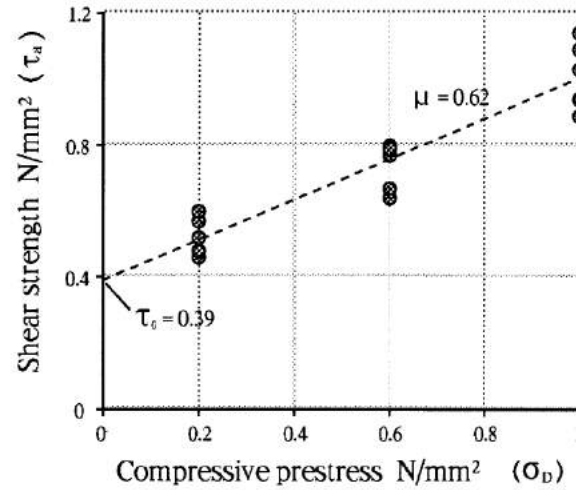


Figure 3.15: Typical Plot from Triplet Test (RILEM, 1996)

3.7 Masonry Compressive Strength

The compressive strength of masonry normal to the bed joints is one of the most important characteristic used by engineers in design. Before numerical methods it was also one of the only relevant structural material properties. As masonry consists of both units and mortar, the failure mechanism thereof is governed by the interaction between the two materials as well as their elastic properties (Lourenço et al., 2004). The main aspects that influence the compressive strength is the strength of the units, the type of mortar used, workmanship and curing (PCA, 1993).

The compressive strength of the unit is the greatest contributing factor to the strength of the masonry. While the mortar strength also influences the strength of the masonry, its effect is vastly lower, with certain studies showing a masonry wall strength increase of only 10 % for a 130 % mortar strength increase. This is largely due to the dimensional difference between the thickness of the mortar joint and the masonry unit in the walls (PCA, 1993).

While the above properties influence the strength of the masonry walls, it is generally accepted that the precursor of failure is the difference in elastic properties between the mortar and the units (Lourenço et al., 2004). For conventional masonry the units generally have a higher strength and therefore a higher stiffness than the mortar. However, with alternative masonry units, such as adobe or compressed earth blocks, this is not always the case.

For cases where the units have a higher stiffness than the mortar, the mortar joint has a tendency to expand laterally more than the units. This results in the mortar being confined by the more stiff unit due to the shear stress at the interface. Thus, the uniaxial compression of the masonry leads to a state of triaxial compression in the mortar and a combination of compression and biaxial tension in the units (See Figure 3.16b). Conversely, when the mortar is stiffer than the unit, a stress state of triaxial compression occurs in the units with axial compression and lateral tension in the mortar (See Figure 3.16c) (Feng et al., 2012).

Chapter 3. Mechanical Characterisation of Masonry Units

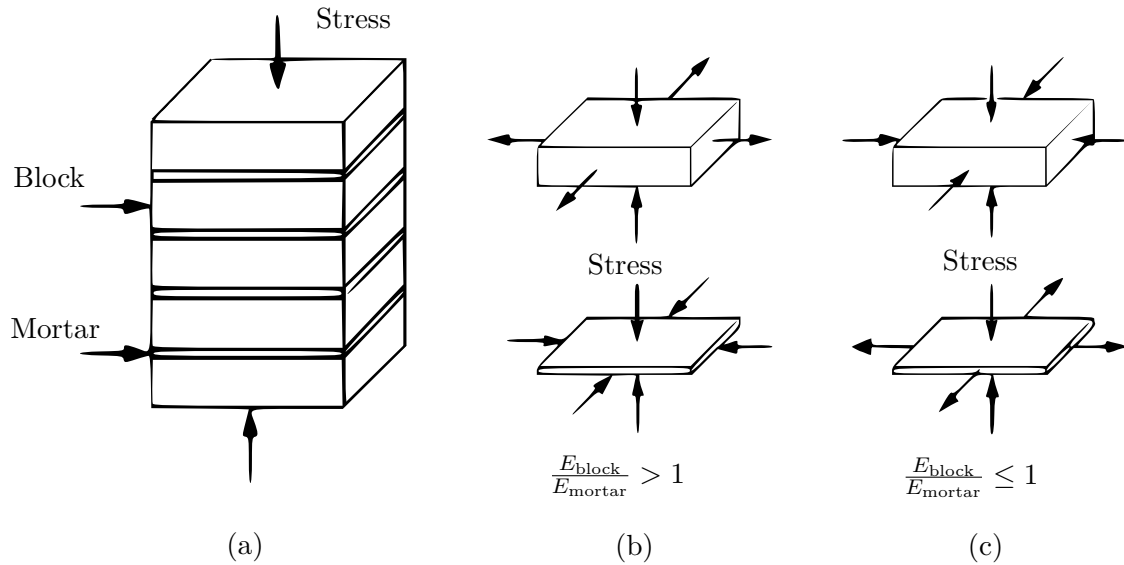


Figure 3.16: (a) Masonry in Compression (b) Stress State for Stiffer Block and Softer Mortar, (c) Stress State for Softer Block and Stiffer Mortar (Feng et al., 2012)

Two of the most common methods used to determine the compressive strength of masonry through experimental testing is the masonry wallets and the stack bonded prisms. Testing of masonry wallets gives the best indication of the real uniaxial compressive strength of masonry normal to the bed joints. However, these experimental set-ups are relatively large and costly to construct and test. The larger surface area of the wallets may also increase the difficulty of obtaining failure for high strength masonry if suitable testing equipment is not available. The prism are smaller and easier to construct, and are therefore often used in literature. Although the wallets give more representative results, the prism tests still show the simultaneous effect of bedding type, unit-mortar interaction and workmanship (De Vasconcelos, 2005).

Figure 3.17 shows a representation of a prism and wallet specimen. Figure 3.17a is representative of the solid unit prism specimens tested by ASTM C1314-11A (2011) for the compressive strength of masonry. Figure 3.17b is representative of the wallet specimens tested by BS EN 1052-1 (1999) for the compressive strength of masonry.

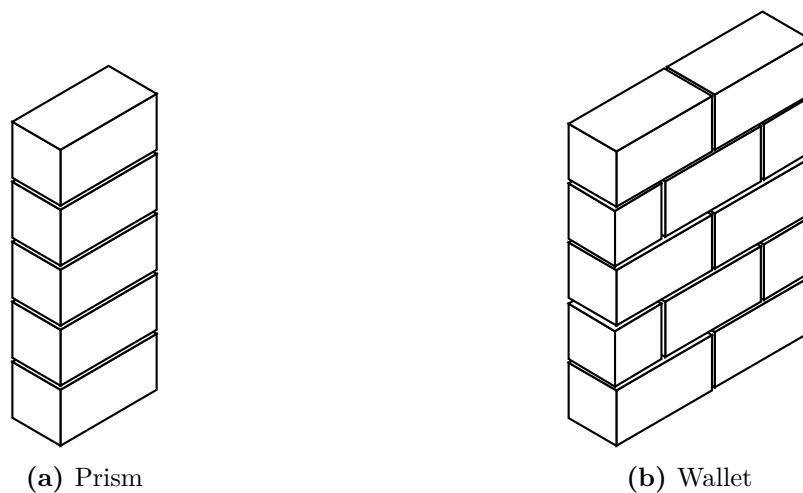


Figure 3.17: Representations of Common Prism and Wallet Specimens

3.7.1 Compressive Strength of Masonry Specifications

Masonry wallets are used in this study due to their better representation of the uniaxial compressive strength. Both BS EN 1052-1 (1999) and SANS 10164-1 (1980) specifies methods for determining the compressive strength of masonry wallets perpendicular to their bed joints, while ASTM C1314-11A (2011) provides guideline for testing masonry prisms. Once again the European standard BS EN 1052-1 (1999) is employed by this study.

Three specimens are created, having dimensions specified by the standard that are dependant on the unit size. The specimens are built on a flat horizontal surface and it must be ensured that the load distribution faces of the specimens are flat and parallel to each other. Steps must be taken to ensure that the test specimens receive appropriate curing in the first three days. Samples of the mortar shall be taken from the mason's board and tested at the same age as the wallet tests (such as at 28 days).

Once the wallets have reached the appropriate age they are placed centrally in the testing machine in such a manner that the top and bottom of the specimen are in full contact with the testing machine. The loading is steadily increased so that failure is reached after 15 to 30 min from the commencement of loading. If the modulus of elasticity is required then the masonry specimens must be fitted with measuring devices that can measure the change in height of the specimen. Figure 3.18 shows the masonry wallet as well as the location at which the measuring devices must be attached.

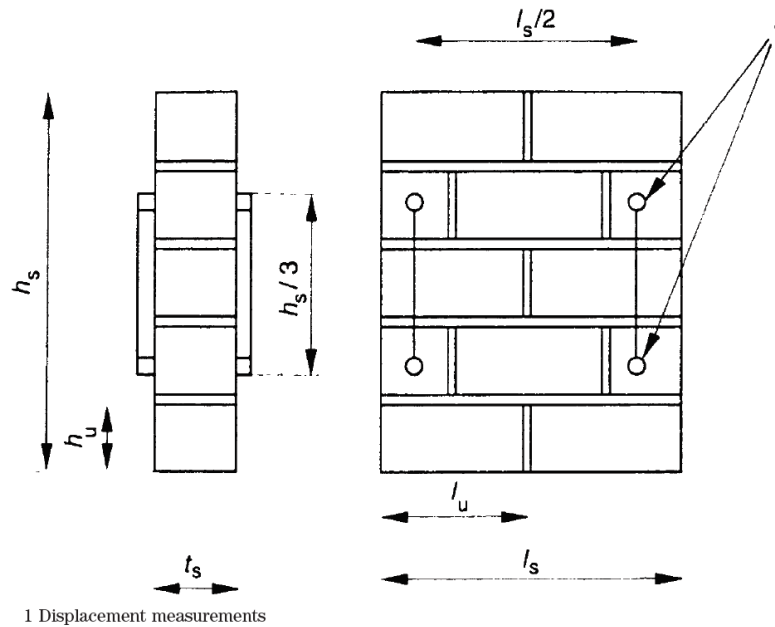


Figure 3.18: Masonry Wallet Specimen (BS EN 1052-1, 1999)

The measurements that should be recorded include: the dimensions of the loaded cross section, the maximum load achieved, the load at which cracks appear, and the length of time from the start of loading until the maximum load. The compressive strength of each masonry specimen can then be calculated using the following formula:

Chapter 3. Mechanical Characterisation of Masonry Units

$$f_i = \frac{F_{i,max}}{A_i} \quad (3.10)$$

where:

f_i compressive strength of masonry specimen [N/mm^2]

$F_{i,max}$ maximum load [N]

A_i cross sectional area of a specimen parallel to the bed joints [mm^2]

The modulus of elasticity is calculated as the secant modulus from the mean of the four measuring positions occurring at one-third of the maximum stress achieved. This is given by the following formula:

$$E_i = \frac{F_{i,max}}{3 \times \varepsilon_i \times A_i} \quad (3.11)$$

where:

E_i modulus of Elasticity [N/mm^2]

ε_i mean of strains at four measuring positions

From these results the mean compressive strength and modulus of elasticity can be calculated for the masonry wallets.

3.8 Conclusion

This chapter discussed the mechanical properties of masonry units that are investigated in this study. Both international standards and previous research are considered. The compressive strength, modulus of elasticity, Poisson's ratio, fracture energy and density of individual masonry units are investigated as well as the compressive strength and modulus of elasticity of masonry wallets. The shear strength between the masonry units and mortar is also studied through the use of triplet tests. The next chapter discusses the materials used in this study as well as the mix designs and the processes employed to create the various masonry units.

Chapter 4

Materials and AMU Creation

This study focuses on the mechanical properties of various masonry units created from a wide range of materials. The masonry types that are investigated include three alternative masonry units (AMUs) as well as a concrete masonry unit (CMU) to be used as a benchmark. The AMUs that are investigated are alkali-activated concrete blocks (AACB), compressed stabilised earth blocks (CSEB), and adobe blocks. Due to the wide range of materials and methods used in the creation of these masonry units, an entire chapter is dedicated to covering the materials, mix design, mixing procedure and curing of the masonry units.

This chapter is organised as follows. First the material characteristics are discussed for all the aggregates and binders used in the study. Next, the specifics of the four types of masonry units are discussed, with the mix design, mixing procedure and curing of each being covered separately. Finally, the mortar used for masonry compressive strength and triplet tests are covered.

4.1 Materials

The materials chosen for the creation of the masonry units were taken from local sources wherever possible to better approximate AMUs that could be created locally. To minimise costs and increase efficiency, aggregates and binders were reused for different masonry material types where applicable. In order to reduce the variables in this study, the aggregate type and origin were kept constant for all the mixes investigated. This section gives an overview of the aggregates, binders, alkaline solution and water used in the study.

4.1.1 Aggregate

Three types of sand were used for the creation of the masonry units. Two of the finer sands, known locally as Philippi and Malmesbury sand, were formed by the natural disintegration of rock. The coarser sand used was a crusher dust that was formed by the mechanical crushing of Malmesbury shale that is locally known as Greywacke stone. A clay soil obtained from the quarry of a local brick manufacturer was used for the CSEB and adobe units. The gradings

of the three sand types and the clay soil were accomplished with dry sieving and are given in Figure 4.1, with the gradings conducted according to SANS 201 (2008).

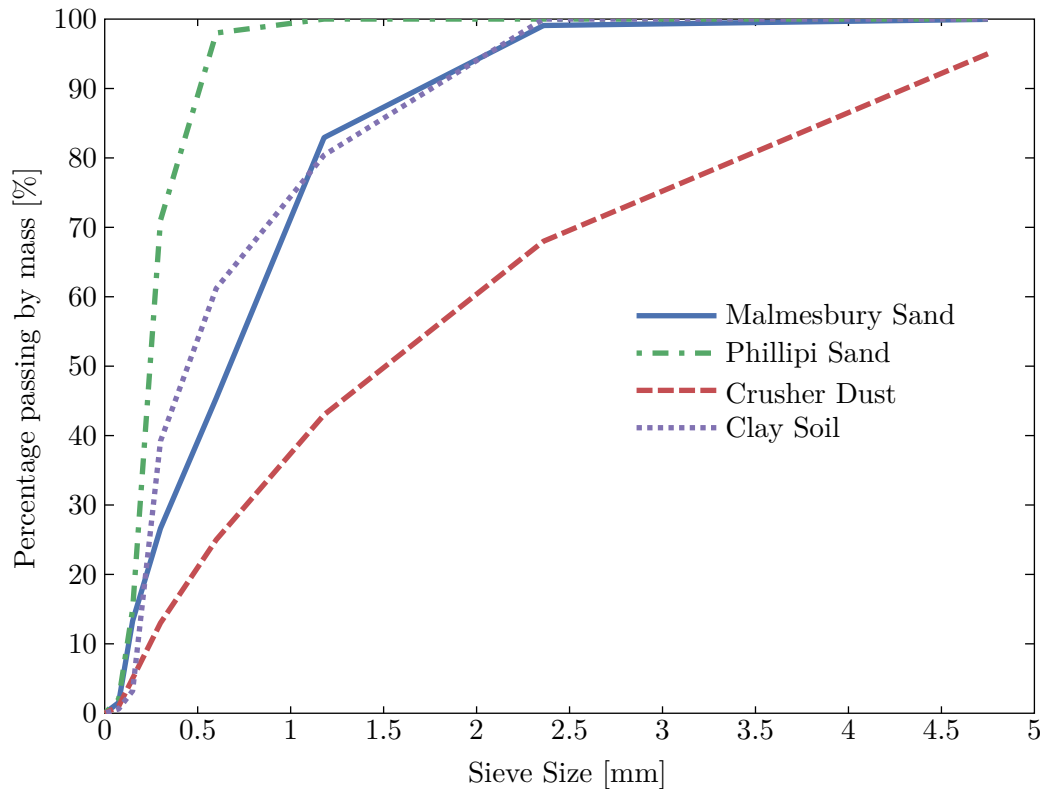


Figure 4.1: Grading of Materials

From Figure 4.1 it can be seen that the Phillipi sand is very fine, with the Malmesbury sand being slightly coarser but still having almost all the material passing the 2.36 mm sieve. Both sands have a poor grading. The crusher dust showed a much better grading, with grain sizes up to 4.75 mm. Due to the poor grading of the fine sands it was often necessary to blend the sands to obtain an appropriate grading.

Table 4.1 gives the fineness modulus (FM), relative density (RD) and particle shapes of the aggregates used, including a 13 mm Greywacke stone. The relative density was determined according to SANS 5844 (2006).

Table 4.1: Aggregate Characteristics

Material	FM	RD	Particle Shape
Malmesbury Sand	2.33	2.62	Round
Phillipi Sand	1.17	2.59	Round
Crusher Dust	3.51	2.71	Angular
13 mm Greywacke stone	-	2.69	Angular

4.1.2 Binders

The binders used in this study consist of two types of Portland cement (CEM II 42.5 N and CEM II 52.5 N), as well as fly ash and ground granulated corex slag (GGCS). No liquid admixtures were used.

Due to the fact that the geopolymerisation process of the AACBs relies mainly on the amount of silica and aluminium available in the mix, it was important to ensure that all the fly ash was from the same power station and the slag from the same steel factory. This reduced the variables that affected the strength of the alkali-activated concrete (AAC). For the same reason the ordinary Portland Cement (OPC) used for the CMUs and CSEBs were also sourced from the same batch acquired from the suppliers.

The fly ash is categorised as ASTM type F fly ash due to its low calcium content. The chemical composition of the fly ash is given in Table 4.2. The GGCS was obtained from the iron production process at Saldanha Steel, Western Cape. The chemical composition of the GGCS is also given in Table 4.2. The negative L.O.I. value in Table 4.2 is suspected to be an anomaly, however it is not key for this research.

Table 4.2: Chemical Composition of Fly Ash (FA) and Ground Granulated Corex Slag (GGCS)

Content	SiO ₂	Al ₂ O ₃	CaO	Fe ₂ O ₃	MgO	K ₂ O	MnO	Cr ₂ O ₃	Na ₂ O	P ₂ O ₅	TiO ₂	L.O.I.
GGCS	33.27	13.90	35.57	1.19	12.07	0.68	0.04	0.00	0.19	0.01	0.48	-1.48
FA	56.00	29.55	4.61	3.58	1.16	0.89	0.03	0.03	0.21	0.48	1.56	0.36

4.1.3 Alkaline Solution

Sodium hydroxide and sodium silicate were used as the the alkaline solution for the AACB mixes in this study.

The sodium hydroxide was obtained from Sigma-Aldrich, Western Cape. It was obtained in pellet form and had to be dissolved in potable tap water. When the pellets were dissolved in water an exothermic reaction would occur and the solution would be left for an hour to cool down prior to mixing. The concentration of the solution required, expressed in Molar, determined the mass of sodium hydroxide pellets per litre of solution.

The sodium silicate used in this study was obtained from Kimix Chemicals, Western Cape. The density of the solution was 1396 kg/m³.

4.1.4 Water

Water is an important ingredient in the creation of concrete mixes as it facilitates the hydration process that gives concrete its strength. It also provide the necessary workability for all the

mixes. The amount of water used depends on the material constituents and the desired state of the final product. For this study ordinary municipal tap water was used which can be classified as potable.

4.2 Concrete Masonry Unit (CMU)

The focus of this study is to investigate the mechanical properties of alternative masonry for low income housing. However, it was decided that a benchmark was required against which to compare the results from the alternative materials. In light of this, a masonry unit was chosen that is regularly used throughout South Africa, namely the conventional concrete masonry unit.

In order to properly compare the CMU to the AMUs all the investigated masonry units needed to have the same dimensions. This prevented any difference in the data due to a shape factor and allowed for ease in assembling the experimental tests. All the tests conducted on the AMUs were first conducted on the CMU. The purpose for this was twofold. First, it allowed a test run of the experimental set-ups to ensure they functioned correctly with the masonry units dimensions and shape. Second, the final results of the CMUs and AMUs could be compared to see the viability of the test set-ups for use on the AMUs, whose unique material properties meant that not all the test procedures would necessarily work.

4.2.1 Mix Design

The mix design used for the CMU was chosen to closely resemble that used in practice. However, due to the method of creation and the size of the units, certain adjustments needed to be made. The mix design procedure that was implemented was adapted from a design method given by Jablonski (1996) that uses the FM to proportion the mix.

According to Jablonski (1996) the FM method is the most used method for designing mixes for concrete masonry. A proper mix design is required to create a unit with improved physical properties such as compressive strength, unit weight, and absorption. A brief overview of this mix design procedure is shown below with the final mix design proportions shown in Table 4.3.

Step 1

The FM of all the aggregates used in the mixtures must first be determined. This was done according to SANS 201 (2008) and can be seen in Table 4.1.

Step 2

Aggregates must be blended together to obtain the desired FM for the total mix. The FM for the mix can be chosen according to what is desired of the final product. Recommended values from industry are: 3.70 for normal weight CMUs, 3.67 for medium weight CMUs, and 3.84 for lightweight CMUs. The final mix must not have an excess of coarse or fine particles, as fine

particles will require more cement to cover the larger surface area and coarse particles will create large voids and a harsh final product.

It can be seen that the recommended FM values require a relatively coarse mixture of aggregates, whereas most of the aggregates that were available for this study were very fine. A mix was therefore designed with a large proportion of crusher dust in an attempt to raise the blended FM.

Step 3

Determine the batch weight of each separate aggregate. This is done by multiplying the total design batch weight with the percentage of the different aggregate types in the mix. The total design batch weight is generally dictated by the mixer size, which was 50 L for this study.

Step 4

If the aggregate is wet then the moisture content must be determined as design weights are for dry aggregate. For this study all aggregate was thoroughly dried before use and this was therefore not necessary.

Step 5

The cement content must be calculated next. For this mix method the cement to aggregate ratio is used rather than the cement to water ratio that is used for ordinary concrete. Jablonski (1996) recommends a range of cement to aggregate ratios for various types of aggregate. For a sand and gravel aggregate he recommends a ratio of 1:8 to 1:12. A ratio of 1:10 was therefore chosen for this study.

Due to the method of forming the CMUs (discussed in Section 4.2.2), the cohesiveness of the mix needed to be increased. To accomplish this fly ash was added to the mix. This was done due to the fact that a material with high fineness increases the cohesiveness of a mix. It was decided to replace 25 % of cement with fly ash.

Step 6

The final step of the mix design is to choose the water content. The required water content is controlled by the aggregate type used, the cement content, type and operation of the block press, and the desired final appearance of the masonry units. Jablonski (1996) recommends that the water content be determined through trial batches. For the CMUs created in this study a large factor in the water content was the ability of the CMUs to retain their shape after demoulding.

Generally, as much water as possible should be added without causing the unit to slump when extracted from the mould or causing other production problems. Mixes that are too dry are difficult to compact properly and therefore produce units of high porosity, low green strength and low compressive strength. Mixes that are too wet tend to stick to the sides of the moulds and are difficult to extrude, as well as causing the units to slump when removed from the mould. Final adjustments of the water content are therefore done by eye and trial batches (Owens, 2009).

Water content for the concrete masonry units is normally between 6 and 9 % of the mass of the green units (Owens, 2009). The optimum water content for this study was found to be 9.1 %.

Table 4.3: CMU Mix Proportions

Constituents	kg/m ³
Malmesbury Sand	607
Crusher Dust	1316
CEM II 42.5	144
Fly Ash	48
Water	212
Total	2328

4.2.2 Mixing and Manufacturing Procedure

CMUs created in practice are formed with compaction in order to allow for immediate demoulding. One common method of compacting the blocks in practice is through the use of an egg laying block machine, where material is fed into the block machine which then compresses the mixture into moulds and ejects the masonry units onto a flat pallet or concrete slab. The advantage of this method is that once ejected onto the pallet the units can be left to cure without moving and with no demoulding being necessary at a later date.

For this study an egg laying block machine was not available and therefore a manual earth block press was used. Previous studies at Stellenbosch University had used this block press for investigations into compressed soil blocks (Malherbe, 2016). The block press was manufactured by Hydraform in South Africa and is shown in Figure 4.2. The process employed by the block press is similar to that seen in Figure 2.4. The manufacturer states that a compaction pressure of approximately 2.90 MPa is applied by the press. The masonry units created by the block press have a length of 290 mm, a width of 140 mm and a height of 116 mm. As these dimensions could not be altered they became the controlling factor for the dimensions of all subsequent masonry unit types, irrespective of the manufacturing procedure. The aspect ratio of all blocks was therefore equal to 0.83.

The materials for the CMU were mixed in a 50 L pan mixer. The dry aggregates and binders were added to the mixer and mixed for approximately 2 minutes. Once a homogeneous mix was achieved the water was added and mixed for approximately 3 minutes. This allowed an even distribution of water among the dry constituents.

The final wet mixture was then weight batched for use in the block press. Enough material was weighed off from the mixer for one block and transported to the block press. Through trial and



Figure 4.2: Manual Earth Block Press

error the optimal mass for ease of compaction and appearance of the final unit was found to be 10.5 kg per block.

The material was placed in the block press in consecutive layers and smoothed on the surface before the lid was placed on top of the mixture and slightly pre-compressed by hand. The lever arm was then used to apply the actual pressure to the unit. Once compacted, the block could be extracted and moved to the curing area.

Difficulty was encountered with this method of compaction for the CMUs as the block press was designed to be used for compressed earth blocks. These blocks are discussed in detail in Section 4.4, but suffice to say that the clay involved in the CSEB manufacturing process resulted in a material that easily held its shape and could therefore be transported from the block press with ease. The CMU did not have any clay in its mix design and therefore the fineness and water content of the mix needed to be adjusted in an attempt to increase its cohesion. Through trial and error a workable mixture was created that could be transported from the block press with great care. It would be beneficial in future studies to create a method of block production that allowed the units to be extracted onto a flat surface and left there until they cured for a day, similar to an egg laying block machine.

In order to test the modulus of elasticity of the CMU according to BS EN 12390-13 (2013), a cylinder of the material needed to be created. Various methods of accomplishing this were attempted. One such attempt was the ‘cookie cutter’ technique, where a cylinder was cut from the freshly pressed block itself. With this method the block was placed on its headface before cutting, as this allowed a cylinder of sufficient height to be extracted. Figure 4.3 shows the frame used for the ‘cookie cutter’ technique. However, this meant that the cylinders would be orientated in such a manner that the force was applied at a 90° angle to the direction of compaction. In effect this meant that the modulus of elasticity results would have to be compared to the headface compression tests rather than the bedface compression tests. It was also not guaranteed that the extraction process did not in some manner damage the units.



Figure 4.3: 'Cookie Cutter' Extrusion Frame (Gous, 2015)

For these reasons another method of creating cylinders was adopted, where the cylinders were compressed in a metal pipe of the correct diameter using a hydraulic press. Rather than attempting to compact the cylinder with the same compaction pressure as the block press, a density method was used instead. This was accomplished by determining the required mass and dimensions of the cylinder in order to achieve the same density as the masonry units from the block press. The required material was then placed in the metal pipe before being compressed until the unit had the correct height and thereby achieved the same density as the blocks.

4.2.3 Curing

The CMUs were cured in curing tanks filled with water kept at a constant temperature of 25 °C. The masonry units then remained in these curing tanks until the day of testing or until they were used to construct wallets and triplets. Figure 4.4 shows one the CMUs after it has been cured for over 28 days.



Figure 4.4: CMU Block

From the figure it can be seen that the exterior of the unit is very rough (similar to those from Maxi-Brick shown in Figure 2.2), however a section of the interior showed that the units do have proper compaction with little to no air voids. A close look at the figure also shows that the bottom of the block has a greater degree of compaction than the top. This was due to the method of compression that the block press applied. Compaction was applied from the bottom of the unit and friction reduced the compaction effort towards the top of the unit.

4.3 Alkali-Activated Concrete Block (AACB)

The first alternative material that was investigated is AAC. There is a significant difference in the mix design of AAC versus conventional OPC concrete. For conventional OPC concrete the strength of the matrix is mainly dependent on the water to binder ratio. Therefore, to design an OPC concrete the water and cement content is calculated, followed by the aggregate content. Conversely, AAC mix designs have more material constituents, making them more complex to design. The factors affecting the strength of the AAC matrix are also more complex as it does not rely only on the water to binder ratio.

The AAC mixes in this study were specifically designed to allow them to set in ambient temperatures through the addition of slag into the mix. Therefore, the final AAC matrix consisted of aggregate (sand and stone), binder (fly ash and slag), and alkaline solution (sodium hydroxide and sodium silicate).

4.3.1 Mix Design

The focus of this study is not on designing various mixes but rather on testing the characteristics of the masonry and masonry units. For this reason significant amounts of time were not dedicated to designing AAC mixes. Rather, a mix was simply modified from a study on AAC conducted at Stellenbosch University by Barnard (2014). This mix design fit the requirements of this study, namely an AAC that could be cured at ambient temperatures and a masonry unit that could be created from local cost-effective materials.

Due to the complex nature of alkali-activated binders, a straight forward mix design procedure does not exist in the same manner as for conventional concrete. Therefore, Barnard (2014) used mixes from literature as a guideline for his mix design. An initial volume assumption of 1 m^3 was made for the mix and the materials were each allocated a percentage of this volume. The constituents of the mixes used by Barnard (2014) are as follows. The aggregates made up 59 to 65 % of the volume, while the remaining mass consisted of binder material, alkaline liquid and water. The fly ash took up 60 to 80 % of the binder material, with the rest consisting of slag. The ratio of sodium silicate to sodium hydroxide was from 0.5 to 2. These mixes gave a large range of mechanical properties for the AAC and allowed it to set at ambient temperature.

It was decided that the strength of the AACBs tested in this study would be reduced to approximately the strength of the CMUs. However, the AAC tested by Barnard (2014) resulted in

strengths much higher than those required. Therefore, the reference mix designed by Barnard was altered in order to achieve a lower strength concrete.

The difficulty in reducing the strength of an AAC material matrix is due to the many factors that influence the strength of AAC. Table 4.4 shows some of the factors that Barnard (2014) found to influence the strength. These factors were adjusted in an attempt to achieve a mix that gave a compressive strength of approximately 20 MPa. Table 4.4 shows what these factors need to be to achieve this strength and what the final value of these factors were for the AAC mix used in this study.

Table 4.4: Factors that lower AAC strength

Factor that influence the strength of AAC	Desired values	Final mix Values
Sodium silicate to sodium hydroxide ratio	0.6 or 2.5	1.8
Fine aggregate to total aggregate ratio	0.50	0.40
Alkaline to binder ratio	0.55	0.22
Binder to sand ratio	0.85-1.10	1.14
Slag content	20 %	23.10 %
Aggregate content	60 %	62 %
Sodium hydroxide solution	3 - 6 M	4 M
Percentage alkaline liquid replaced by water	25 %	30 %

Table 4.5 gives the reference mix used by Barnard (2014) as well as the final AAC mix design used in this study. For the fine aggregate Philippi sand was used, and the coarse aggregate was 13 mm Greywacke stone.

Table 4.5: AAC Mix Proportions from Barnard (2014) and Mix Proportions Used in this Study

Constituents	Barnard (2014) mix design (kg/m ³)	Used mix design (kg/m ³)
Philippi Sand	520	570
13 mm Stone	858	858
Fly Ash	394	150
Slag	259	500
Sodium Silicate	108	90
Sodium Hydroxide	92	50
Water	90	102
Total	2321	2320

4.3.2 Mixing and Manufacturing Procedure

The mixing of the AAC was conducted in 50 L pan mixers. All the dry materials were first mixed in the pan mixer for 2 minutes. The alkaline solution and water was then added separately and mixed for a further 2 minutes. It was found that the AAC mix used in this study set extremely quickly and therefore once a homogeneous mix was attained the material was immediately cast into moulds.

Wooden moulds were created with the same dimensions as that of the block presses internal chamber, namely a length of 290 mm, a width of 140 mm and a height of 116 mm. These moulds could be disassembled to remove the AACBs after curing. Figure 4.5 shows the wooden moulds used for the AACBs. For the cylinders created for the modulus of elasticity tests conventional cylindrical moulds, available in the laboratory, were used.



Figure 4.5: Wooden Mould for AACBs

Due to the caustic nature of the sodium hydroxide in the mix, careful handling was necessary to avoid skin contact with the mixture. Safety gear was therefore worn when working with the mixture. The safety concerns of the AAC mix will cause complications when used in practice and it is recommended that more research be conducted on how to avoid this.

4.3.3 Curing

Curing of AAC is dependent on the binder material in the mix. When fly ash is the only binder in the mix then heat curing is generally necessary. This study specifically looked at an AAC that could be cured at ambient temperatures and therefore slag was introduced into the mix.

Once the AACBs were cast they were left to cure in their moulds for one day. After one day the units were demoulded and the samples were further cured in a temperature and humidity controlled room. The room was kept at a temperature of $24 \pm 2^\circ\text{C}$ and $65 \pm 5\%$ relative humidity. The masonry units remained in the curing room until the day of testing or until they were used to construct wallets and triplets.

Figure 4.6 shows one of the AACBs after curing for over 28 days.



Figure 4.6: Alkali-Activated Concrete Block (AACB)

4.4 Compressed Stabilised Earth Block (CSEB)

The second alternative masonry material that was investigated is CSEBs. The mix design procedure for the CSEBs was once again adopted from a previous study at Stellenbosch University. This study was conducted by Malherbe (2016) on The Characterisation of Compressed Earth Blocks Stabilised with Cement and Agro-Industrial Residue. The mix design was able to produce a block that gave a good representation of those used for construction in the housing developments of South Africa.

4.4.1 Mix Design

The mix design that was chosen from Malherbe's study was a CSEB with a binder content of 10 %. The mix design consisted of two soils, a sandy soil and a clay sandy soil, combined with various binders. However, for this study the only binder that was included was a CEM II 52.5N. Similar soils as those used by Malherbe were also used to ensure that the mix design required as little adjustment as possible. The fine Philippi sand used showed similar characteristics as the sandy soil used by Malherbe (2016). For the clay sandy soil, soil was taken from the same local quarry as that used by Malherbe. The total volume of both soils was taken from a single batch to eliminate the variability that using different batches would cause.

The clay soil that was acquired from the local quarry contained large clay clumps. The soil was therefore mechanically crushed in the lab with a heavy roller. The crushed clay was then sieved through a 2.36 mm sieve aperture to ensure that the clay particles were fine enough for the mix.

As explained in Section 2.8.2, the soils were blended in such a manner that the final percentages of clay, silt, sand and gravel were similar to those recommended in literature. This ensures a material that holds its shape well, can be extracted easily and does not shrink or crack due to excessive clay.

Section 2.8.2 also discusses the method used to obtain the water content of CSEBs. This was accomplished by determining the optimum moisture content (OMC) of the soil through the use of the modified Proctor test. The values from Malherbe's study were used for this investigation and a final moisture content of 10 % was found to produce a workable mix that resulted in a well compacted CSEB.

The final mix design can be seen in Table 4.6.

Table 4.6: CSEB Mix Proportions

Constituents	kg/m ³
Philippi Sand	1198
Clay Soil	798
CEM II 52.5 N	200
Water	231
Total	2427

4.4.2 Mixing and Manufacturing Procedure

The mixing and manufacturing procedure for the CSEBs was very similar to that of the CMUs as the same Hydraform block press method was used. Once again the material was mixed in the 50 L pan mixer. The dry materials were added first and mixed for 2 minutes followed by mixing in the water for an additional 3 minutes.

Due to the low water content and clay in the mixture, clumps were formed from the rotation of the pan mixer. These were then broken up by hand to ensure an even distribution in the block press. As with the CMUs the material was weight batched for the block press. 9.4 kg of material was weighed off for each block; this material was then placed in the block press and compacted. The units therefore also had a length of 290 mm, a width of 140 mm and a height of 116 mm. Once compacted the blocks were extracted and moved to the curing area.

For the cylinders created to test the modulus of elasticity of the material, the same density method was implemented as that used for the CMU cylinders (See Section 4.2.2). Due to the clay in the mixture both the blocks and the cylinders held their form much better than the CMUs and therefore extraction and transport of the units was easier.

4.4.3 Curing

Once the units were extracted from the block press they were placed on polythene sheets in the laboratory. These units also had a polythene sheet placed over them to limit evaporation and ensure hydration of the cement particles. The units were sprayed with a fine mist of water

every 24 hours for seven days to ensure proper curing. After seven days the units were moved to the curing room with a temperature of $24 \pm 2^\circ\text{C}$ and $65 \pm 5\%$ relative humidity. The masonry units remained in the curing room until the day of testing or until they were used to construct wallets and triplets. Figure 4.7 shows a CSEB cured for more than 28 days.



Figure 4.7: Compressed Stabilised Earth Block (CSEB)

4.5 Adobe Block

The final material that was investigated is adobe blocks. These blocks were created in an attempt to achieve a material with vastly different material characteristics from the blocks that were stabilised through cement or geopolymerisation. Unlike other block types, adobe does not generally have a mix design, instead a natural soil near the build site is selected and used. Other materials are then added to this soil if it is found that the soil is lacking in some regard.

As soils vary considerably from location to location, the adobe mix designed for this study did not use a specific natural soil. Rather, a soil was created with the necessary characteristics through the blending of materials available from previous masonry materials. Blended soils allow greater control over factors such as grading and minimise the inclusion of organic matter.

4.5.1 Mix Design

The main considerations for choosing a soil are similar to those considered for CSEBs. The clay, silt, sand and gravel percentages of the soil are generally used in literature to determine if a soil is acceptable for adobe creation. Section 2.7.2 discussed some of the percentages that are recommended for adobe and which were used to determine the ratio with which the various materials should be blended together.

Based on the recommended percentages, it was decided that the Philippi sand, Malmesbury sand and clay soil would be combined to form a material mixture to be used for the adobe blocks. Due to the reliance on the clay for strength in the adobe mix, the clay was sieved through a 1.18 mm

sieve aperture to ensure a very fine material. The water content was determined through trial and error until an optimum water content of approximately 13 % was found.

Table 4.7: Adobe Mix Proportions

Constituents	kg/m ³
Philippi Sand	809
Malmesbury Sand	809
Clay Soil	534
Water	275
Total	2428

Once a base water content and material blend was chosen, trial batches were performed to determine the workability of the mix. Numerous trial batches were created due to difficulty in the forming of the adobe blocks (See Section 4.5.2). A final mix that satisfied the requirements of the adobe blocks was achieved through these trial batches and the mix proportions can be seen in Table 4.7.

4.5.2 Mixing and Manufacturing Procedure

In order to produce the required number of adobe blocks quickly and efficiently, the same method was adopted for manufacturing blocks as that used in practice. A wooden mould without a base, similar to those shown in Figure 2.3 but with room for only one block at a time, was constructed and the material mix was placed into the mould and tamped down. The wooden mould was then immediately lifted off the fresh masonry unit, which was then carefully moved to the curing area. It should be noted that, unlike the CMU and CSEB mixes, the adobe mix was not weighed off before each unit was formed, instead enough material was simply placed in the wooden mould to fill it, resulting in the possibility of increased variability in the test results. This was done due to the hand compaction method not working well with a pre-determined amount of material.

Difficulty was encountered with the original mixes due to the quick demoulding of the units. If the material was too dry then the compaction would not remove all the air voids. If the material was too wet then it would slump as the wooden mould was removed. The large amount of clay in the mixture also caused the blocks to stick to the sides of the mould, thereby deforming the blocks as the wooden mould was removed. This effect was reduced by lining the interior of the mould with plastic to decrease the friction as the units were extracted.

Trial batches were therefore conducted in order to arrive at a mix that created a block which held it's shape. The material proportions that were adjusted in these trial batches were the water content, clay content, and fine to coarse aggregate ratio. A workable mix was eventually found that minimised the deformation of the units due to the demoulding. These units were of an acceptable quality for use in practice, however due to the sensitivity of the tests conducted

on the units many needed to be levelled on their top surface to ensure proper contact with the testing equipment.

The cylindrical specimens created for the modulus of elasticity tests were formed in conventional cylindrical moulds. The mixture was placed in the moulds and tamped down in the same manner as the blocks. Once compacted, the material was left in the mould for 2 days before carefully demoulding due to the fact that the slenderness of the cylindrical specimens caused them to deform if demoulded too soon.

4.5.3 Curing

Adobe's curing process consists of simply leaving the units to dry until they are strong enough for construction. Care must be taken to ensure that the units do not get rained on and that they do not dry out too quickly, causing cracks. Unfortunately, the creation of the adobe blocks for this study took place in winter and therefore the rainy season limited the sunlight the blocks could acquire. The lower temperatures also caused the blocks to dry out slower than they would in summer.

Three options for curing were therefore available. The first was to move the units outside into the sun when possible and back into the laboratory when it rained. It was decided that this movement could damage the blocks and the variability of sunny days would result in the different batches of blocks receiving different amounts of sun. This would cause greater variability in the units strength but possibly create stronger units.

The second option was to place the blocks in the curing room which at the time had a slightly higher temperature than the ambient temperature. However, the higher humidity in the curing room decreased the evaporation of water out of the units and therefore delayed the drying time even more.

For this reason it was decided to cure the units in the general laboratory area. There would be less variability in the strength of the units but they would be of a lower strength than if they received direct sunlight. Figure 4.8 shows one of the adobe blocks after curing for 28 days.

4.6 Mortar Design

This study investigated various properties of individual masonry units as well as the properties of masonry; where masonry is an assemblage of masonry units laid in a specified bonding pattern and jointed together with mortar. The masonry characteristics that were tested included the compressive strength and the initial shear strength. To test the compressive strength small wallets were constructed of approximately 0.5 by 0.5 m. For the initial shear strength, triplets were constructed that consisted of three bricks laid on top of each other. Chapter 5 discusses both masonry types in more detail. For both types of masonry tests mortar was used to bind the masonry units together.

**Figure 4.8:** Adobe Block

The mortar that was used in the masonry tests was designed to have a similar compressive strength to that of the masonry units involved in the tests. For this reason four different mortar mixes were designed in an attempt to approximate the different masonry units' strength. The mortar was designed through a simple trial and error process using the water to cement ratio to adjust the strength as necessary.

Table 4.8 shows the mix designs for the mortars. It can be seen that different sands and cement were used for the different mortars. This was simply due to having the material available at the time and the choice of material was not influenced by strength considerations.

Table 4.8: Mortar Mix Proportions

Constituents (kg/m ³)	CMU Mortar	AACB Mortar	CSEB Mortar	Adobe Mortar
Malmesbury Sand	1655	-	-	-
Philippi Sand	-	626	664	865
CEM 52.5 N	-	1148	1033	-
CEM 42.5 N	732	-	-	425
Water	54	95	99	123
Total	2441	1869	1796	1413

4.7 Conclusion

This chapter considered the materials and creation of the masonry units used in this study. First an overview is given of the all the materials used in the creation of the various masonry units.

The mix design, mixing and manufacturing procedure, and the curing of each masonry type is discussed next. The masonry material types covered are: CMUs, AACBs, CSEBs and adobe blocks. Finally, the mortar mix designs used in the construction of the interface tests is covered.

It can be seen that this study does not focus on creating and optimising various mix designs but rather adopted them from other sources where possible. This is due to the fact that this study focused on the actual testing procedure more than the creation of alternative masonry units. It is therefore possible to enhance these mixes and thereby the masonry units in further studies as they are not optimised. For convenience, all the mix proportions for the different masonry unit types are given in Table 4.9. Chapter 5 discusses the set-up and execution of the various tests conducted on the masonry specimens in this study.

Table 4.9: Masonry Units Mix Proportions

Constituents (kg/m ³)	CMU	AACB	CSEB	Adobe
Malmesbury Sand	607	-	-	809
Philippi Sand	-	570	1198	809
Crusher Dust	1316	-	-	-
13 mm Stone	-	858	-	-
Clay Soil	-	-	798	534
CEM II 42.5 N	144	-	-	-
CEM II 52.5 N	-	-	200	-
Fly Ash	48	150	-	-
Slag	-	500	-	-
Sodium Silicate	-	90	-	-
Sodium Hydroxide	-	50	-	-
Water	212	102	231	275
Total	2328	2320	2427	2428

Chapter 5

Experimental Design

To allow for the further development and acceptance of alternative masonry units (AMUs), the characterisation and evaluation of their mechanical properties is necessary. This is achieved through a wide range of experiments on the various masonry unit types as investigated in this study.

Chapters 3 and 4 can be seen as a foundation to the work covered in this chapter. Chapter 3 discussed the basic principles behind the mechanical properties generally tested for in masonry as well as specifications set forth in international standards to determine these properties. Chapter 4 discussed the creation of the different masonry types that are investigated in this study. This chapter follows on these by applying the experimental tests of Chapter 3 on the units discussed in Chapter 4.

The set-up and execution of the compressive strength, modulus of elasticity, Poisson's ratio, wedge splitting, density, triplet and compressive interface tests are all detailed in this chapter. Each test was conducted on the benchmark concrete masonry unit (CMU) first, followed by the alkali-activated concrete block (AACB), compressed stabilised earth block (CSEB) and adobe masonry units.

5.1 Masonry Units Compressive Strength Tests

The compressive strength of individual masonry units was determined according to the procedure set out in BS EN 772-1 (2011). The units were tested in the bedface orientation at 7, 14, 28, 56 and 91 days. Further tests were also conducted on units in the headface orientation at 28 days. To ensure that the average compressive strength was representative of the particular group in consideration, a total of seven specimens were tested at each age and orientation.

The testing machine employed for the tests is a 2 MN Instron Materials Testing Machine. As per BS EN 772-1 (2011) a loading rate was chosen that resulted in failure of the specimen after a minimum of 1 minute. Due to the great difference in masonry material types and therefore a difference in their expected strengths, a slow loading rate of 0.75 mm/min was chosen and kept constant for all the tests. The slow loading rate resulted in the higher strength masonry

units taking up to 10 minutes to reach failure. The test was continued until the applied load decreased to 75 % of the maximum load.

The units were placed between two 20 mm thick steel plates in the centre of the testing set-up. The test set-up for units tested in the bedface orientation can be seen in Figure 5.1 and the headface set-up in Figure 5.2. After each test the steel plates were cleaned to ensure a smooth contact surface on the faces of the specimens.

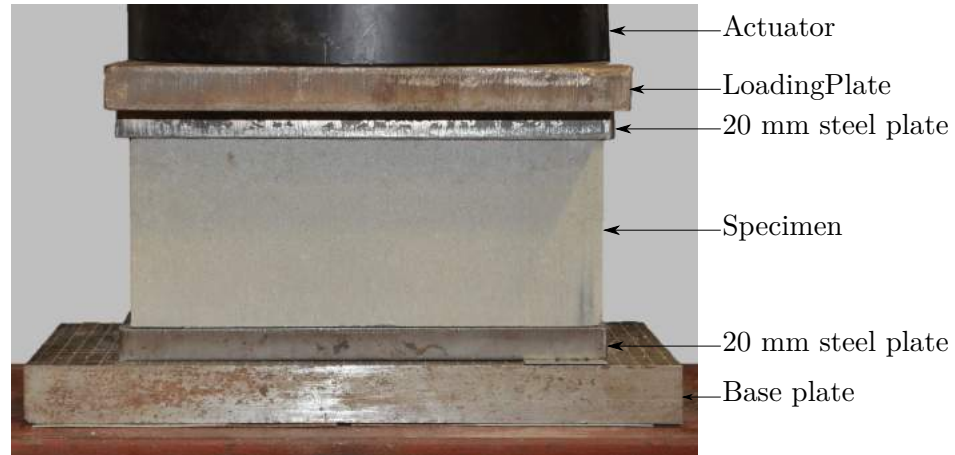


Figure 5.1: Compressive Strength Bedface Test Set-up



Figure 5.2: Compressive Strength Headface Test Set-up

The maximum load from the Instron and the loaded area of each specimen were recorded from the tests. These were used to determine the final compressive strength for each masonry type, orientation and age, as explained in Section 3.1.2.

5.2 Modulus of Elasticity Tests

Modulus of Elasticity tests were conducted according to BS EN 12390-13 (2013) on seven cylindrical specimens at a curing age of 28 days. The CMU and CSEB specimens had a height

of 220 mm and a diameter of 106 mm, while the AACB and adobe specimens had a height of 200 mm and a diameter of 100 mm. All four types of cylinders that were investigated can be seen in Figure 5.3. The difference in dimensions was due to the casting methods employed for the different masonry types as discussed in Chapter 4.



Figure 5.3: Cylinders for Elastic Modulus Tests

A 2 MN Instron Materials Testing Machine was used for testing the specimens. Figure 5.4 shows a cylinder in the test set-up. All specimens had their loading faces ground level to ensure proper contact with the loading plates. The specimens were then placed centrally in the set-up between two pot bearings to account for any deviation in the planeness of the specimens.

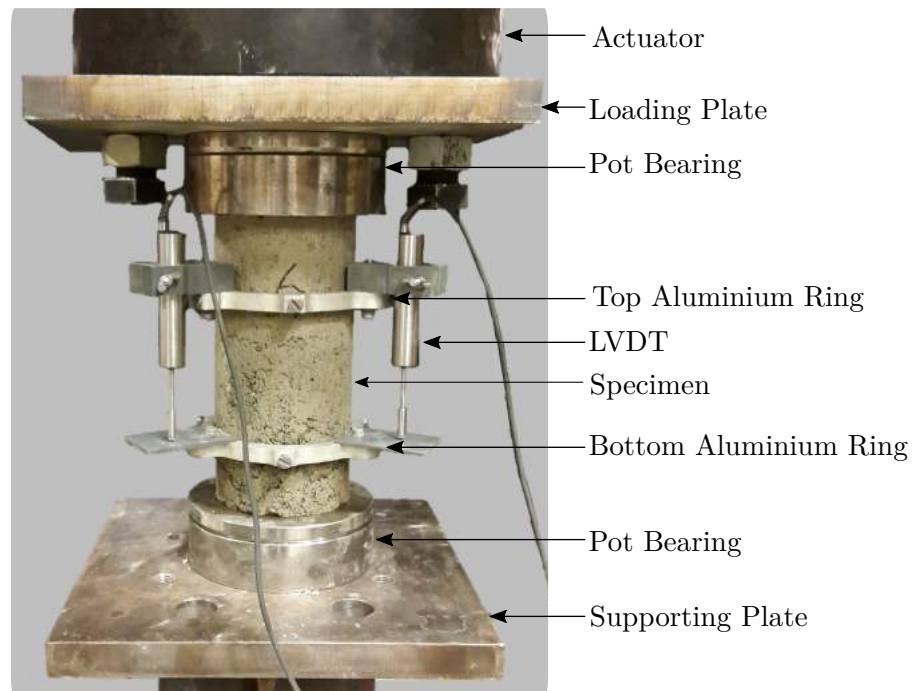


Figure 5.4: Elastic Modulus Tests Set-up

In order to measure the deflections of the specimen as the test progressed, three linear variable

differential transducers (LVDTs) were fitted around the specimen. These were attached to a frame designed for the specimens. The frame consisted of two aluminium rings that were held in place by three blunt screws. These screws tightened onto the surface of the specimens. The frame was positioned in such a way that the measurements occurred over the mid-height of the specimen with a gauge length of 112 mm.

In order to apply the correct loading patterns for the modulus of elasticity test (covered in Section 3.2.1), the masonry material's maximum load must first be known. Therefore, the compressive strength at 28 days on a masonry block was always tested before the modulus of elasticity tests were conducted. Using the blocks maximum load and a shape factor of 0.8, the equivalent cylindrical strength could be determined. The preload and upper load could then be calculated as specified in BS EN 12390-13 (2013). Using the stress and strain data from the tests the stabilised secant modulus of elasticity could be determined as shown in Section 3.2.1. After the tests the compressive strength of the cylinders were determined by testing the specimens to destruction.

All tests were successfully executed according to the specification of BS EN 12390-13 (2013) except for the adobe blocks. Due to the low strength of this material the loading rate of 0.6 ± 0.2 MPa/s was too high and the testing machine could not properly complete a stable loading cycle. Therefore, the loading rate was decreased by a factor of 10, to approximately 0.04 MPa/s and the test could be completed without further issues.

5.3 Poisson's Ratio Tests

Tests for Poisson's ratio were conducted according to the guidelines from ASTM C469/C469M (2010) as discussed in Section 3.3.1. The tests were conducted at the same time and on the same specimens as the modulus of elasticity tests. This allowed both the transverse and longitudinal strain to be measured simultaneously under the same loading procedure.

ASTM C469/C469M (2010) states that either an unbonded extensometer or two bonded strain gauges are to be used for determining the transverse strain, however these were not used in this study. A compressometer-extensometer was not available in the laboratory and was not purchased due to their high costs. Bonded strain gauges were also not used due to concerns about their performance on the AMUs. The extremely brittle and low tensile strength of the CSEBs and the adobe blocks (especially on the surface) could result in the strains on the surface of the specimens not being fully transmitted to the strain gauge.

For this reason an attempt was made to create a set-up that could measure the transverse strains. Two different methods were attempted to measure the strain. The first method involved placing a ring around the specimen at mid-height, which could then follow the circumferential deformation. Figure 5.5 shows a schematic of a similar measuring system proposed by Štemberk and Kohoutková (2005). One drawback of such a system is the friction between the ring and the specimen's surface. Štemberk and Kohoutková (2005) solved this by using a ring made of small cylinders which are connected to a chain.

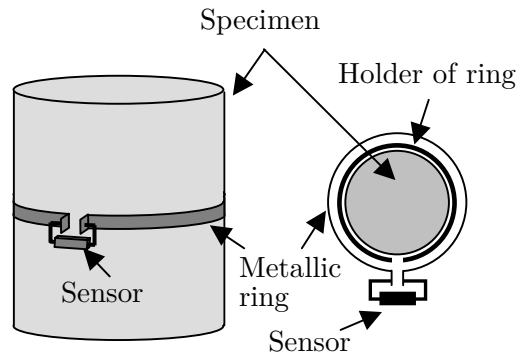


Figure 5.5: Ring method for Poisson Tests from Štemberk and Kohoutková (2005)

The test in this study was set-up with a steel wire instead of a ring made of small cylinders. The measuring device employed was a clip gauge attached to the steel wire. As the stress was applied, the specimen expanded circumferentially and the steel wire measured this expansion. Figure 5.6 shows the set-up for Poisson's ratio on a CMU cylinder. It can be seen that this set-up was applied alongside the modulus of elasticity set-up.

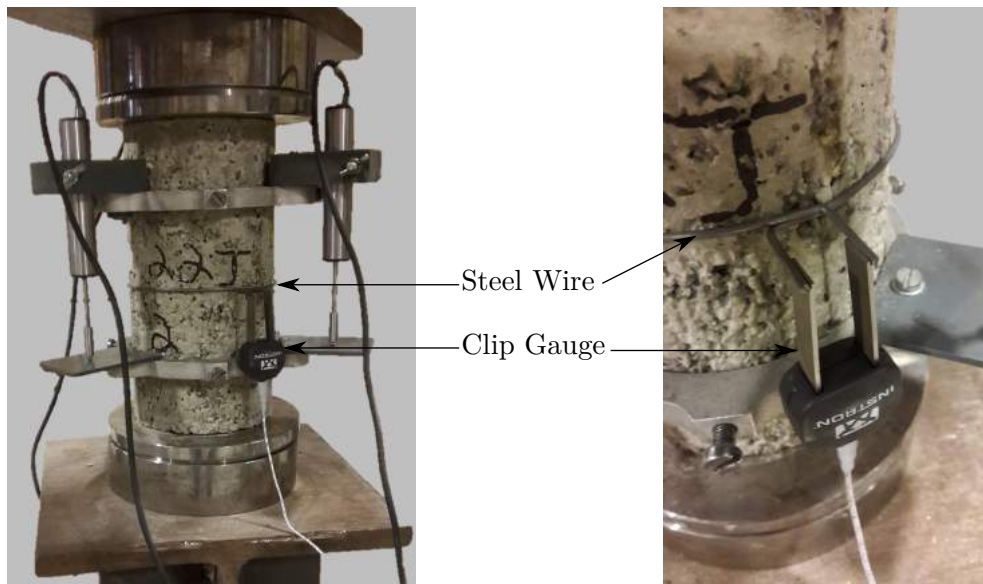


Figure 5.6: Poisson's Ratio with Circumferential Wire Set-up

After the first tests a number of immediate issues were encountered. Firstly, there was the possibility of large variability in the set-up. The wire and clip gauge were not very stable on the units, with small movements causing the clip gauge to fall off and with the wire not hugging the specimen tightly. It was also very difficult to ensure that the wire had proper contact around the entire specimen. Repeatability of the test was therefore a concern.

Due to the concerns with the steel wire test another method was developed to determine Poisson's ratio. Three LVDTs were placed around the specimen to measure the change in radius at mid-height. The LVDTs were spaced at equal intervals around the unit and connected to the base of the set-up with electro magnetic LVDT stands. Six LVDTs were therefore employed for the combined modulus of elasticity and Poisson's ratio tests; three LVDTs to measure longitudinal strain and three to measure transverse strain. This test set-up was easier to assemble and

provided better repeatability than the steel wire test set-up.

Figure 5.7 shows a cylinder in the test set-up surrounded by the LVDTs. The three transverse LVDTs can be seen as well as two of the longitudinal LVDTs. As the tests were conducted at the same time as the modulus of elasticity tests the same loading procedure was applied (see Section 5.2 for the loading procedure).

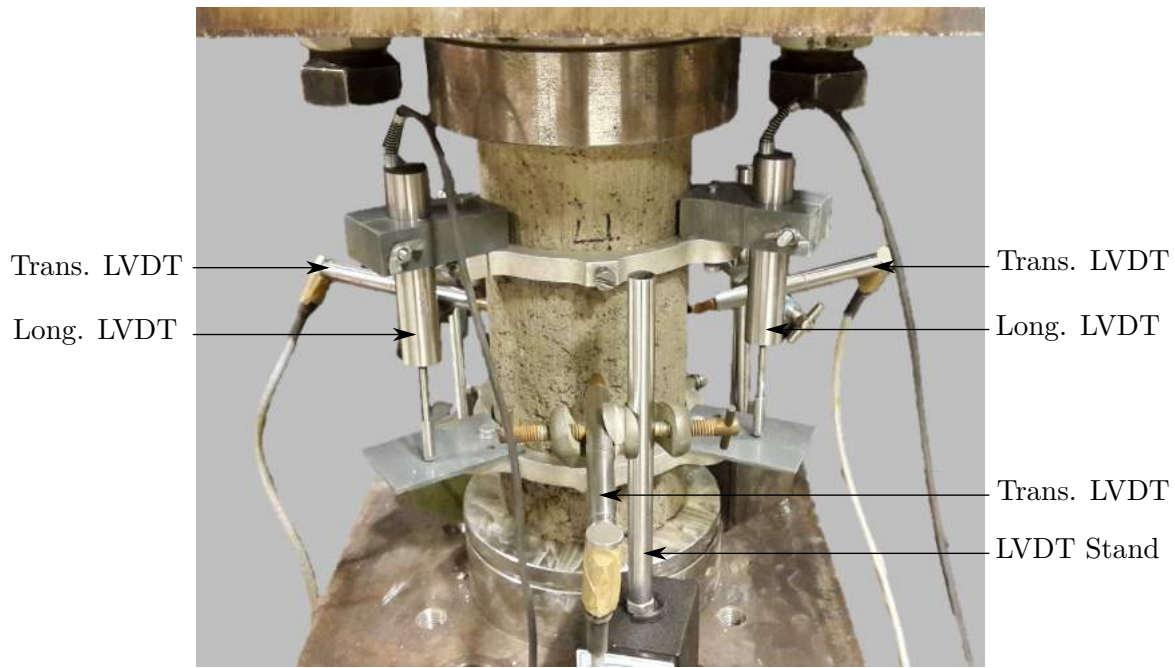


Figure 5.7: Poisson's Ratio Set-up with Longitudinal (Long.) and Transverse (Trans.) LVDTs

5.4 Wedge Splitting Tests

The wedge splitting tests were conducted as laid out by Brühwiler and Wittmann (1990) (covered in detail in Section 3.4.1) to determine the specific fracture energy of the masonry. The tests were conducted on cubical specimens with a notch at the top and a starter groove in the notch, seen in Figure 5.8. Due to the sensitive nature of the tests between 6 and 12 units were tested, all at a curing age of 28 days.

Due to the different masonry materials having different casting processes, the wedge splitting specimens did not all have the same dimensions. The CMU and CSEB specimens were created in the block press with a wooden mould used to form the notch and a 38 mm starter groove. The units formed in this manner had a length of 290 mm, a width of 140 mm and a height 108 mm. These units were then cut into nearly cubical specimens with a length of 100 mm and a width of 140 mm, as seen in Figure 5.8a. The AACB and adobe specimens were cast in $100 \times 100 \times 100$ mm moulds with a wooden plug forming the notch. A 30 mm starter groove was then saw cut into the unit, as seen in Figure 5.8b. Both types of specimens had a notch with dimensions of 20×30 mm. The dimensions were chosen in such a manner that the crack surface area was the same for both specimen types, namely 100 mm by 50 mm.

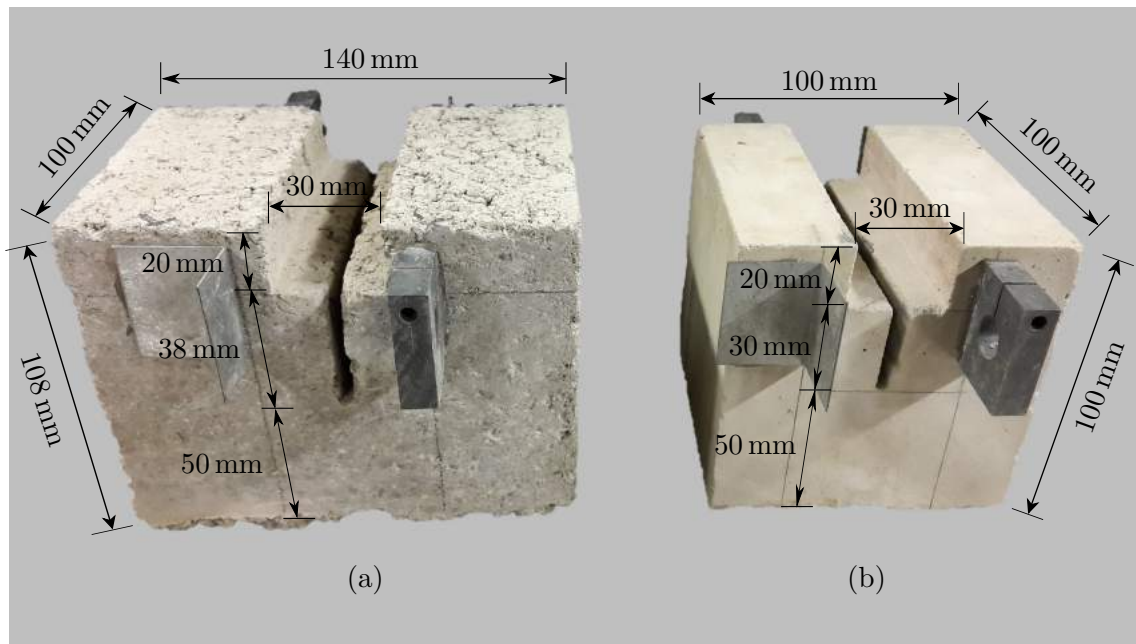


Figure 5.8: Dimensions of Wedge Splitting units

A 50 kN servo-hydraulic actuator fixed to a testing frame was used for testing the specimens. The set-up consisted of the testing machine, steel wedges with a 14° angle, two loading plates with 25 mm diameter roller bearings, a base plate with two line supports and two LVDTs. Figure 5.9 show a close up of a specimen in the test set-up.

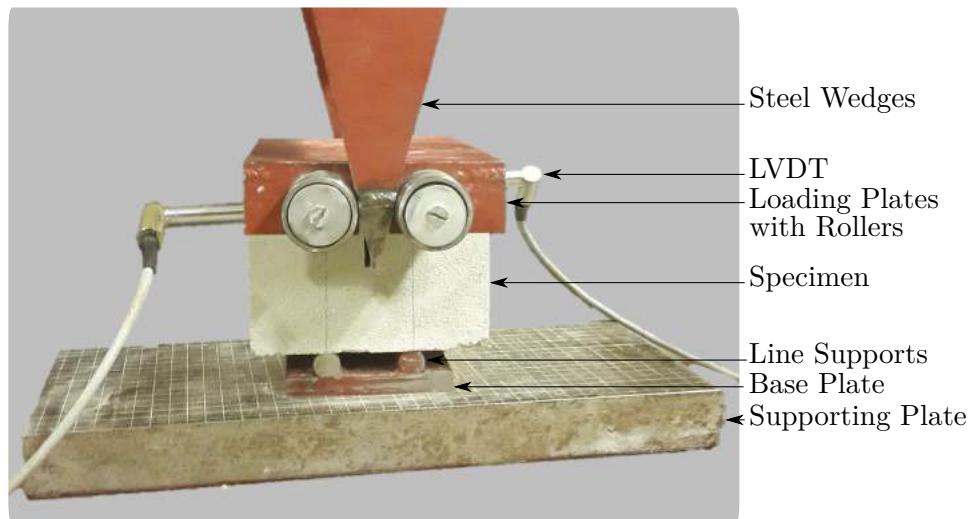


Figure 5.9: Close up of Wedge Splitting Set-up

In preparation of the specimens, two LVDT mounts were glued onto both sides of the specimen with a 50 mm gauge length (the LVDT mounts can be seen on the specimens in Figure 5.8). These LVDTs were used to measure the crack opening displacement (COD) of the specimen as the test progressed.

Once the LVDTs were attached, the specimens were carefully placed on the base loading plate in such a manner that the LVDT mounts lined up with the two line supports. Two line supports

were used as recommended by Trunk et al. (1999) rather than the one support originally used by Brühwiler and Wittmann (1990). The loading plates with the attached rollers were then slotted onto the notch at the top of the specimen. Using the testing machine, the steel wedges could slowly be lowered in-between the rollers. The downward force of the steel wedges was then transferred into a horizontal force with the help of the rollers. Figure 5.10 shows the entire wedge splitting set-up.



Figure 5.10: Total Wedge Splitting Set-up

Once the specimens were in place a preload of 100 N was applied. The preload helped settle the set-up and ensure that the rollers and steel wedges were in proper contact. The preload was successfully employed for the CMU, AACB and CSEB specimens; however, the 100 N load was too high for the adobe specimens and they would split in two before the preload was fully applied. As this load was already at the minimum for the testing machine another method had to be found to begin the tests. Therefore, it was decided to lower the steel wedges onto the specimen by eye. Once contact was made between the steel wedges and the rollers the test was immediately started rather than increasing the load to the preload. This had the side effect of not allowing the set-up to settle properly.

The loading of the specimen was controlled through the displacement caused by the crack opening at the starter notch. This displacement, and therefore the actuator control, was measured and controlled by the two LVDTs. The position of the LVDTs was chosen in such a manner that the COD reading occurred at an early stage, even before the crack started to develop at the starter notch.

The loading rate applied to the specimens varied between the material types. The weaker

materials, such as adobe, needed a very low loading rate or a stable fracture could not be formed. The loading rates were all determined through trial and error and are given in Table 5.1.

Table 5.1: Loading Rates of Wedge Splitting Units

Masonry Material	Loading Rate (mm/s)
CMU	0.035
AACB	0.035
CSEB	0.02
Adobe	0.01

A successful test resulted in a vertical crack forming from the starter notch to the bottom of the specimen. The fracture was considered stable if there was no sudden drop in the load being applied. Using the data recorded during the tests, a splitting force-COD curve could be created for each sample using the methods in Section 3.4.1. From there the specific fracture energy could be calculated.

5.5 Density

Dry density tests were conducted according to BS EN 772-13 (2000). Six units from each masonry material were tested at 28 days. All density tests were conducted on units that were dried to a constant mass in a ventilated oven at a temperature of 70 °C.

The units were placed in the oven for 24 hour intervals. After 24 hours the units were allowed to cool before being weighed. Constant mass was reached when a mass loss of less than 0.2 % of the total mass was achieved between subsequent weighing sessions. The density of the units was then calculated by dividing the constant mass with the units volume.

5.6 Triplet Tests

To analyse the shear behaviour of masonry, triplet tests were conducted according to BS EN 1052-3 (2002) on the various masonry materials investigated in this study. The initial shear strength of the masonry was derived from small masonry samples tested to destruction. Method A of the standard was implemented, whereby different pre-compression levels were applied to the samples. All specimens were tested at 28 days.

The masonry samples were created by mortaring three units together. The lowest unit was placed on a clean level surface, with the next unit placed on top in such a manner that a final mortar joint thickness of 8 to 15 mm was achieved. The units were checked for linear alignment and level using a spirit level. The procedure for the second unit was then repeated for the third unit. Immediately after constructing the specimens a pre-compression load of 3 N/mm² was

applied to the specimens by placing an equivalent weight on top of the specimen. Figure 5.11 shows one of the CSEB triplet specimens. All the triplets were built by the same person to ensure uniformity between the different specimens and materials.



Figure 5.11: CSEB Triplet Specimen

The specimens were constructed after curing the masonry units for three weeks. As the triplet tests were conducted at four weeks, this allowed one week for the mortar to cure to its final strength. A mortar sample was taken during the construction of each triplet batch and its strength was tested at the same age as the final specimens. The mortars were designed to give $\pm 20\%$ of the final masonry unit strength after one week (Section 4.6 discusses the mortar mixes).

The tests were executed with three different pre-compression loads. The code specifies for Method A that units with compressive strengths over 10 N/mm^2 , use pre-compression loads of 0.2 N/mm^2 , 0.6 N/mm^2 and 1.0 N/mm^2 . While units with compressive strengths less than 10 N/mm^2 , use pre-compression loads of 0.1 N/mm^2 , 0.3 N/mm^2 and 0.5 N/mm^2 . However, the pre-compression loads used in this study were adjusted from those used in the code. Due to limits of the testing set-up a pre-compression load over 0.5 N/mm^2 could not be achieved, therefore even though certain units reached strengths greater than 10 N/mm^2 the pre-compression for units less than 10 N/mm^2 was applied to all tests.

Another adjustment made to the test procedure was that instead of applying the first pre-compression load of 0.1 N/mm^2 , no pre-compression load was applied. This was to ensure that even if the test set-up could not properly apply the pre-compression levels needed for Method A, enough data would be available to complete Method B (see Section 3.6.1 for more information on the two methods). The three pre-compression levels that were applied to the specimens were therefore 0 N/mm^2 , 0.3 N/mm^2 and 0.5 N/mm^2 .

Due to the weakness of the adobe specimens, when pre-compression levels equal to or higher than 0.3 N/mm^2 were applied, the units would crush before shear failure occurred. Therefore,

pre-compression levels of 0 N/mm^2 , 0.05 N/mm^2 and 0.1 N/mm^2 were applied to the adobe specimens. This still allowed the friction angle to be plotted from the results.

The test set-up can be split into two types, the first one consisted of a set-up that tested the units with zero pre-compression. This set-up was much simpler to construct and use. The second type of set-up was used to test the units with an applied pre-compression. This set-up expanded the zero pre-compression set-up by adding a method to apply a horizontal force. Both set-ups are discussed next.

The zero pre-compression set-up used a 2 MN Instron Materials Testing Machine to apply a vertical force on the specimens. Figure 5.12 shows the testing configuration. The specimen was carefully placed on two supporting steel plates which were each positioned on top of two steel roller bearings. The supporting plate's dimensions were the same as the head face of the specimens, namely 140 mm by 116 mm. They were positioned so that only the two outer units were touching the plates and not the mortar joint. Another supporting plate was then positioned in the same manner on the top of the middle unit. Two roller bearings were also placed on top of this plate. Next another steel supporting plate was placed on the roller bearings, upon which a pot bearing was set to assist in assuring everything was level. All the steel supporting plates have a thickness of at least 12 mm, and the steel roller bearings a diameter of 12 mm. The testing machine then applied the load onto the specimen at a rate of 0.5 mm/min until shear failure occurred.



Figure 5.12: Triplet Set-up for Zero Pre-Compression

In order to test specimens with pre-compression the set-up was modified to apply a horizontal force as well as the vertical force. This was accomplished with the aid of a hydraulic jack and a 20 kN external load cell. Using a system of channel sections and a steel spring, the

pre-compression could be applied to the specimen. The vertical force was applied in the same manner as that used for the zero pre-compression set-up.

A close up of a specimen in the test set-up is given in Figure 5.13. It can be seen that the zero pre-compression set-up is still used for applying the vertical forces on the specimen. Supporting plates are added on the sides of the specimen in order to apply the pre-compression loads. These plates are not resting on anything but are held between the unit and the channels, thereby reducing any friction and constraints that may result from contact with the base of the set-up. The load cell in the figure was used to measure the pre-compression that was placed on the specimen by the hydraulic jack.

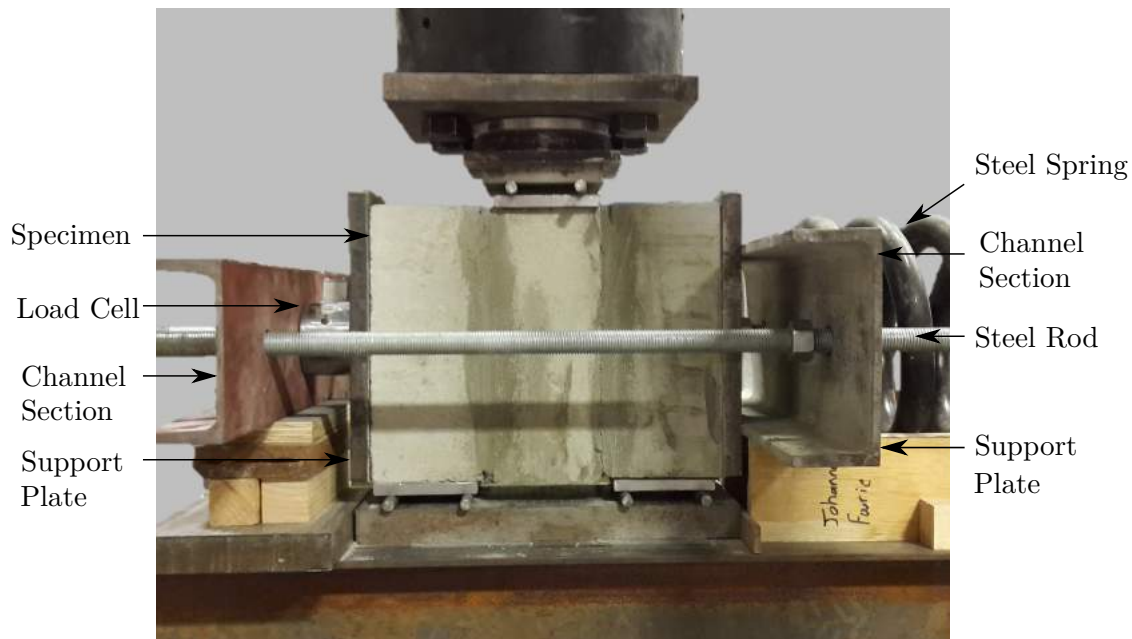


Figure 5.13: Close up of Triplet Set-up for Pre-Compression

Figure 5.14 gives a labelled image of the entire set-up, which functioned as follows. Four steel channel sections were connected with steel rods and held in place with bolts. The back/fourth channel supported the hydraulic jack. The jack pushed against the third channel which compressed the steel spring. The steel spring then pressed on the second channel which laid against a supporting plate. This plate held up the one side of the specimen itself. On the other side of the specimen was another supporting plate, which bordered on the load cell. The load cell was connected to the first channel, holding the entire set-up together.

The code specifies that the applied pre-compression load stay within $\pm 2\%$ of the initial value. However, as the masonry units shear and displace vertically, the dilatancy causes them to displace horizontally as well. This horizontal displacement would cause an increase in the pre-compression load if it was fully constrained. For this reason the steel spring was added to the set-up. It reduced the constraint on the units as they displaced and thereby helped to keep the pre-compression load as close to the initial load as possible. As mentioned earlier in this section, the set-up could not apply pre-compression forces higher than 0.5 N/mm^2 , this was due to the steel spring having a maximum capacity of just over 0.5 N/mm^2 . If higher forces were applied

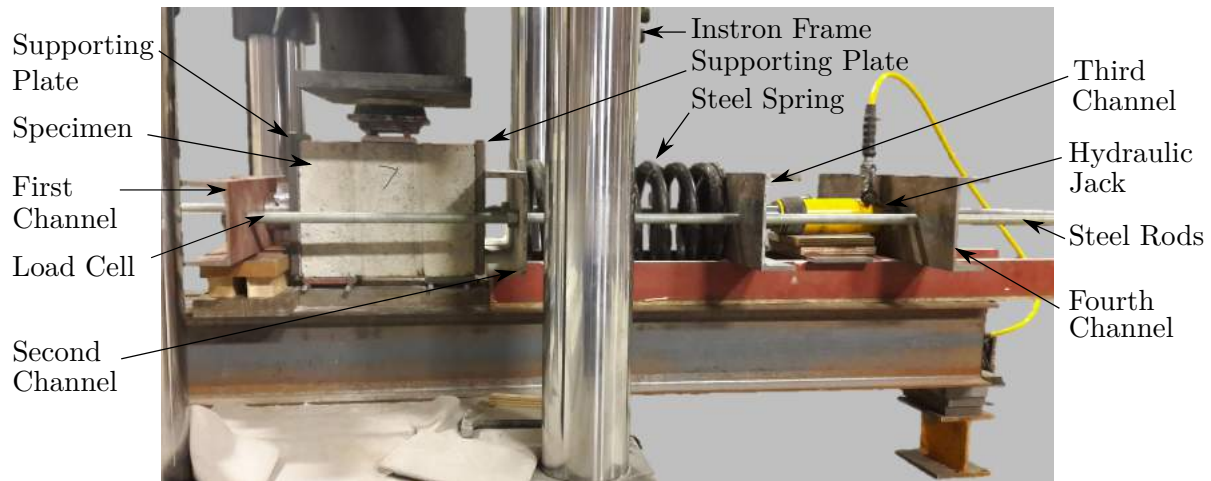


Figure 5.14: Full Triplet Set-up for Pre-Compression

the spring was compressed completely and would effectively be meaningless.

As mentioned in Section 3.6.1, specific failure mechanisms are required by the code. These include shear failure in the unit-mortar joint and shear failure only in the mortar. If during the tests any of the other failure mechanisms occurred, the test results were discarded. The majority of failure occurred due to shear failure in the unit-mortar joint. During the zero-compression tests, failure generally occurred at only one of the unit-mortar joints. Conversely, during the pre-compression tests failure was more likely to occur at both joints simultaneously or occur one after the other as the load increased.

The data that was taken from successful tests included the pre-compression load applied and the maximum vertical force applied. With this data and the mortar joint area, the initial shear strength and angle of internal friction could be determined.

It can be seen in Figure 5.14 that the set-up consisted of many loose components, these were often only held in place by self-weight, clamps or bolts. This resulted in a lot of movement in the set-up itself, resulting in more variability in the results. It is therefore recommended that future studies attempt to construct a set-up that is more stable and solid. This will be discussed in more detail in Section 7.2.6. The set-up discussed thus far worked well for the tests, however another method that can be investigated in future studies is to use the servo-hydraulics of the Instron to control the normal load and use the hydraulic jack to slowly apply shear.

5.7 Masonry Compressive Strength Tests

The compressive strength of masonry wallet specimens was determined according to the specifications in BS EN 1052-1 (1999). Both the compressive strength and the modulus of elasticity were determined on wallet specimens tested at 28 days. Four wallets were tested for compressive strength, with three of these used to obtain the modulus of elasticity.

BS EN 1052-1 (1999) bases the dimensions of the wallets on the size of the individual masonry

units. Using these guidelines a wallet was chosen that consisted of ten masonry units, with a height of approximately 610 mm and a length of 590 mm. The mortar joint thickness was kept between 10 and 15 mm. A spirit level was used to ensure the specimen's loading faces were flat and parallel to one another and at right angles to the main axis of the specimen. All the wallets were built by the same person to ensure uniformity between the different specimens and materials.

The specimens were built on a level surface inside a steel channel section. This ensured a level base for the unit and allowed easy transportation of the wallets to the testing set-up. In order to determine the modulus of elasticity of the wallet, LVDTs were attached at four points to the specimen. These were attached with LVDT mounts and were positioned 360 mm apart with a gauge length of 210 mm. The distances used were slightly larger than those suggested by BS EN 1052-1 (1999) (see Figure 3.18 in Section 3.7.1) but were chosen in order to fit the specimens dimensions properly. Figure 5.15 shows one of the AACB wallets with attached LVDT mounts.



Figure 5.15: AACB Wallet

The same time frame for testing the specimen was used as that of the triplet tests, namely specimens were constructed three weeks after the units were created. The mortar therefore had an age of one week at the time of the tests. Once again the week old mortar was designed to give $\pm 20\%$ of the 28 day masonry unit strength. A mortar sample was taken from each batch mixed for the wallet construction and tested after one week.

The test set-up consisted of a 2 MN Instron Materials Testing Machine, with a steel spreader beam attached to its actuator. The wallets were placed centrally in the set-up and it was ensured that the top and bottom of the wallets were in full contact with the testing machine. A 10 mm rubber mat was placed between the wallet and the spreader beam to help ensure full contact. Figure 5.16 shows an adobe wallet in the test set-up.

Once the specimen was in the set-up, a loading rate was used so that the specimen failed within

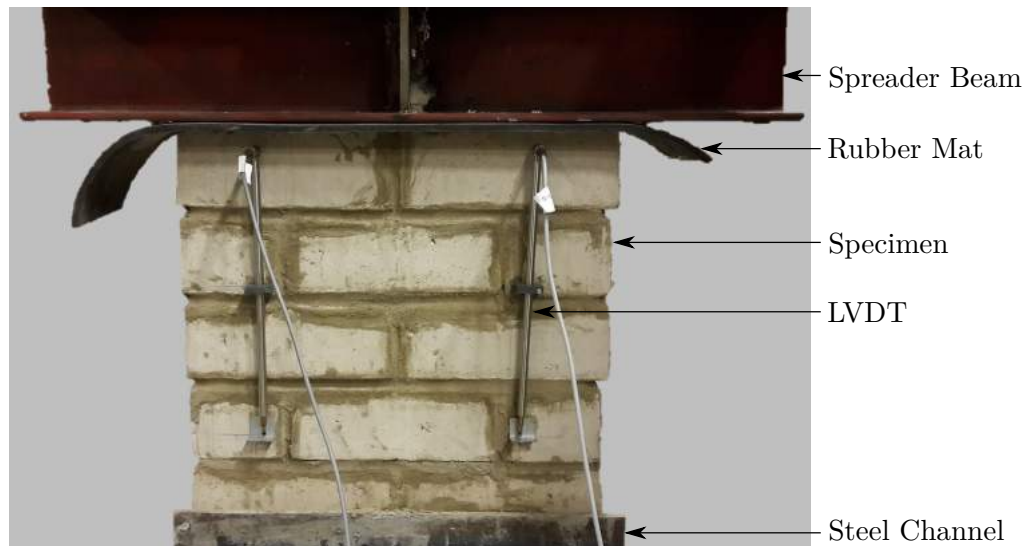


Figure 5.16: Masonry Compressive Strength Set-up

15 to 30 minutes from commencement of loading. As each material had a different strength, the loading rate was adjusted for each specimen. With the CMU, AACB, CSEB and adobe specimens having a 0.33 mm/min, 0.3 mm/min, 0.25 mm/min and 0.2 mm/min loading rate respectively.

Different loading rates were used to ensure that the tests were performed in accordance with the standard, however, generally the faster the loading rate the higher the resistance of a material. This means that the strength results from the different materials can not be directly compared for these wallets. As this study focuses on determining whether standards for testing the mechanical properties of conventional masonry units can be successfully applied on alternative materials as well as to determine reliable mechanical properties for a variety of AMUs, a direct comparison between materials was deemed to be less important than following the standards closely.

Four specimens were tested for each material. The first specimen of each type was tested without any LVDTs in order to determine its maximum load. The remaining three wallets had LVDTs attached, which were removed at approximately 50 % of the maximum load. This was to ensure that the LVDTs were not damaged when the wallet failed.

From the tests the maximum load as well as the displacement of the LVDTs were recorded. Using the equations in Section 3.7.1 the mean compressive strength and modulus of elasticity could be determined.

5.8 Conclusion

This chapter covered the experimental tests that were conducted to acquire the mechanical characteristics of the various masonry types investigated. The tests that are investigated included compression tests on individual masonry units, modulus of elasticity tests, Poisson's ratio tests, wedge splitting tests, density tests, triplet tests and compression tests on masonry wallets. Four masonry materials were experimented upon, namely: CMU, AACB, CSEB and adobe masonry.

Each test's specimen preparation, testing set-up and any issues are discussed in their relevant sections. Almost all tests were conducted successfully and without major deviation from international standards. The one material that did cause some deviation was the adobe masonry. The low strength of the adobe units resulted in adjustments to the testing conditions for the modulus of elasticity, wedge splitting and triplet tests. Chapters 6 and 7 discusses the results of these tests.

Chapter 6

Experimental Results

Several tests were conducted on the concrete masonry units (CMUs), alkali-activated concrete blocks (AACBs), compressed stabilised earth blocks (CSEBs) and adobe masonry specimens in order to determine their mechanical characteristics. The tests included: the compressive strength tests on masonry units, modulus of elasticity tests, Poisson's ratio, wedge splitting tests, density tests, triplet tests, and compressive strength tests on masonry. The test set-ups and procedures of these tests are discussed in Chapter 5.

This chapter discusses the mechanical properties that are determined from the tests. Each test's results are given and any relevant points of interest are reported. Chapter 7 covers the comparisons and discussions between the various mechanical properties and tests, as well as the appropriateness of the tests for use on the various masonry materials.

6.1 Compressive Strength of Masonry Units Results

The compressive strength of individual masonry units is one of the most common mechanical properties used to determine the size of a structure in masonry structural design. Therefore, compressive strength testing is generally conducted when investigating the mechanical characteristics of masonry. This study is no exception and an extensive series of tests were conducted to determine the strength gain of masonry over 91 days on the four masonry materials investigated.

The compressive strength of the masonry was determined at 7, 14, 28, 56 and 91 days for the CMU, AACB, CSEB and adobe masonry units. Each test was conducted on seven units to allow a reliable comparison of strengths for the different ages and materials. All the masonry units were created with the same dimensions to allow easy comparison between the ages and materials. The test procedure employed is explained in detail in Section 5.1.

The 28 day strength results were of special significance due to the fact that all other mechanical tests conducted in this study occurred when the masonry units reached 28 days of age. Therefore, the 28 day strength results were used to compare the strength of the units with its other characteristics. The results were also used in certain tests to determine the expected failure load beforehand.

The influence of the orientation of masonry samples was also investigated. Units were tested in their headface orientation at 28 days in order to compare them to the bedface tests. These tests allowed a more comprehensive understanding of the masonry's mechanical behaviour and the influence of the shape factors and casting direction of the units. This section first considers the strength gain of the various masonry materials followed by the effect of orientation on the unit's strength.

The results shown for the compressive strength tests in the following sections are not normalised strengths corrected for dimensions, but measured strengths. The normalised strengths for both the bedface and headface tests are given at the end of Section 6.1.2.

6.1.1 Strength Gain of Masonry Units

The results of the compressive strength tests, measured on the four masonry types over 91 days, can be seen in Figure 6.1. The bars represent the average compressive strength measured for each group, increasing with age from 7 to 91 days. The variability among the compressive strength is shown by the standard deviation error bars. It can be seen that the masonry units gained strength over time.

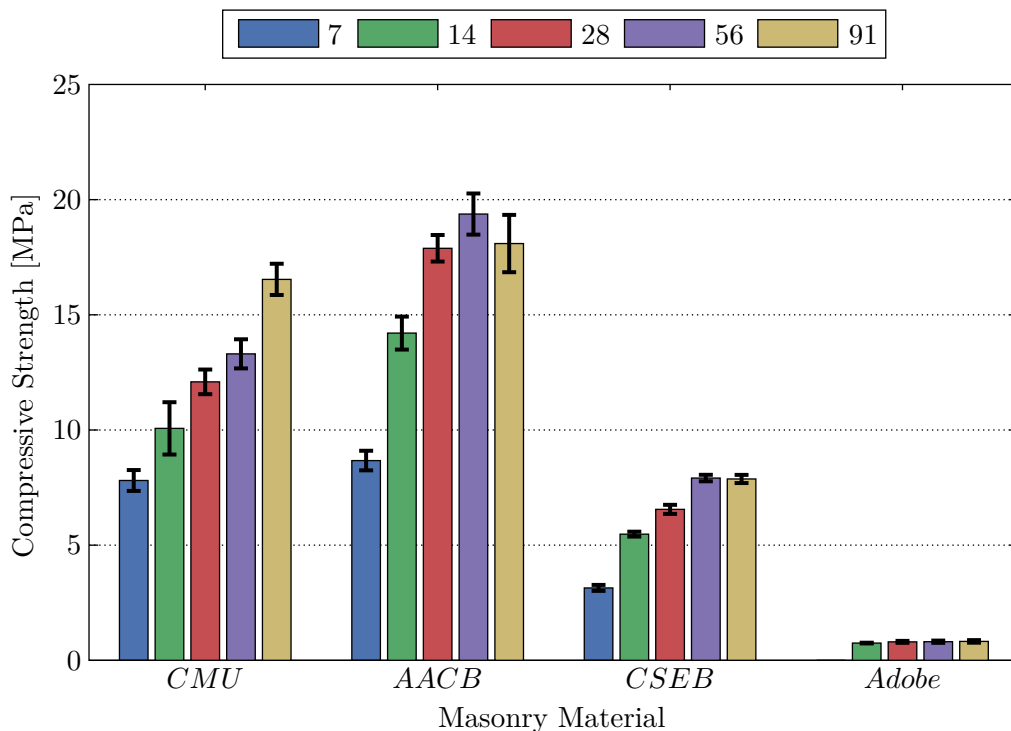


Figure 6.1: Compressive Strength Values for 7, 14, 28, 56 and 91 day strength for CMU, AACB, CSEB and Adobe

From Figure 6.1 the relative differences in the masonry materials and testing ages can clearly be seen. The AACBs showed the highest strength of all the materials, with the benchmark CMUs having the second highest strength. As expected the CSEBs showed the third highest strength, with their 91 day results being only marginally stronger than the CMUs 7 day results. The adobe units were by far the weakest, not even reaching half the strength of the CSEBs 7 day

strength.

It is important to note that while the CSEB and adobe mixes were designed to give as high a strength as possible, this was not the goal of this study. In other words, their mix designs were not optimised or improved by a large amount of trial batches. Therefore, it is entirely possible to achieve higher strengths from these materials. The CSEB could easily be made stronger by adding more cement to the mix, however this would defeat the purpose of making a cost-effective environmentally friendly alternative masonry unit. Equally important is the fact that the CMU and AACB mixes were not designed to give as high a strength as possible. In fact the strength of initial trial batches were higher than the final implemented mix designs. Their mix designs were adjusted in order produce a cheaper and more environmentally friendly unit, while still retaining strength similar to conventional concrete masonry units used in practice. Therefore, the fact that in this study the AACBs are stronger than the CMUs does not mean that it would always be the case.

The average compressive strengths of each group shown in Figure 6.1 is also given in Table 6.1. The coefficient of variation (COV) associated with the average compressive strength for each batch is also given in the table. The COV gives an indication of the variability within one group of units. It can be seen that almost all COV values are under 10 %, which is acceptable for masonry units. There is no data for the adobe 7 day strength due to the fact that at 7 days the adobe mixture had not set yet and was too wet to properly transport and test.

Table 6.1: Average Compressive Strength Values (f_c) presented in Figure 6.1 and the Coefficient of Variation (COV)

Material	CMU		AACB		CSEB		Adobe	
Age	f_c (MPa)	COV	f_c (MPa)	COV	f_c (MPa)	COV	f_c (MPa)	COV
7 days	7.81	(5.8 %)	8.67	(4.9 %)	3.14	(4.1 %)	-	-
14 days	10.07	(11.3 %)	14.21	(5.0 %)	5.48	(2.0 %)	0.75	(2.3 %)
28 days	12.09	(4.4 %)	17.89	(3.2 %)	6.55	(3.0 %)	0.80	(5.3 %)
56 days	13.30	(4.8 %)	19.37	(4.6 %)	7.91	(1.8 %)	0.81	(6.0 %)
91 days	16.54	(4.1 %)	18.09	(6.9 %)	7.87	(2.2 %)	0.82	(6.7 %)

6.1.1.1 Compressive Strength Discussion

The results from the compressive strength tests show the expected trends for the materials. As expected the CMU, AACB and CSEB masonry batches show an increase in strength with age. This is a direct result of the hydration process in the cement based units (CMU and CSEB), and the geopolymerisation process in the AACBs.

An important aspect of strength gain is the increase in strength over the first 28 days. The compressive strength for the 7 day specimens was 65 %, 48 % and 48 % of the 28 day strength

for the CMU, AACB and CSEB specimens respectively. The rapid strength gain within the first 7 days shows the necessity for providing proper curing conditions for the units. The CMU's strength gain is approximately the same as conventional concrete's strength gain (generally accepted to be between 65 % and 80 % (Mindess et al., 2003)). The long term strength gain from 28 to 56 days is similar for the CMUs and AACBs, having a strength gain of 10 % and 8 % respectively. The CSEB had a higher strength gain of 20 % from 28 to 56 days.

The adobe units showed almost no strength increase with time. This was due to the fact that the adobe units do not have anything similar to a hydration process. Instead, once the units were dry, they were near their final strength.

There are some concerns with the results of the compressive strength tests, particularly the 91 day strengths. For the CMUs there was a larger strength gain from 56 to 91 days than from 28 to 56 days. This is contrary to what is expected as the strength gained should decrease with time. Therefore, it is recommended that the 91 day strength for the CMU be redetermined in future studies. The 91 day strength of the AACBs also showed irregularities. The 91 day strength was lower than the 56 day strength, once again raising concern over these values. These issues could be due to variabilities in the creation or testing process. Finally, the 91 day strength of the CSEB was almost identical to the 56 day strength.

Certain variabilities must be accounted for in the compressive strength results due to the method of creating the units. A batch of seven units was created for each age, consequently different ages were created from different batches. This introduces the possibility of variability between the various testing ages if there was any deviation in the mixing process. Another area where variability was introduced is in the curing of the units. Efforts were made to ensure that all units within one material type were cured under the same conditions. For instance, the CMUs were placed in temperature controlled water tanks and the AACBs and CSEBs were placed in a temperature and moisture controlled room. Even with these measures some variability could still occur. The units tested at 91 days had the greatest chance of variability developing simply due to their greater age.

The CMU and AACBs still had to set for the first day in the general laboratory workspace. Large differences in the first day's temperature or moisture conditions could have an influence on the strength, especially early age strength. The CSEBs had to set for an entire week in the general laboratory workspace before being moved. This increased the effects of temperature and moisture on the units. The adobe units had the largest chance for variability as they were not placed in a controlled environment but left to harden in the general laboratory workspace.

In an attempt to reduce variability, due to differences in climate conditions within each masonry material's test groups, the batches for one material type were produced within as short a time as possible. However, due to the large amount of masonry that needed to be created and tested, each material type was still produced over three to four weeks.

6.1.1.2 Compressive Strength at 28 Days

The 28 day compressive strength of the masonry units are compared with masonry strengths found in literature or standards in order to determine if the various materials are within an acceptable range for the material type. This simply confirmed whether the material mixes used in this study could be categorised as conventional CMU, AACB, CSEB and adobe materials.

The CMUs are the easiest to compare as international standards give a wide range of acceptable strengths. As discussed in Section 3.1.1, solid CMUs are widely available in a range of 7 to 21 MPa. The CMUs created in this study are near the centre of this range and can therefore be categorised as a good representation of concrete masonry, at least with regards to the compressive strength.

While there are many studies into various AAC, there are not as many into AACBs and even less into AACBs cured at ambient temperatures. Some results from literature are given here that resembled the material in this study as closely as possible. Abdullah et al. (2015) investigated fly ash based geopolymer bricks and found a strength of 21.1 MPa at 28 days, however the curing methods are not explicitly given and it is expected that some temperature curing was conducted. Manjunath et al. (2011) achieved a range of approximately 2 to 28 MPa for a geopolymer mortar, however these results were only taken at 7 days. These results from literature show that the alkali-activated concrete (AAC) strengths found in this study are within the range of results from other researchers.

The mixes and curing procedure of the AAC by Barnard (2014) are the closest to those of this study, even though they were not specifically created for masonry. However, when looking at the entirety of Barnard's testing regime a range of strengths from 6 to 72 MPa was found, showing the great range of strength that AAC can achieve.

For the CSEBs, a range of 4 to 14 MPa was reported by Morel et al. (2007) and Riza and Rahman (2015), while Malherbe (2016) found strengths of 3.5 to 6.5 MPa. These ranges show that the CSEB strengths found in this study are acceptable. It should be noted that the close correlation to Malherbe's results are due to the mix design of this study being based on Malherbe's work.

As mentioned in Section 3.1.1, the strengths of adobe specimens commonly fall within 0.8 to 3.5 MPa. This means that the results from this study are within the lower spectrum of adobe strengths and can be deemed acceptable.

6.1.2 Influence of Masonry Orientation

The influence of the orientation of the masonry units on the compressive strength was investigated by also testing units in the headface orientation at 28 days, as opposed to the bedface orientation as discussed in the previous section. Figure 6.2 shows the results from the headface tests compared to the bedface tests for the CMU, AACB, CSEB and adobe specimens. The variation amongst the specimens is indicated with the use of error bars showing the standard deviation.

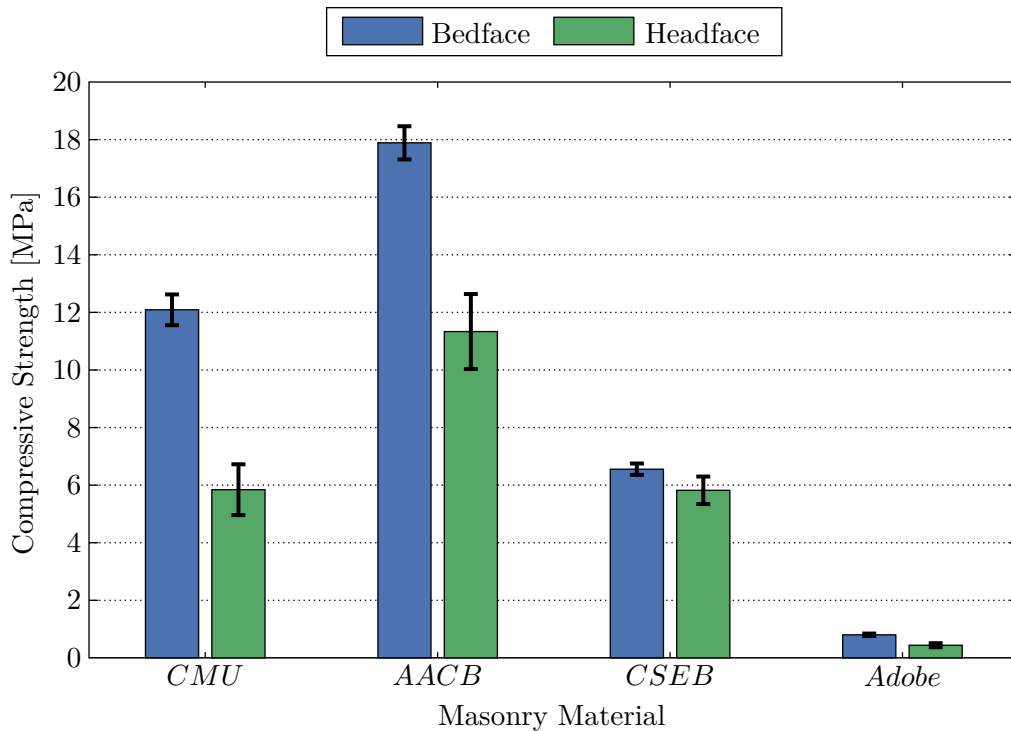


Figure 6.2: Compressive Strength Values of CMU, AACB, CSEB and Adobe Bedface and Headface Units

From Figure 6.2 it can clearly be seen that the bedface strengths are higher than the headface strengths. One of the major reasons for this can be attributed to a larger contact area between the bedface specimen's surface and the upper platen of the testing machine, resulting in a higher degree of confinement. The higher confinement resists against lateral expansion due to Poisson, resulting in more compressive strength. This is often categorised with the shape factor of the units. Another major cause of the reduced strength in the headface orientation is the increased slenderness of the cylindrical specimens, and the effect this has on the development of tensile forces and resulting cracking pattern.

The lower strength in the headface specimens is also caused by an increased probability of eccentricities. If the units are not perfectly formed, some eccentricity may occur during the loading of the specimen, resulting in a lower final strength of the unit. The casting direction versus the loading direction also influences the strength of the units. The bedface specimens are compressed perpendicular to the casting direction, which is also the direction compression is applied in the creation process for the CMU, CSEB and adobe specimens; this causes an increase in the strength of the bedface specimens versus the headface specimens due to the better arrangement of the particles.

Table 6.2 shows the average compressive strength values presented in Figure 6.2 as well as the COV. It can clearly be seen that the COV of the headface tests are higher than the bedface tests. This is most likely due to eccentricities created during the forming of the units, which has a larger effect on the more slender headface units than the low bedface units. All the material types' COV percentages are above 10 % for the headface tests, except for the CSEB values.

Table 6.2: Average Compressive Strength Values Presented in Figure 6.2 and the Coefficient of Variation (COV)

Material	CMU	AACB	CSEB	Adobe
Average Bedface Strength (MPa)	12.09	17.89	6.55	0.80
(COV)	(4.4 %)	(3.2 %)	(3.0 %)	(5.3 %)
Average Headface Strength (MPa)	5.84	11.33	5.82	0.44
(COV)	(15.1 %)	(11.5 %)	(8.2 %)	(15.9 %)

The headface strength for the different masonry types are, 48 %, 63 %, 89 % and 55 % of the bedface strength, for the CMU, AACB, CSEB and adobe units respectively. This shows that the CSEB's headface and bedface strengths were much closer to each other than the other materials. The high headface strength for the CSEBs is unusual and an explanation for this could not be found. Therefore, it is recommended that the CSEBs be retested in this regard.

By using the shape factors given by BS EN 772-1 (2011) (shown in Table 3.1 in Section 3.1.2), both the headface and bedface units can be normalised. Using linear interpolation, the shape factor for the bedface tests is determined to be 0.814 and the headface specimens shape factor 1.37. A further factor of 1.2 can be applied to the CMUs due to their conditioning by immersion. Table 6.3 shows the headface and bedface strengths when these shape factors are applied. It can be seen that using the shape factors brought the CMU's respective orientation strengths within 20 % of each other, and the AACB's and adobe's strengths within 10 %. The outlier was the CSEB's normalised strengths, being only within 33 % of each other, this relates back to the fact that the headface strength for the CSEBs was unusually high.

These results show that the shape factors could be applicable for these units. However, as only one batch of each material was tested, it is suggested that a more extensive study be carried out focusing on these shape factors before any final conclusions are drawn.

Table 6.3: Normalised Bedface and Headface Strength at 28 Days Age

Material	CMU	AACB	CSEB	Adobe
Bedface Strength (MPa)	11.81	14.56	5.33	0.65
Headface Strength (MPa)	9.60	15.52	7.97	0.60

6.2 Modulus of Elasticity Results

The modulus of elasticity was measured by applying a compression loading on a cylinder specimen, while simultaneously measuring the strain in a direction parallel to the stress. Section 5.2 outlines the test procedure employed to accomplish this. The tests were conducted on all four material types (CMU, AACB, CSEB and adobe) at 28 days.

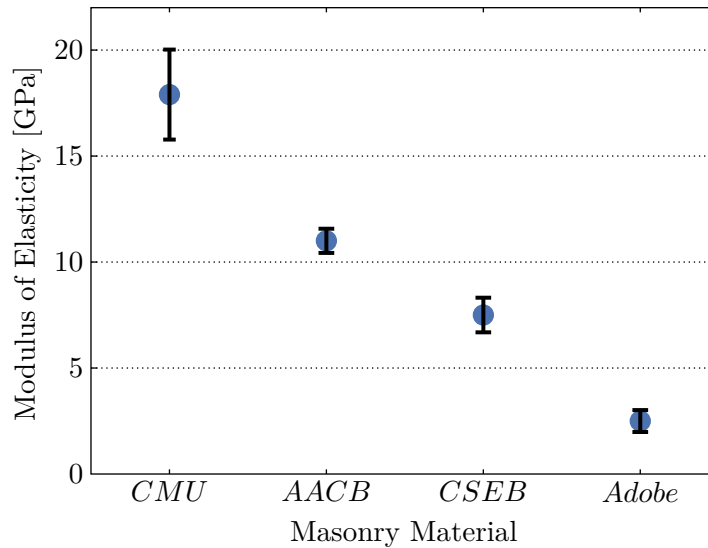


Figure 6.3: Mean Modulus of Elasticity Measured at 28 Days for CMU, AACB, CSEB and Adobe Specimens

The calculated mean modulus of elasticity values for each material are presented in Figure 6.3, along with error bars showing the standard deviation of the samples. It can clearly be seen that the CMU specimens showed the highest modulus of elasticity, followed by the AACB and then the CSEB specimens. Adobe specimens showed the lowest modulus of elasticity.

The mean values shown in Figure 6.3 are also given in Table 6.4, along with each group's COV. It can be seen that the COV values of the modulus of elasticity tests are higher than the COV values from the compressive strength tests. This is due to the greater chance of variability because of the more complicated nature of the tests. The height of the specimens also likely played a roll, adding variability in a similar manner to that of the headface tests conducted on the masonry units as discussed in Section 6.1.2.

The CMU and CSEB specimens were both formed by using a hydraulic press as discussed in Chapter 4. This along with the uncontrolled nature of the particle orientation in the forming chambers, resulted in a greater possibility of variability than the AACB specimens. The AACB specimens showed the lowest variability due to their self compacting ability, allowing consistent specimens to be created. The adobe specimens' high COV is a result of the low consistence in the forming process due to the hand compaction conducted on the cylindrical specimens, as well as the natural weakness of the material.

Table 6.4: Modulus of Elasticity Values Presented in Figure 6.3 and the Coefficient of Variation (COV)

Material	CMU	AACB	CSEB	Adobe
Elastic Modulus (GPa)	17.9	11.0	7.5	2.5
(COV)	11.9 %	5.2 %	10.9 %	20.9 %

6.2.1 Influence of Material Type on Modulus of Elasticity

Table 6.5 shows the modulus of elasticity of common masonry construction materials (Domone and Illston, 2010). It shows that the CMU's modulus of elasticity falls near the middle of the range for dense concrete masonry. The AACB's modulus of elasticity is towards the bottom of the range for dense concrete and relates closer to lightweight aggregate concrete. CSEB's modulus of elasticity is closer to that of autoclave aerated concrete masonry, while adobe is lower than any other common material.

Table 6.5: Modulus of Elasticity of Common Construction Materials (Adapted from Domone and Illston (2010))

Masonry Material	Modulus of Elasticity (GPa)
Mortar	20-35
Dense concrete	10-25
Lightweight aggregate concrete	4-16
Autoclave aerated concrete	3-8
Clay brickwork	14-18

The CMU's modulus of elasticity falls within an acceptable range for the material type, therefore acting as an appropriate benchmark for the test set-up. The stiffness of the AACB material, on the other hand, is low when compared to a concrete of similar strength. According to SANS 10100 (2000), a concrete with strength of 20 MPa should provide an approximate modulus of elasticity of 25 GPa. However, the AACB with a strength of 17.89 MPa provided a modulus of elasticity of only 11.0 GPa.

This corresponds with work found in literature, with both Barnard (2014) and Fernandez-Jimenez et al. (2006) finding that similar AAC mixes also achieved low stiffness for higher strengths. Some of their mixes had strengths of over 30 MPa, but a modulus of elasticity less than 20 GPa, similar to the results of this study. Lee and Lee (2013) also found modulus of elasticity values of between 10 GPa and 21 GPa for similar AAC mixes. These authors all used a AAC mix with the addition of fly ash and slag. While the low stiffness of the material could be a problem for large buildings constructed of cast concrete or AAC, for masonry buildings it is not as large a concern, as seen by some of the low modulus of elasticity values in Table 6.5.

The modulus of elasticity of the CSEB specimens was found to be relatively low for a masonry material, but still within an acceptable range. The modulus of elasticity found in this study is similar to that found by Malherbe (2016), even though a different test procedure was employed (tests were conducted on blocks rather than cylinders).

The adobe specimens showed a very low modulus of elasticity, of only 2.5 GPa, which is to be expected for such a low stiffness material. This low stiffness should be accounted for during structural design. The values in this study are, however, much higher than found by other researchers. Martins and Varum (2006), Quagliarini and Lenci (2010) and Silveira et al. (2012)

all found adobe specimens to have a modulus of elasticity of between 0.10 GPa and 0.40 GPa. These values are a lot lower than that found in this study, however a direct comparison is difficult due to the inherent variability in adobe masonry. The different soils, forming method, and the addition of fibres all have large influences on the stiffness of adobe.

6.3 Poisson's Ratio Results

The tests to determine Poisson's ratio were conducted simultaneously with the modulus of elasticity tests. The procedure for the Poisson's ratio set-up is discussed in Section 5.3, where two methods are covered. The first method involved a test set-up with a steel wire measuring the change in circumference, and the second method involved three linear variable differential transducers (LVDTs) measuring the change in radius. Both methods requires their measurements to be transformed into transverse strains.

The first method was only tested on the CMUs before it was discarded due to high variability in the test and low repeatability, as well as physically impossible results. These results also showed a COV of nearly 100 % and were therefore discarded.

The second method was much more stable, however the results from these test were also unsatisfactory. Table 6.6 shows the Poisson's ratio found for the four materials as well as the COV from the tests.

Table 6.6: Results from Poisson's Ratio Tests

Material	CMU	AACB	CSEB	Adobe
Poisson's Ratio	1.73	1.33	1.19	0.79
(COV)	(15 %)	(18 %)	(11 %)	(21 %)

These results are unsatisfactory due to the fact that a material cannot have a Poisson's ratio greater than 0.5. This would mean that the material is expanding under pressure, which is an impossibility (Domone and Illston, 2010). It is therefore clear that there was either an error in the test set-up or in the calculations from the tests.

The results from the modulus of elasticity tests fell within recognised ranges as shown in Section 6.2. This implies that the error was not in the loading procedure of the specimens or in longitudinal strains, but in the transverse strain measurements or calculations.

The calculations are straightforward. First the change in radius measured by the transverse LVDTs are converted to a change in circumference. Next, using the change in circumference and the original circumference, the transverse strain can be calculated, and with the use of the transverse strain and the longitudinal strain Poisson's ratio can be calculated (using Equation 3.4). It is therefore concluded that the bulk of the problem with the Poisson's ratio results lay with the test set-up. The issues with the test set-up that may have caused the errors are investigated in Section 7.2.3.

6.4 Wedge Splitting Results

The fracture energy (G_f) of the masonry materials was determined through the use of the wedge splitting test. The tests were conducted on six specimens of each material at 28 days, subjected to the test method described in Section 5.4. Each specimen's splitting force versus crack opening displacement (COD) was plotted in order to calculate the fracture energy.

A typical splitting force-COD curve is shown in Figure 6.4 for each the four material types. From the figure a few observations are immediate obvious. First, the maximum COD varied greatly between the different materials. This has a large influence on the final fracture energy of the materials. The general order of COD from greatest to smallest was: CMU, AACB, CSEB then adobe. Secondly, the maximum horizontal splitting force varied between the materials, however, it did not necessarily correspond with the compressive strength of the material. This is the most obvious with the CSEB maximum splitting force being higher than the CMU's splitting force. The order of the splitting forces corresponds with the order of the tensile strength of the materials. Finally, it can be seen that the adobe's curve is far below, and much smaller than, the other materials. As mentioned in Section 5.4, the adobe material could not support the 100 N minimum pre-load of the testing machine and the tests were therefore started at practically zero pre-load.

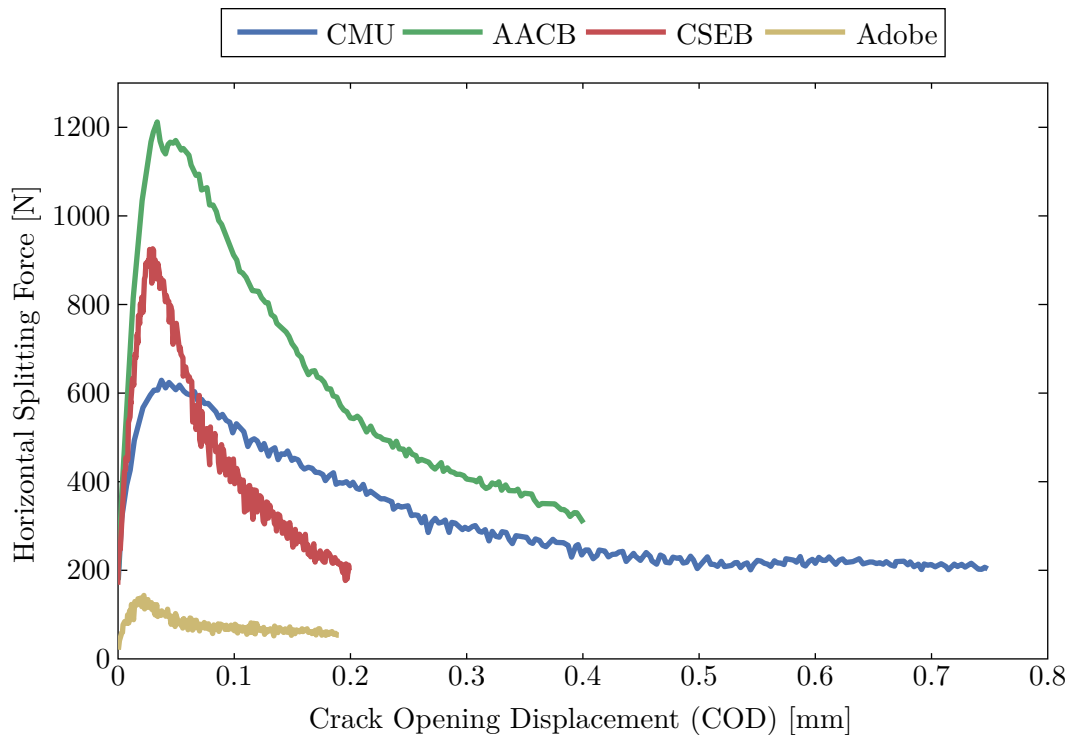


Figure 6.4: Typical Splitting Force-COD Curve for the CMU, AACB, CSEB and Adobe materials

Figure 6.5 shows the fracture energy as well as the standard deviation for the different materials, calculated through splitting force-COD curves such as those shown in Figure 6.4. By comparing Figure 6.5 with the average compressive strengths of the different materials, it can be seen that the compressive strength of the materials relate to the fracture energy of the specimens. The strongest masonry unit, AACBs, also has the largest fracture energy, with this trend continuing

for all the materials. The figure also shows that the standard deviation for the materials was very high for the fracture energy.

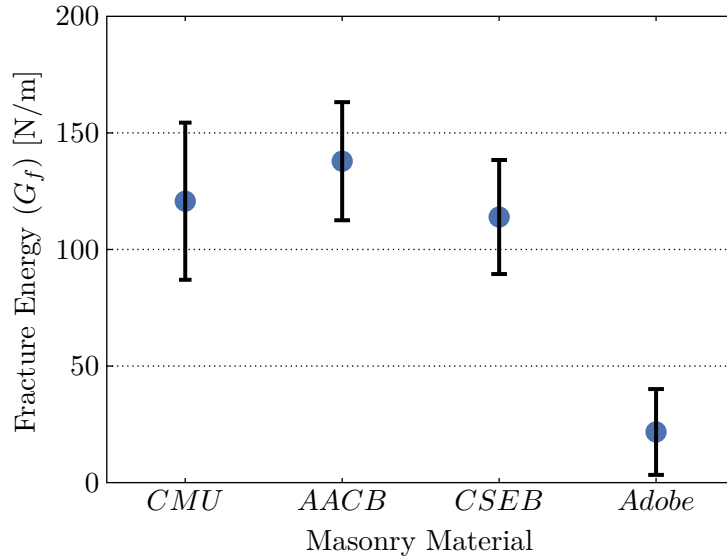


Figure 6.5: Fracture Energy of CMU, AACB, CSEB and Adobe Specimens

Table 6.7 shows the results from the wedge splitting tests. The maximum splitting force, tensile strength, fracture energy and final COD is given for each material, as well as the COV for these results. These results confirm the statements made with regards to Figure 6.4.

From Table 6.7 it can be seen that the COD values differ greatly from one material to another. However, there were also differences in the COD values from one material between specimens, albeit smaller differences. The splitting force-COD curves were very similar from within one material type batch of tests, with similar peaks and shapes, the major difference being the length of the curve. This was due to the specimen failing at different COD widths.

The final COD lengths of each material's results were reduced in order to better compare each individual material's fracture energy and reduce the variation in the results. The COD values used in the calculations were reduced to 75 to 80 % of the average COD length. This greatly reduced the COV percentage of the COD values for the CMU, CSEB and AACB results, however, the adobe COD values were much more scattered and therefore their average was simply used.

Table 6.7: Results from Wedge Splitting Tests

Results	CMU		AACB		CSEB		Adobe	
	Average	COV	Average	COV	Average	COV	Average	COV
$F_{s,max}$ (N)	692	(25 %)	1183	(12 %)	871	(8 %)	116	(30 %)
$\sigma_{tens,max}$ (MPa)	0.14	(27 %)	0.25	(12 %)	0.18	(8 %)	0.03	(30 %)
G_f (N/m)	121	(28 %)	138	(18 %)	114	(21 %)	22	(85 %)
COD (mm)	0.75	(0 %)	0.40	(3 %)	0.20	(4 %)	0.19	(41 %)

Wittmann (2002) conducted the same wedge splitting test on two normal and one high strength

concrete specimens, with a compressive strength of 35.3 MPa, 57.4 MPa and 112.2 MPa respectively. The resultant fracture energy from these tests was 123.55 N/m, 152.05 N/m and 158.70 N/m respectively, increasing with the compressive strength. It can be seen that the AACB fracture energy from this study is higher than the 35.3 MPa concrete, while the CMU fracture energy is slightly lower due to its lower compressive strength. The results of Wittmann were higher than both the CSEB and the adobe specimens due to the much weaker nature of these alternative masonry units (AMUs).

Wittmann et al. (1988) states that the loading rate and the maximum aggregate size both influence the fracture energy of a material. Wittmann shows that an increase in the loading rate causes an increase in the fracture energy. As different loading rates were used in this study, this must be taken into account when looking at the results. The loading rates were higher for the stronger materials and lower for the weaker materials (loading rates are given in Table 5.1). This may have increased the resulting difference in their final fracture energy values.

An increase in maximum aggregate size also causes a corresponding increase in the fracture energy. This has the largest influence on the AACB material, as it was the only mix with large aggregate (13 mm stone), thereby increasing its fracture energy compared to the other materials. Wittmann (2002) developed the following power function that describes the fracture energy of concrete based on the maximum aggregate size:

$$G_f = 80.6\phi^{0.32} \quad (6.1)$$

where ϕ is the maximum aggregate diameter. When this equation is used with the maximum aggregate sizes from Chapter 4, the values in Table 6.8 are calculated. These are compared with the actual fracture energy determined from the tests. From the results it can be seen that the CMU and CSEB specimens achieved a fracture energy close to that calculated by Equation 6.1. This is most likely due to the fact that both use cement hydration to gain strength, which makes them the closest materials to the concrete used by Wittmann (2002) to develop Equation 6.1.

The AACBs showed a much lower fracture energy than that of Equation 6.1. This is likely due to AACB's different material properties from concrete, possibly its different modulus of elasticity. The adobe mixture also showed a great difference between the results and Equation 6.1. Again, this is due to the different material properties of concrete. Especially as there is no stabilising compound in the adobe mixture.

Table 6.7 shows that the large standard deviations of the tests caused large COV percentages. The large COV percentages for this test can be attributed to a few causes. Firstly, the test is very sensitive and was conducted on relatively weak and very brittle materials. A degree of variation is therefore expected.

Next, it can be seen that the CMU and CSEB specimens have a higher COV than the AACB. This could be a result of the method employed to form the blocks. Both the CMU and CSEB wedge splitting specimens are cut from one large block created in the block press, whereas the

Table 6.8: Comparison of Fracture Energy from the Equation by Wittmann (2002) to the Experimental Results

Material	G_f (N/m)		Max Aggregate Size (mm)
	From Tests	From Equation	
CMU	121	130	4.5
AACB	138	183	13
CSEB	114	106	2.36
Adobe	22	101	2

AACB specimens are formed individually as discussed in Chapter 4. Due to the fact that the block press method creates blocks with density variations throughout the unit, the two specimens cut from the block press units could differ from each other as they are not obtained from the same position in the block, thereby increasing the variability of the test.

Another factor that increases the COV of the tests is the crack path itself. The fracture energy is calculated through the use of the fracture area, i.e. the area where the crack takes place. However, the crack does not always occur along the same path. Instead it formed in slightly different paths between specimens, thereby increasing the variability in the results. Figure 6.6 shows two wedge splitting specimens illustrating how some of the different cracks formed.

**Figure 6.6:** Cracked Wedge Splitting Specimens

Table 6.7 shows that the adobe COV percentage for the fracture energy is very high. One of the causes of this could be the extreme weakness of the material as well as the fact that there was no stabilising content in the mix design. Another factor that could have increased the variability is the hand compaction that was used on the specimen, increasing the variability between specimens in the creation process.

The COV could also have been increased due to the method of testing the adobe specimens. Section 5.4 explained how the testing machine was lowered onto the adobe specimens without a pre-load due to the weakness of the material. This could have caused an increase in the variability of the test for two reasons. Firstly, without the preload the specimen and set-up could not settle properly before commencement of testing. The pre-load allows the steel wedges

to gain proper contact with the rollers, as well as making sure that the entire set-up is stable. Secondly, due to the weakness of the material, and the fact that the steel wedges were lowered visually, there is a chance that the specimens were damaged, reducing the effectiveness of the COD control.

While the adobe specimens have a very high COV, it can be seen from Figure 6.5 that its standard deviation was similar to the other materials. The high COV was therefore also due to the very low fracture energy values from the adobe specimens.

6.5 Density Results

The dry density of the different masonry materials was determined by oven drying the blocks to a constant mass at 28 days, as explained in Section 5.5. The density of the units can be used as a quality control measure and relates to the other mechanical characteristics of the material. Figure 6.7 shows the density determined for each of the four masonry materials investigated along with error bars indicating the standard deviation.

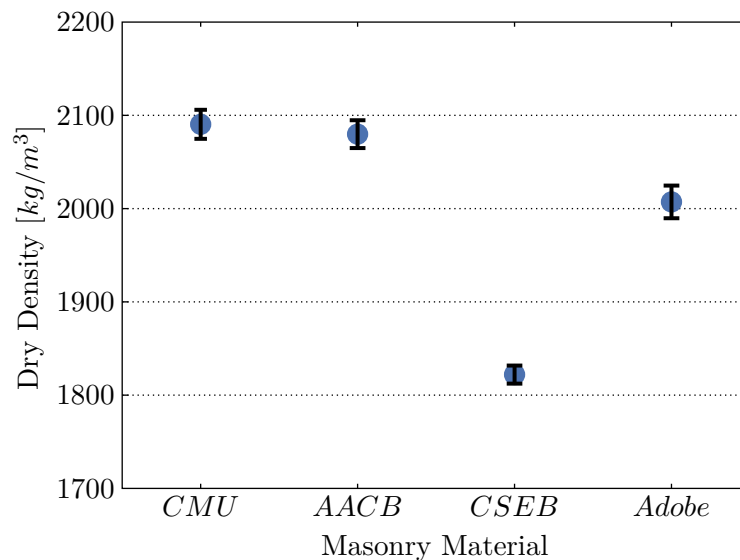


Figure 6.7: Mean Dry Density of CMU, AACB, CSEB and Adobe Specimens

From Figure 6.7 it can be seen that the CMU's density is lower than the accepted average for cast concrete (2300 kg/m^3). This is due to the dry nature of the mix, resulting in air voids even after compaction in the block press. The density does however fall within the range of dense masonry concrete, discussed in Section 3.5.

The CMUs and AACBs have similar density, with the AACBs also falling within the ranges found by researchers within literature as given in Section 3.5. The fact that the CMU's and AACB's densities are so similar to each other is counter intuitive as the AACBs had a self-compacting nature, whereas the CMUs had a dry mix. However, the AACBs contained much larger coarse aggregate in its mixture than the CMU specimens. This corresponds to the results from Barnard (2014), who found that the aggregate content had the largest influence on the AAC's density, with an increase in the fine aggregate content causing an increase in the density.

The CSEB mixture's density was the lowest of all the materials, due to the fact that it was the driest of the mixes. While its water content was higher than the CMU's mix, it had a much higher fines content. As a higher fines content increases a mix design's water demand, this resulted in a very dry mix, with a higher percentage of air voids. The CSEB's density also fell within the range of values found in literature, however, it is towards the lower range of these findings. This indicates that it was a very dry mix even for CSEBs and could explain why the compressive strength is towards the lower spectrum of literature's findings.

The adobe specimen had a higher density than the CSEB, even though the CSEB used a compacting force in its formation and the adobe specimens did not. Therefore, the higher density is a result of the much higher water content in the adobe mixture, thereby reducing the air voids even without compaction. The adobe specimen's density was also within the range of values found in literature, however, it was towards the upper limit of this range. This indicates that the mixture was wetter than those commonly found in literature. The adobe specimens in this study were also tamped with a wooden bar, the compaction applied may have been higher than that commonly seen in literature. However, this is difficult to confirm as little is stated about how much compaction should be applied.

Table 6.9 shows the density values presented in Figure 6.7 as well as the COV. It can be seen that the coefficient of variation is very low for the density tests, suggesting very little variation in one mix for each material. The adobe specimens have the highest COV, a result of the higher degree of variability in their creation due to the fact that the adobe mix was not weighed off before being formed, as discussed in Section 4.5.2. The adobe was also compacted by hand, rather than by machine, which adds to the possibility of variation if the applied force and number of strokes were not always constant. As the variability shown here is just for one batch, it can be assumed that there would be greater variability between different batches, due to the possibility of differences in the mixing procedure, forming process and curing conditions. This is likely one of the major causes for the adobe mix's mechanical results generally having a higher degree of variability than the other materials.

Table 6.9: Density Values Presented in Figure 6.7 and the Coefficient of Variation (COV)

Material	CMU	AACB	CSEB	Adobe
Density (kg/m^3)	2090	2080	1822	2007
(COV)	(0.7 %)	(0.7 %)	(0.5 %)	(0.9 %)

6.6 Triplet Results

The triplet tests, discussed in Section 5.6, provided the initial shear strength and the friction coefficient of the four masonry materials. These results are obtained by plotting the maximum shear strength of the specimens against the normal pre-compressive stress. Using the guidelines from BS EN 1052-3 (2002), five specimens were tested at each of the three different

pre-compression loads.

A line of best fit is plotted against the data points using linear regression. The mean initial shear strength (τ_o) is obtained from the intercept of the line with the vertical axis (at zero normal stress). The friction coefficient (μ) is obtained from the slope of the line. This line represents the sliding failure of the triplets and can be described by the classical Mohr-Coulomb's failure criterion:

$$\tau_a = \tau_o + \mu\sigma_D \quad (6.2)$$

where σ_D is the normal stress and τ_a is the shear stress. The friction coefficient is also sometimes represented as the internal angle of friction (ϕ_f) and is determined with the following conversion:

$$\phi_f = \arctan(\mu) \quad (6.3)$$

Figure 6.8 shows the lines of best fit as well as the data points for the CMU, AACB, CSEB and adobe triplet specimens. The data points are grouped at each of their respective pre-compressive stresses and a linear regression is conducted. Results were removed from the sample data if a failure type other than A1 or A2 occurred (see Section 3.6.1) and if a visible inspection of the test set-up showed an error. However, at least three specimens were tested successfully for each pre-compression load, thereby satisfying the standard's requirements.

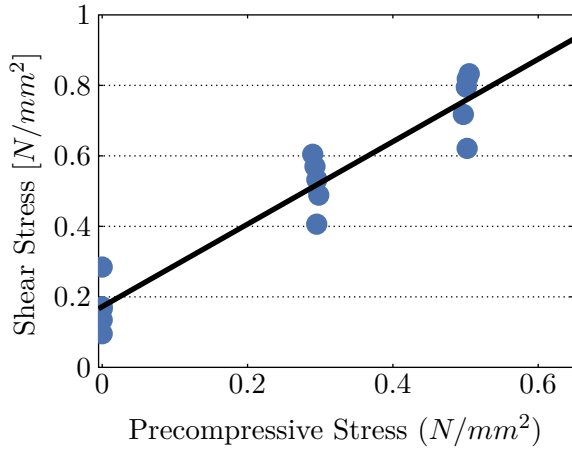
As it is difficult to visually compare the linear regression lines in four separate figures, Figure 6.9 shows all four material types' lines. In the figure, it can be seen that the CMU specimens showed the highest initial shear strength as well as the largest angle of internal friction. The AACB specimens showed the lowest angle of internal friction but a similar initial shear strength to the CSEB specimens. The CSEB and adobe specimens showed similar friction coefficients, however the adobe specimens had the lowest initial shear strength.

Returning to Figure 6.8, it can be seen that the data points are not always directly on the line. In order to qualify how closely the line fits the data a statistical measure, called the coefficient of determination (R^2), is applied.

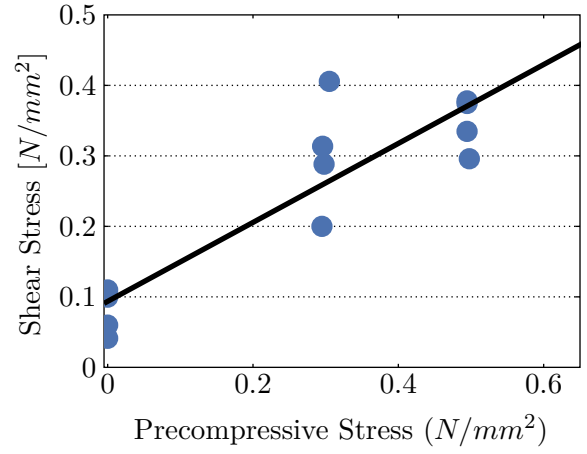
The R^2 value is a statistical measure of the functional dependency of two variables under consideration, in this case the regression line of the shear data. The closer R^2 is to one, the better the fit of the data to the line. Table 6.10 shows the initial shear strength, friction coefficient, mortar strength as well as the R^2 value. The internal angle of friction is also given for ease of comparison with other studies. It can be seen that the R^2 values are all very similar to each other for the different materials, except for the AACB masonry, which has a lower value.

SANS 10164-1 (1980) gives the calculations for the characteristic shear strength of masonry. The specified initial shear strength is given as 0.35 N/mm^2 for Class I mortar and 0.15 N/mm^2 for Class II mortar. Class I mortar is defined as having a compressive strength of 14.5 MPa at 28 days, and Class II mortar as 7 MPa at 28 days. SANS 10164-1 (1980) also states that the

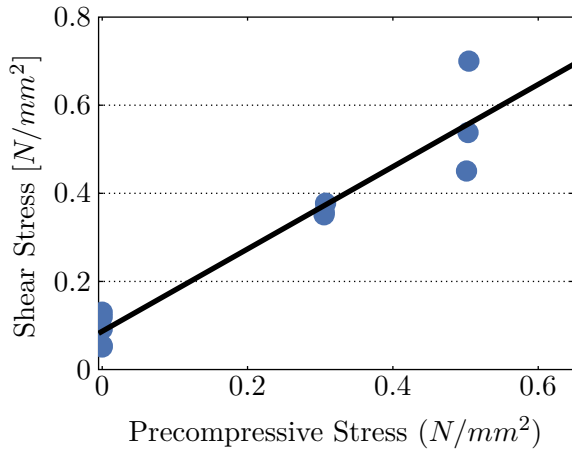
Chapter 6. Experimental Results



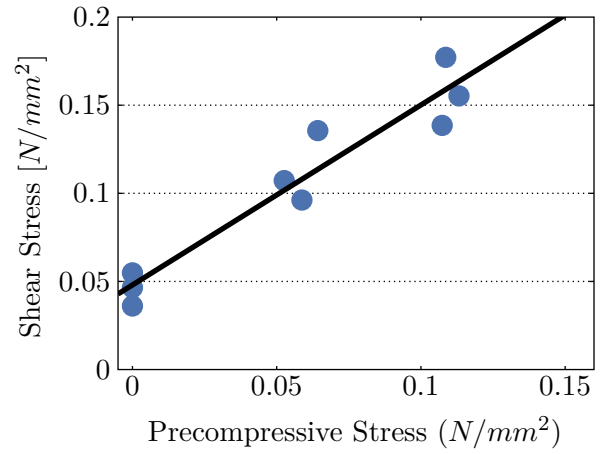
(a) CMU Triplet Specimens



(b) AACB Triplet Specimens



(c) Adobe Triplet Specimens



(d) CSEB Triplet Specimens

Figure 6.8: Shear Stress versus Pre-compressive Stress from Triplet Tests

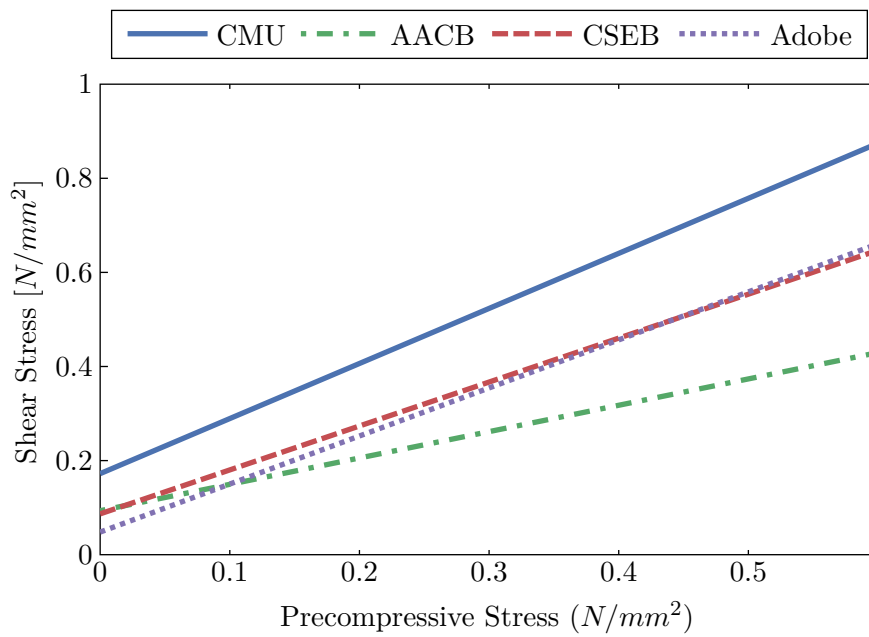


Figure 6.9: Regression Lines from Triplet Results for CMU, AACB, CSEB and Adobe

Table 6.10: Triplet Test Results

Material	CMU	AACB	CSEB	Abode
Initial Shear Strength (N/mm^2)	0.172	0.094	0.087	0.050
Friction Coefficient	1.17	0.56	0.93	1.02
Internal Angle of Friction ($^\circ$)	49.5	29.2	42.9	45.6
Coefficient of Determination – R^2	0.92	0.80	0.92	0.92
Mortar Strength (N/mm^2)	10.3	15.3	9.9	0.8

coefficient of friction must not exceed 0.6. EN 1996-1-1 (2005) states that an initial friction value of $0.20 N/mm^2$, for a mortar strength range of 10 to 20 MPa, can be assumed in the absence of experimental data.

The mortar specimens in this study were tested at the same age as the mortar in the triplet samples, namely at 7 days. Therefore, the 7 day mortar strength is used rather than the 28 day strength. From Table 6.10 it can be seen that the mortar for the CMU and CSEB falls between the two mortar classes, while the AACB mortar is above a Class I mortar. The adobe mortar is far below a Class II mortar. The differences in mortar strength is due to an attempt to create a mortar that was within 20 % of the 28 day compressive strength of its respective masonry units.

The only masonry material that resembles the initial shear strengths given by SANS 10164-1 (1980) and EN 1996-1-1 (2005) is the CMUs, with $0.172 N/mm^2$. The other materials are far below the lower value of $0.15 N/mm^2$. However, the codes were developed for conventional masonry (such as concrete and clay bricks) and not AMUs. This implies that when designing with AMUs, the initial shear strength values must be investigated to ensure they are sufficient for masonry design. The adobe specimens, in particular, had only one third of the initial shear strength that the code specified. This was due to the very low strength of the adobe specimens, the weakness of its cohesion, and the low mortar strength. The adobe specimen contained no stabilising content, and therefore it's outer surface could be scratched or pulled off with great ease. The unit-mortar interface was therefore particularly weak for the adobe.

Conversely, the coefficient of friction given by SANS 10164-1 (1980) is much lower than that of the masonry materials investigated. The AACB masonry was the only material that was slightly lower than the codes value. The low coefficient of friction from the AACB specimens was due to the extremely smooth nature of the unit's faces. Whereas, the other materials had a coarse outer face that allowed a good bond between the mortar and the masonry units, the AACBs also contained little air voids or indentations for the mortar to join to. From inspection it could be seen that the friction coefficient gave a good indication of the roughness of the different material's unit faces. The CMU had the coarsest face, followed by the adobe, then the CSEB and finally the AACBs. This corresponds with the order of decreasing friction coefficient.

It is important to note that the bond between block and mortar is not controlled by just the block but also by the mortar and the entire masonry system. An investigation into the appropriate

mortars for AMUs is well beyond the scope of this study and further research is required to determine which mortars are most suitable for different AMUs. For instance, Heath et al. (2012) shows that sodium silicate based mortars are the most appropriate for use on unstabilised load-bearing earth masonry, rather than cement based mortars. It is therefore possible that other AMUs will also function better with different mortars than those investigated in this study.

The failure of most triplet tests was due to shear failure in the unit-mortar joint (failure Type A1/1 and A1/2 in Figure 3.14). Figures 6.10a and 6.10b show examples of A1/1 and A1/2 failure, respectively. The only other failure type that occurred for certain units was failure by crushing or splitting of the units (failure Type A3). Failure Type A3 only occurred in the CSEB and adobe specimens due to their low compressive strength, and the results from those tests were discarded.



(a) Failure Type A1/1



(b) Failure Type A1/2

Figure 6.10: Shear Failure Types from Triplet Tests (a) Failure Type A1/1 (b) Failure Type A1/2

6.7 Compressive Strength of Masonry Results

The compressive strength of masonry wallets was determined through the procedure set out in Section 5.7. Four masonry wallets were tested for the CMU, AACB, CSEB and adobe materials. The compressive strength of the wallets was determined from the specimens tested to destruction. Modulus of elasticity tests were conducted on three of the specimens before destruction.

The compressive strength of the masonry units is shown in Figure 6.11, along with the standard

deviation indicated with the use of error bars. The results show expected trends, with the AACBs having the highest strength and the CMUs being slightly weaker, followed by the CSEB specimens and finally the adobe specimens. This correlates with the strengths of the individual masonry units for the different materials. An in depth comparison of these strength results are compared with the masonry unit results in Section 7.1.1.

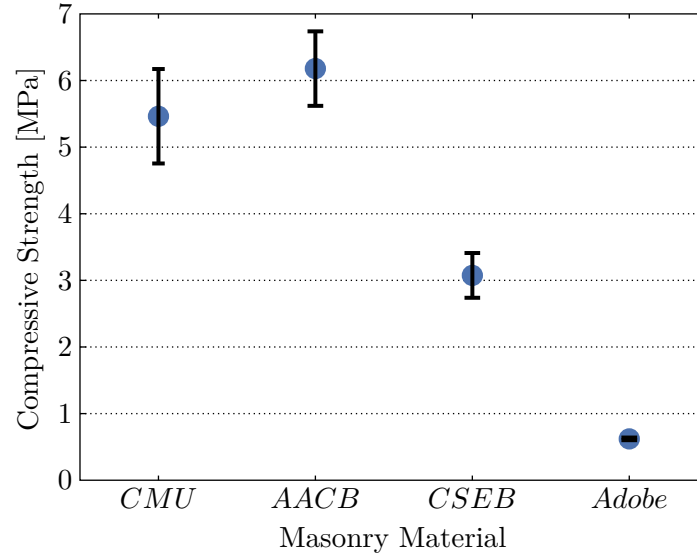


Figure 6.11: Compressive Strength of Masonry Wallets

The modulus of elasticity was determined for only three of the four wallets. This was due to the first wallet of each material being tested to destruction without LVDTs. Once the first wallet was tested, the maximum wallet compressive strength was known and in the following tests the LVDTs could be removed before failure, thereby avoiding damage to the equipment. Figure 6.12 shows the average modulus of elasticity determined for the three wallets of each material. The standard deviation was once more indicated through the use of error bars.

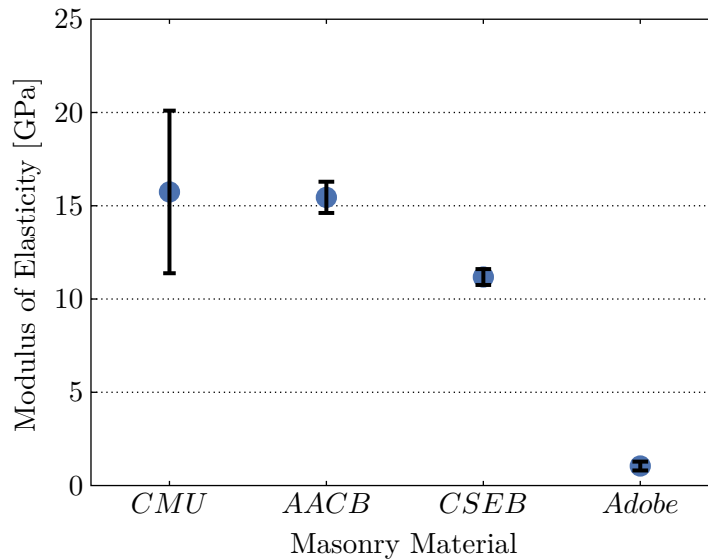


Figure 6.12: Modulus of Elasticity of Masonry Wallets

A comparison between the modulus of elasticity results from the wallets with the results from the individual cylinders shows similar trends between the masonry units and the masonry tests,

with the largest modulus of elasticity measured for the CMUs and then decreasing from the AACBs to the CSEBs to the adobe specimens. The compressive strength is compared with the modulus of elasticity in Section 7.1.2.

There were concerns with the CMU's modulus of elasticity results. At the time of testing the CMU modulus of elasticity only three LVDTs were available, resulting in one corner of the wallet not having an attached LVDT. This increased the variability in the test by a large margin, with one wallet's modulus of elasticity result being classified as an outlier. Therefore, only two results were recorded for the CMU, and as can be seen in Figure 6.12, there is a large standard deviation between these two results. For this reason it is recommended that the modulus of elasticity results for the CMU wallet be retested at a future date. All AMUs wallets were tested with four LVDTs and it can be seen that their standard deviation is acceptable.

Table 6.11 shows the masonry wallets compressive strength and their modulus of elasticity, along with the COV for both results. It can be seen that a higher strength does not necessarily mean a higher modulus of elasticity, as shown by the AACB wallets having a greater strength than the CMU, but a lower modulus of elasticity.

Table 6.11: Compressive Strength, Modulus of Elasticity and COV Results from Masonry Wallets

Materials Results	CMU		AACB		CSEB		Adobe	
	Mean	COV	Mean	COV	Mean	COV	Mean	COV
Strength (MPa)	5.5	(13 %)	6.2	(9 %)	3.1	(11 %)	0.6	(3 %)
Elastic Modulus (GPa)	15.7	(28 %)	15.5	(5 %)	11.2	(4 %)	1.0	(23 %)

The loading rates for the different material types were chosen so that failure of the wallet occurred between 15 to 30 minutes. However, the loading rate was estimated due to the final strength of the wallets not being known beforehand. In an attempt to reduce variability, once a loading rate was chosen for a material, it was kept constant for all subsequent wallets of that material, even if the resulting testing time did not fall precisely in the guidelines. As mentioned in Section 5.7, the loading rates for the CMU, AACB, CSEB and adobe specimens were 0.33, 0.3, 0.25 and 0.2 mm/min respectively. To check whether these loading rates were within the guidelines of BS EN 1052-1 (1999), the time until failure of each wallet was recorded. The average of these times were 14.4, 16.0, 12.1 and 24.8 minutes for the CMU, AACB, CSEB and adobe wallets respectively. It can be seen that two of these times were slightly under the guidelines of BS EN 1052-1 (1999), due to overestimation of the required loading rate. The adobe specimens had a far longer testing time (yet still within the guidelines) due to the material having a much lower strength than the other materials, but only a slightly lower loading rate.

6.7.1 Masonry Failure Mechanisms

During the tests conducted on the masonry wallets, the mode of failure was recorded with both written descriptions and photographs. The failure modes of the different materials were

remarkably similar. However, the adobe specimens showed some deviation from the general failure modes.

The masonry wallets predominately failed due to splitting, with a vertical crack forming down the head face of the specimens. Figure 6.13 illustrates two representative wallets (one CMU and one AACB wallet) showing the vertical crack pattern parallel to the loading direction. The CSEB and some of the adobe specimens also showed the same cracking pattern. This failure mode was also observed by other researchers (Feng et al., 2012; Vermeltfoort et al., 2007; Sassoni et al., 2014).



Figure 6.13: Vertical Crack on Head Face of Masonry Wallet

Another general occurrence in the wallets was crushing at the top course of the masonry units, causing some spalling of the material. The crushing of the masonry wallets rarely continued past the top course of masonry units. This was due to the failure by vertical splitting before the load increased enough for crushing of the second course of masonry.

While the cracking pattern seen in Figure 6.13, occurred in almost all specimens at failure, the side face cracking pattern differed between the wallets. However, three main cracks were recorded in nearly all wallets on the large side face. Figure 6.14 shows two representative wallets with all three cracking patterns, labelled as Cracks 1, 2 and 3. These cracks generally occurred in one of four variations. Either Cracks 1 and 3 would occur (such as Figure 6.13a), or Cracks 1 and 2 (such as Figure 6.13b), or Cracks 2 and 3, or Crack 2 would occur alone. While these cracks contributed to failure, final failure only occurred when the vertical splitting crack suddenly increased in size. Minor cracks would also occur across the large side face of the specimen, especially in the top two courses of masonry units.

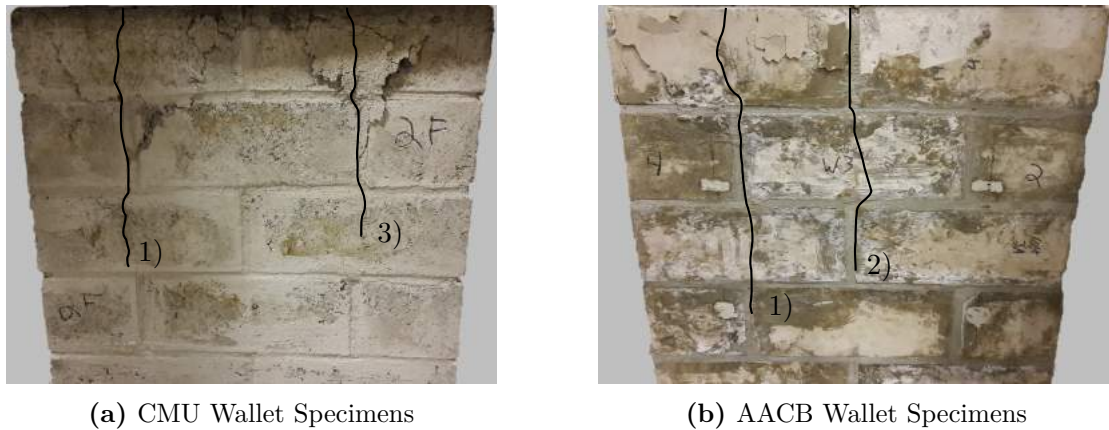


Figure 6.14: Crack Pattern on Side Face of Masonry Wallet

The load at which the cracking of the specimens first occurred could not be deduced from the load-deformation diagrams. This was due to the cracks forming slowly and initiating at several places at once. Instead, through visual assessment it was determined that the cracking became visible at approximately 70 to 85 % of the maximum load. This coincides with observations by Vermeltfoort et al. (2007).

As mentioned earlier the adobe wallets failed in a slightly different manner to the other materials. Firstly, a larger amount of crushing occurred at the top course of masonry units in the adobe wallets, most likely due to the weakness of the material. Secondly, while some of the adobe wallets showed a small vertical crack on the head side, failure mainly occurred due to Cracks 1, 2 and 3 described above. The most common failure mode was due to a large crack at 2, with occasional smaller cracks occurring at 1 and 3.

6.8 Conclusion

This chapter documented the results obtained from the mechanical tests conducted on the CMU, AACB, CSEB and adobe materials. Tests were conducted to determine the compressive strength of individual masonry units, modulus of elasticity, Poisson's ratio, fracture energy, density, shear characteristics of the mortar/unit joint and the compressive strength of masonry wallets. While most of the tests can be classified as a success with regards to the reliability, the results from Poisson's ratio tests were not successful and are therefore discarded.

For each material property, the results are given in graph and table format, as well as a discussion of any relevant observations or concerns from the results. This chapter only discussed the material properties separately, whereas Chapter 7 discusses the interactions between the various material properties as well as the effectiveness of the test set-ups for determining these properties.

As a summary, Table 6.12 shows the main results from all the tests conducted on the units. Due to the issues with the Poisson's ratio test results, they are not included in the table.

Table 6.12: Main Results from All Tests Conducted in this Study

Material Property	Units	CMU	AACB	CSEB	Adobe
Compressive Strength of Unit Tests					
Bedface					
7 days	MPa	7.81	8.67	3.14	-
14 days	MPa	10.07	14.21	5.48	0.75
28 days	MPa	12.09	17.89	6.55	0.80
56 days	MPa	13.30	19.37	7.91	0.81
91 days	MPa	16.54	18.09	7.87	0.82
Headface					
28 days	MPa	5.84	11.33	5.82	0.44
Modulus of Elasticity Tests					
Modulus of Elasticity	GPa	17.9	11.0	7.5	2.5
Wedge Splitting Tests					
Splitting Force	N	692	1183	871	116
Tensile Strength	MPa	0.14	0.25	0.18	0.03
Fracture Energy	N/m	121	138	114	22
COD	mm	0.75	0.40	0.20	0.19
Density Tests					
Density	kg/m ³	2090	2080	1822	2007
Triplet Tests					
Initial shear strength	N/mm ²	0.172	0.094	0.087	0.050
Friction Coefficient		1.17	0.56	0.93	1.02
Compressive Strength of Masonry Tests					
Compressive Strength	MPa	5.5	6.2	3.1	0.6
Modulus of Elasticity	GPa	15.7	15.5	11.2	1.0

Chapter 7

Comparisons and Discussions

This study considered various mechanical properties of concrete masonry units (CMUs), alkali-activated concrete blocks (AACBs), compressed stabilised earth blocks (CSEBs) and adobe blocks. These mechanical properties help to better understand the alternative masonry units (AMUs) and can also be utilised in numerical modelling of masonry structures. Though these results are useful in these regards, a major goal of this study is to determine whether standards and tests used for conventional masonry can also be utilised for a wide range of alternative masonry.

The compressive strength of masonry is one of the most commonly tested material properties and is closely linked to the durability of masonry, thereby giving an indication of quality. However, other mechanical properties of masonry also influence how a building behaves during its lifespan and are often linked to each other.

This chapter first discusses prediction methods given in literature or international standards that are used to determine mechanical properties of masonry. These prediction methods use the interconnectedness of the mechanical properties to determine properties that are difficult to achieve experimentally.

A second section is then dedicated to discussing the test set-ups and whether it was found that these set-ups properly categorised the mechanical properties of the AMUs. All the test set-ups that were used are discussed, namely the compressive strength test for individual masonry units, modulus of elasticity test, Poisson's ratio test, wedge splitting test, density test, triplet test, and the compressive strength tests for masonry wallets.

7.1 Prediction Methods

The factors influencing the material properties of masonry are often interlinked and researchers have used this to develop prediction methods. These prediction methods are employed by international standards to determine certain material characteristics that are more difficult to discover experimentally.

As this study conducted an extensive investigation into the different material properties of

masonry, both sides of the prediction methods are generally known. For example, prediction methods exist to determine the compressive strengths of masonry from the compressive strength of individual masonry units. This investigation has results for both of these, and therefore the accuracy of prediction methods for the materials in this study can be examined.

This section discusses prediction methods relating compressive strength of masonry and units as well as compressive strength and modulus of elasticity. An important caveat is that many of these prediction methods were developed for only conventional masonry units, such as clay bricks or concrete blocks, and therefore the AMUs of this study does not always fit the prediction methods.

7.1.1 Compressive Strength of Units and Wallets

For all construction projects, including low income housing, the strength of the masonry is important as it yields values required for structural design. Design codes such as EN 1996-1-1 (2005) recommend that these values be tested for in masonry specimens that include the mortar/unit joint in order to give the best indication of the real uniaxial compressive strength of masonry normal to the bed joints. However, a simplified method is given in Annex D of EN 1996-3 (2006) to determine the characteristic strength of masonry from the normalised mean compressive strength of a masonry unit and the mortar class.

According to EN 1996-3 (2006) the mortar classes are determined according to their compressive strength, and are classified as the letter M followed by the compressive strength in N/mm^2 . The mortars of the CMU, AACB, CSEB and adobe masonry specimens are classified as M10, M13, M9 and M1 respectively. Section 6.1.2 already determined the normalised bedface strengths of the masonry units at 28 days (f_b), with these values given in Table 6.3.

Using these values and Annex D of EN 1996-3 (2006), the characteristic compressive strength of masonry determined from the simplified method ($f_{k,s}$) can be determined. These values are compared here with the characteristic compressive strength of masonry (f_k) determined from the compressive strength tests. Figure 7.1 shows the $f_{k,s}$ and f_k values for the different material types.

It can be seen that the f_k values are different from the mean compressive strength results given in Section 6.7. This is due to the fact that the results in Section 6.7 are the mean compressive strengths, while the f_k values are the characteristic compressive strengths. EN 1996-3 (2006) states that the characteristic compressive strengths are to be taken as the smallest of either the minimum individual masonry wallet strengths or the mean strength divided by 1.2. For this study the mean compressive strength divided by 1.2 always resulted in the lower value and was therefore used as f_k .

The results from Figure 7.1 show that the actual characteristic compressive strengths are lower than those calculated with the simplified method for all materials considered. This is a cause for concern as the values from the simplified method are expected to be more conservative.

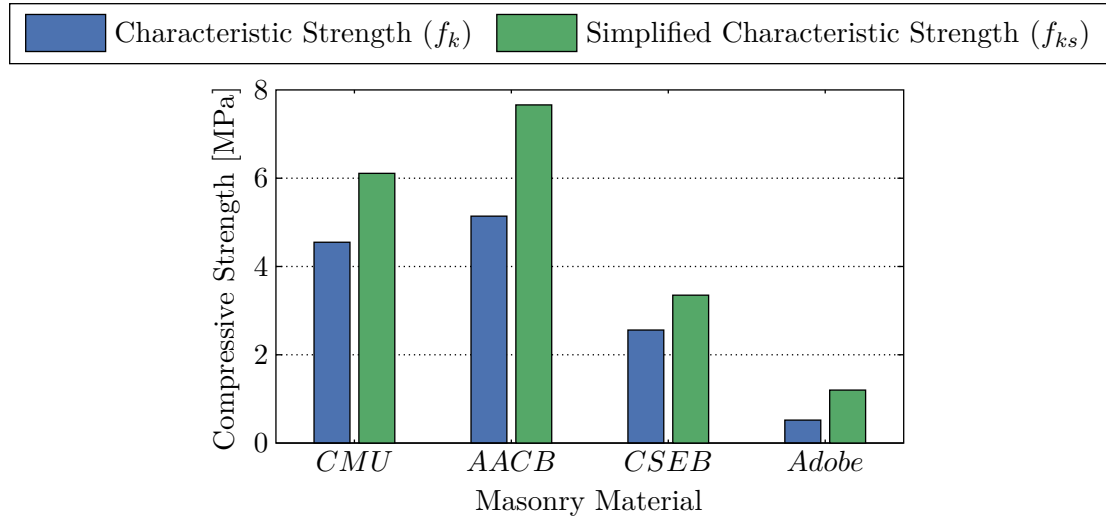


Figure 7.1: Comparison Between Characteristic Compressive Strength from the Tests (f_k) and the Characteristic Compressive Strength of Masonry Determined from the Simplified Method ($f_{k,s}$)

Both the CMU and the CSEB characteristic compressive strengths are approximately 75 % of the simplified method, while the AACB units were only 67 % of the simplified method. The adobe units were added to Figure 7.1, however the simplified tables in Annex D have a minimum value of 1.2 MPa, which is more than double the adobe results.

It is important to note that the values taken from Annex D in EN 1996-3 (2006) are for concrete containing aggregate and therefore were designed only for the CMU material. This helps explain the unexpected results of the AMUs but does not explain why the simplified CMU values are so high.

7.1.2 Compressive Strength and Modulus of Elasticity

Various predictions methods are given in literature to determine the secant modulus of elasticity of masonry from the other mechanical properties of either the masonry or masonry units. One such prediction method is given by EN 1996-1-1 (2005) in Clause 3.6.1, which relates the modulus of elasticity to the characteristic compressive strength of masonry. Another prediction method is a composite model that uses the compressive strength of the masonry units and mortar, as well as the effect of water absorption from the mortar to determined the modulus of elasticity of the masonry (Brooks, 2015).

The relationship from EN 1996-1-1 (2005) is given as $K_E f_k$, where K_E has a recommended value of 1000 and f_k is the characteristic compressive strength of masonry. The characteristic compressive strength has already been determined in Section 7.1.1. This relationship shows that the modulus of elasticity (in GPa) is numerically equal to the characteristic strength (in MPa). This is an oversimplification that is assumed to be conservative.

The composite model for concrete blockwork as discussed by Brooks (2015) was developed by using a relationship between the modulus of elasticity of the masonry (E_{wy}), blocks and mortar. However, as the modulus of elasticity of the blocks and mortar are not always known, their

values are substituted with functions relating the strength of the mortar (f_m) and units (f_b) to their modulus of elasticity. The relationship is given by the equation:

$$\frac{1}{E_{wy}} = \frac{1.058}{f_b} + \frac{A_m}{A'_m} \frac{0.06}{\gamma_e f_m} \quad (7.1)$$

where A_m and A'_m are the gross and net area respectively, and γ_e is the mortar elasticity reduction factor. For this study solid units are investigated where the gross to net ratio is taken as 1. Brooks (2015) states that if the units are wetted or docked before laying then the mortar elasticity reduction factor can be taken as 1, which is done in this study.

Figure 7.2 shows a comparison between the prediction method from EN 1996-1-1 (2005), the composite model, and the values determined from the experimental tests. The results show that the method given by EN 1996-1-1 (2005) vastly underestimates the modulus of elasticity of the masonry, while the composite method gives closer, but still mostly underestimated, results. It should be noted that the method from EN 1996-1-1 (2005) was developed only for conventional masonry and the composite model was developed for only concrete masonry.

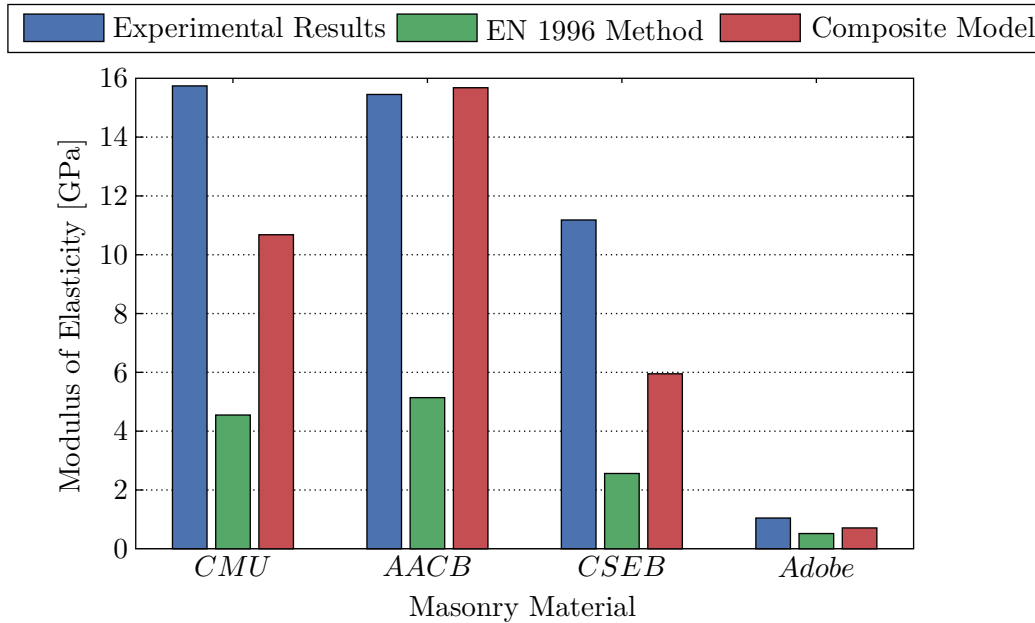


Figure 7.2: Comparison Between the Modulus of Elasticity Determined from Experimental Results, a Prediction Method given by EN 1996-1-1 (2005) and a Composite Model

The prediction method from EN 1996-1-1 (2005) is a very simplified approach and as expected is conservative towards the experimental results. However, the values are perhaps more conservative than would be appropriate and can be deemed as inaccurate for this study. Brooks (2015) also found that EN 1996-1-1 (2005) underestimated the modulus of blockwork.

The composite model gave much closer results to the experimental tests, but were also conservative for the CMU, CSEB and adobe specimens. The results from the composite model for the AACB modulus is slightly larger than those of the experimental tests. This could relate back to the low modulus of elasticity of the AACB units (see Section 6.2), as the composite model was

not designed for AACB masonry.

7.1.3 Concluding Remarks

The prediction methods shown in this section demonstrate the relationship between the compressive strength of units and masonry specimens, as well as the relationship between the compressive strength and modulus of elasticity of masonry.

EN 1996-3 (2006) simplified method of determining a masonry specimen's compressive strength is shown to overestimate the results from the experimental tests. The overestimation of the concrete based masonry units is approximately 25 % while that of alternative materials is even higher. This overestimation of the CMU specimens is unexpected as traditionally a simplified method of determining a material characteristic provides a conservative result. Therefore it can be concluded that the masonry specimens investigated in this study are weaker than average when related to the individual masonry units strength. The weakness of the adobe and CSEB specimens are, however, not as unexpected as they have much lower strengths than conventional concrete.

The prediction method from EN 1996-1-1 (2005) and the composite model from Brooks (2015) compared the compressive strength of units and wallets with the modulus of elasticity. Both prediction methods showed a conservative results when compared with the experimental results. The prediction method from EN 1996-1-1 (2005) resulted in a much lower modulus of elasticity than that of Brooks (2015), which, according to Brooks, is to be expected. The amount with which the experimental results are larger than the prediction models indicates that the moduli of elasticity for these materials in this study are higher than those used to develop the prediction models. The exception is the AACB, whose low unit modulus of elasticity led to a lower masonry wallet modulus of elasticity.

7.2 Suitability of Test Set-ups

To allow for the further development and acceptance of AMUs the characterisation and evaluation of their mechanical properties is necessary. Many standardised tests were implemented in this study, however these tests were developed for conventional masonry units. It must therefore be determined if these tests are suitable for use on AMUs due to the difference in material properties between AMUs and conventional masonry units.

This section discusses the results from the experimental tests in order to determine if the tests were successfully executed on the AMUs. Each test that was conducted is discussed, namely: the compressive strength tests on masonry and masonry units, modulus of elasticity, Poisson's ratio, wedge splitting, density and triplet tests.

7.2.1 Compressive Strength of Masonry Units Test

The compressive strength test procedure and set-up (explained in Section 5.1) produces one of the most important mechanical characteristics of masonry, namely the compressive strength of individual masonry units. The procedure set out by BS EN 772-1 (2011) for determining compressive strength is used on clay, calcium silicate, concrete, autoclaved aerated concrete, manufactured stone and natural stone masonry units. The mechanical properties of these materials vary to different degrees from those investigated in this study.

The uncomplicated nature of the test procedure made it easy to apply for all masonry materials in this study. The fact that all masonry units had the same dimensions also helped with reducing the complications in the testing procedures and removing the need for aspect ratios when comparing between materials.

Currently, the most common testing procedure for determining the compressive strength of conventional masonry units and AMUs is direct, confined tests on single units (like those used in this study). It can be seen from the discussion in Section 6.1.1.2 that this test produced consistent results with those found in literature for all material types investigated and that none of the materials showed signs of major problems during the tests.

Nonetheless, a few areas of concern exist with regards to implementing the results of the tests in standards. In this study all specimens had the same dimensions and therefore results could easily be compared. However, in practice masonry units come in a variety of shapes and sizes. Clay brick masonry is often the most geometrically consistent, followed by concrete masonry. Conversely, CSEBs and adobe blocks have almost no standard sizes.

Units with various sizes result in different amounts of restraint being applied to the units, thereby changing the compressive strength results (see Section 3.1). Different methods exist for standardising these units. The most efficient method would be to adopt a few standard masonry block sizes for the materials. This would be similar to the standardisation of concrete tests through the use of cubes and cylinders. However, this method is unlikely to be implemented simply due to the difficulty in converting existing systems. A method applied by the European standards (EN 1996-1-1, 2005) is to group the masonry units according to their geometrical specifications.

Another method that is implemented is the use of aspect ratios as geometric correction factors, thereby removing the platen restraint effect. This is often used on clay and concrete masonry units as they have had extensive study into their aspect ratios. However, when applying this method to AMUs such as CSEB or adobe, the same aspect ratios are applied as for the conventional masonry. These aspect ratios show great variation when applied to the AMUs, and may be unsuitable without further research (Morel et al., 2007; Aubert et al., 2013).

If one of these methods is not researched and applied to AMUs then the next step would be to implement a different test procedure for testing the compressive strength of alternative masonry. Two possible testing methods that could be applied are a three point bending test or a stack bonded prism (Morel et al., 2007), however both come with their own concerns as well.

The three point bending test is considered an indirect compressive strength test and the forces required are 80 to 150 times lower than those required for direct compressive tests. While this is advantageous as it allows greater ease for on site testing, the adobe specimen's low strength may cause difficulty with such a test. The test is also subject to considerable scatter (Morel et al., 2007). This scatter may become more pronounced with AMUs, especially those with low strengths.

The stack bonded prism was proposed by the RILEM Technical Committee 164, for the testing of compressed earth blocks. The platen restraint effect is reduced by halving the blocks and then stack bonding them using an earth mortar bed joint. This method reduces the effect of the block geometry, however it may give masonry strengths rather than masonry unit strengths. The results are also reliant on the mortar characteristics as well as the quality of preparation of the prism (Morel et al., 2007).

It is clear that further research is necessary in order to understand the geometric effects on compressive strength characteristics if a standardised test procedure is to be developed and widely accepted for AMUs. However, for the purpose of this study the unit compressive strength testing procedure provided acceptable results for all the AMUs.

7.2.2 Modulus of Elasticity Test

The modulus of elasticity test procedure followed (BS EN 12390-13, 2013) was developed for testing cylinders of hardened concrete. A standard testing procedure could not be found that specifically tests the secant modulus of elasticity of individual masonry units. It is more common to see the modulus of elasticity of masonry prism or wallets studied in literature and not that of individual units.

However, when the modulus of the individual masonry units are tested, they are usually tested on masonry bricks or blocks and not on cylinders. Due to the low height of most masonry units, the modulus is more commonly calculated between header faces, i.e. in the headface orientation shown in Figure 5.2 and not the bedface orientation. Fewer sources look at the modulus in the bedface orientation.

Brooks (2015) showed that pressed and extruded clay bricks, as well as calcium silicate bricks, are anisotropic, i.e. the bedface and headface modulus of elasticity differ. He also showed that solid concrete blocks are isotropic.

Due to the methods of forming material in this study it was assumed that the units would be anisotropic, with the possible exception of the AACBs. This was due to the nature of the forming process employed for the units. Both the CMU and CSEB units were compacted in the bedface orientation in the block press, which resulted in different densities along the height of the units. The adobe specimens were also compacted in the bedface orientation, with possible differences in the density and thereby the strength, over the height of the units. The AACBs was the only material that was cast in a method similar to concrete, thereby reducing the likelihood of anisotropic behaviour.

While most studies look at individual masonry units in block form, certain studies conduct tests on cylinders extracted from buildings or from the cores of masonry units (Martins and Varum, 2006; Brooks, 2015). Brooks (2015) showed that modulus of elasticity results from tests conducted on cylinders cored from concrete blocks gave similar results to tests conducted on the blocks themselves. However, the act of drilling cores may have changed the specimen properties, especially for low strength materials.

In order to determine the bedface modulus of elasticity, tests were not conducted on blocks but rather on cylinders that were created in such a manner that they were representative of the masonry in the bedface orientation. This allowed results to be compared with the bedface strength results. The methods of creating these cylinders for the different materials are discussed in Chapter 4.

Every effort was made to ensure that these cylinders resembled the masonry block's strength and modulus of elasticity. In order to check these results the 28 day strength of the masonry blocks is compared with the strength of the cylinders in Figure 7.3. The block results have been multiplied by a 0.8 shape factor to convert them to cylindrical strengths. This is not completely accurate as this shape factor was determined for cube to cylinder shapes.

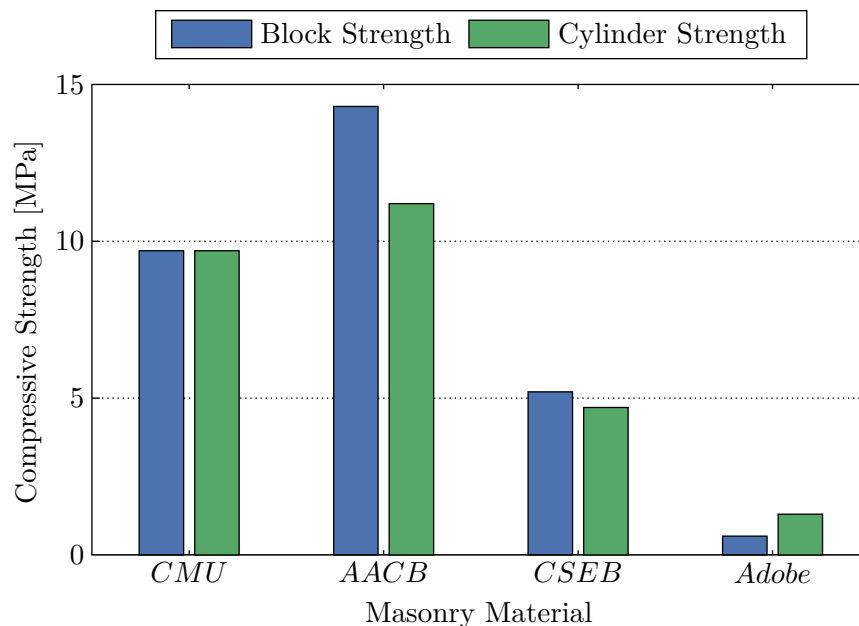


Figure 7.3: Comparison Between Block and Cylinder Compressive Strength

The results from Figure 7.3 show a close correlation between the block and cylinder strengths for the CMU and CSEB materials. This shows the compaction method for the cement based cylinders was successful. The AACB results showed a greater difference between blocks and cylinders. These results are unexpected as both the cylinder and block units were simply cast in the same manner as conventional concrete. The discrepancies in the results could therefore be due to unintended variations in the mixing and casting procedure, or it may be that the shape factors developed for concrete do not apply to alkali-activated concrete (AAC) materials. The adobe results differed by a large degree, however the compressive strength tests conducted on

the adobe cylinder specimens were conducted in a testing machine which has difficulty recording low strengths. Therefore, the strength results of the adobe cylinders are considered to be testing errors. Even with the checks conducted on the cylinders, it is possible that the specimens used in the modulus of elasticity tests are not exact representations of the blocks.

The testing procedure conducted on the cylinders did not produce any issues that would indicate that they could not be used for the AMUs and the modulus of elasticity values were found to be within acceptable ranges. However, without conducting separate modulus of elasticity tests on bedface and headface specimens it is not possible to fully determine the effectiveness of the tests on the cylinders.

The modulus of elasticity results for the adobe specimens are suspect due to the fact that they are nearly 10 times that found in literature, however a direct comparison is difficult due to the inherent variability in adobe masonry. There are a few possible reasons for this discrepancy. Firstly, the adobe created in this study may naturally have a much higher modulus of elasticity than found in some other studies. Secondly, the method of creating the adobe specimen cylinders in this study may have influenced the mechanical results and therefore not be suitable. Lastly, the modulus of elasticity set-up implemented in this study may not be suitable for testing the very weak adobe.

In conclusion, this study found no reason that the testing method of cylinders could not be implemented on alternative masonry materials. However, it is recommended that the results be compared to tests conducted on blocks in the headface and bedface orientation. It is also recommended that taking core samples from the blocks be investigated as a method that produces results with less chance of variability. Finally, it is recommended that the modulus of elasticity of adobe specimens be reinvestigated to determine what caused the high modulus of elasticity results.

7.2.3 Poisson's Ratio Test

Section 6.3 showed that the results from the Poisson's ratio tests were unsatisfactory. It was also concluded that the problems were due to the test set-up and not the calculations. It can also be seen from the results that this error was not isolated to the various AMUs, but that the CMU was also affected.

To try and determine the cause of the error the raw data from the tests were investigated. Figure 7.4 shows the stress versus transverse strain results from a typical test on the cylinders. From the figure it can be seen that Strain 1 was positive while Strain 3 was negative. Strain 2 was similar to the average of the three strains. These results are typical of all the tests investigated and indicate that the specimens likely underwent bending during the test procedure.

Due to the very small displacements measured in order to determine Poisson's ratio, the bending of the specimen could have a major influence on the end results, to the point where they must be discarded. As the Poisson's ratio and modulus of elasticity tests were conducted on the same specimen, it means that the modulus of elasticity results were also affected by the bending.

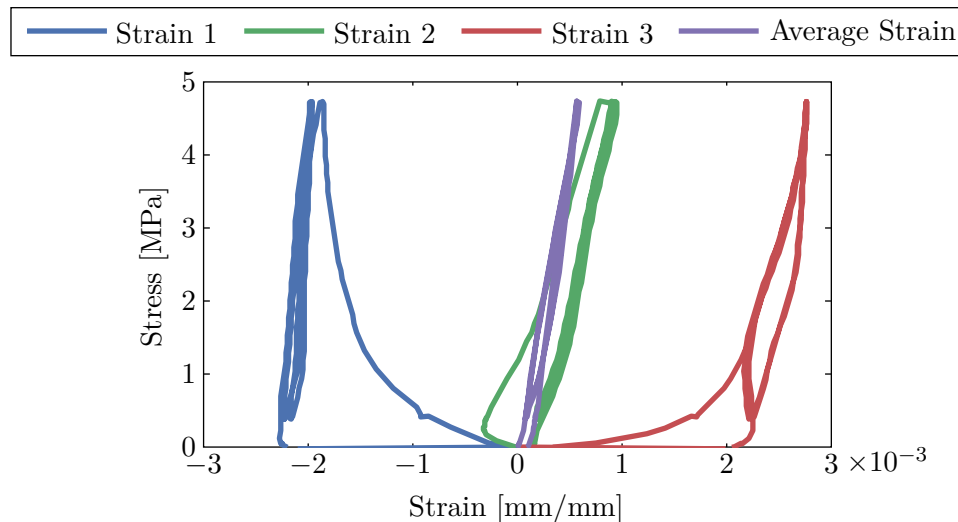


Figure 7.4: Typical Stress/Strain Curve from Poisson Tests

Therefore, even though the modulus of elasticity results fall within recognised ranges, the final values are suspect due to the bending of the specimens. However, they seem to be less affected than the Poisson's ratio results.

There are two possible reasons for the specimens to undergo bending in the set-up. The first possibility is that the specimens were misaligned within the test set-up. The alignment of the specimens is important to ensure that only vertical forces are applied to the cylinders. While pot bearings were placed in the test set-up, it is possible that there was little room for self-levelling once the specimens made contact. The second possibility is that the set-up lacked stiffness in the supporting base. The test set-up's base was a portion of a steel I-section with plate stiffeners welded to the web. Due to the relatively low forces applied to the weak AMUs it was assumed this would be sufficient.

A few recommendations can therefore be made to improve the chances of preventing the bending of the specimens:

- Take extreme care in placing the specimens centrally to ensure the pot bearings have to do as little self levelling as possible
- Grease the pot bearings
- Ensure the base of the set-up and the testing machines actuator are perfectly parallel
- Stiffen the base of the set-up by welding additional plates onto the sides of the I-section

Another possible reason for the failure of the Poisson's ratio tests may be that the method employed with the three linear variable differential transducers (LVDTs) was not suitable for measuring the transverse strain of the cylindrical specimens, and that this coupled with the bending caused the test to fail. However, no definitive reason could be found for this method to not provide satisfactory Poisson's ratio results and it is thought that the bending is the most likely culprit. It is not believed that the creation of the cylinders was at fault for the flawed results as the different material's cylinders were created with different methods, yet all gave

equally flawed results.

In conclusion, it is believed that the bending of the specimens negatively influenced the Poisson's ratio results to such a degree that they could not be used. The modulus of elasticity results would therefore also have been influenced and it is recommended that future studies once again investigate these tests with an emphasis on preventing the bending of the specimens. It is unclear to what extent the modulus of elasticity results were influenced as they still fell within acceptable ranges. The issues with this test are not related to the alternative materials tested but rather the set-up itself, therefore it is predicted that if the bending of the specimens can be prevented, then these tests can be applied on AMUs.

7.2.4 Wedge Splitting Test

The wedge splitting test is not prescribed by any international standard, however due to the advantages mentioned in Section 3.4 it was chosen as the method to determine the fracture energy of the masonry specimens. From the results in Section 6.4 it can be seen that the fracture energy determined from the wedge splitting tests coincided with results from literature.

The CMU and CSEB specimen's results are very similar to those determined from the equation by Wittmann (2002). The AACB's results are not the same as that calculated from the equation, however as the equation was derived for concrete specimens this was expected. The AACBs showed no signs of not behaving properly in the test set-up, as its tensile strength was even higher than the cement based materials. It is concluded that the wedge splitting set-up does properly determine the fracture energy of these materials.

Difficulty was encountered with the adobe specimens in the wedge splitting tests. The extremely weak nature of the material made it difficult to properly test and the resultant coefficient of variation (COV) percentages are very high. However, this issue was due to the weak nature of the material itself and less with the testing method.

Four methods for determining fracture energy are given in Section 3.4, namely the uniaxial tensile test, the notched three point bending test, the compact tension test and the wedge splitting test. Of these four the wedge splitting method was chosen as the most suitable candidate. It is doubtful if one of the other methods would have performed better with the adobe specimens.

The uniaxial tensile test is a difficult test to execute, and the very low tensile strength of adobe would result in even more complications. However, without conducting such a test it is impossible to conclusively say if it would be worse than the wedge splitting test, especially if very sensitive equipment is employed.

The three point bending test would most likely not have been an appropriate method for the adobe material as it is documented that the self weight of the concrete specimen influences the fracture energy. The adobe's extremely low fracture energy would therefore be greatly influenced by the self weight of the specimen. The compact tension test has a very compact specimen shape

that would be difficult to form with the low strength adobe specimens, and a specimen of its shape and size would be easily damaged or destroyed.

For these reasons it is believed that the wedge splitting test is still the best option for determining adobe fracture energy. It is recommended that future tests on adobe specimens with the wedge splitting method be conducted with a testing machine that is capable of a lower pre-load, thereby possibly reducing the variability in the tests.

In conclusion, the wedge splitting test method employed on the alternative materials was successful for all materials but with high variability on the adobe specimens. Nonetheless, it is still recommended that this method be employed for determining fracture energy, with the possibility of more sensitive equipment being employed.

It should be noted that unlike traditional wedge splitting tests on conventional concrete that can easily be cast into any shape, this study looked at masonry units that were solid and rectangular. Therefore, extra effort was required to create specimens of the correct shape for the wedge splitting test (the creation of these specimens was discussed in Section 5.4). While every effort was made to keep the wedge splitting specimens representative of the actual solid masonry specimens, there is still the chance that some of the mechanical properties were influenced. An investigation could be conducted in future studies where the wedge splitting specimens are cut from solid masonry units after 28 days, rather than crafting them at a young age.

7.2.5 Density

As with many of the previous tests, the density test from BS EN 772-13 (2000) was developed for conventional masonry units. However, the test procedure is easily applied to AMUs as well. There are no forces or loading rates that would affect the tests capabilities on weaker materials. Neither do the results from the density tests show any irregularities. It is therefore concluded that the density tests conducted in this study are applicable to alternative masonry.

7.2.6 Triplet Test

The triplet test set-up discussed in Section 5.6 according to BS EN 1052-3 (2002) was designed for masonry. However, once again it was designed for conventional masonry units. Nonetheless, in this study it is shown that the test provided good results for all the materials investigated.

However, certain adjustments were made to the guidelines provided by BS EN 1052-3 (2002), specifically to the pre-compression levels. These are explained in detail in Section 5.6. The adjustments to the pre-compression were due to the method employed to keep the pre-compression levels stable (the steel spring) and due to the low strengths of the adobe units. With the adjustments the tests were conducted successfully.

In order to determine the effectiveness of the steel spring in keeping a constant pre-compression, the percentage change of the pre-compression was measured during the entirety of each test.

Table 7.1 shows the mean percentage that the pre-compression changed during the course of the tests, both over and under the initial pre-compression. BS EN 1052-3 (2002) states that the pre-compression must be kept within $\pm 2\%$ of the initial value.

From the results in Table 7.1 it can be seen that the pre-compression increased more than it decreased during the tests, as explained in Section 5.6 this is expected. The values for the CMU and CSEB specimens are close to the 2% recommended by BS EN 1052-3 (2002), while the AACB and especially the adobe specimens are not near to this value. The large variation in the adobe specimens pre-compression can be attributed to the very low levels of pre-compression applied to it. A small change in these low levels would show as a much larger percentage, than the same change in the other specimens pre-compression. In fact, when considering the magnitude of the change rather than the percentage, the adobe specimens were very similar to the other materials.

Table 7.1: Percentage Change in Pre-Compression During Triplet Tests

Percentage Change (%)	CMU	AACB	CSEB	Adobe
Over Initial Value	3.68	8.18	2.89	31.05
Under Initial Value	2.03	0.39	1.46	1.45

As stated in Section 5.6, the set-up was comprised of many loose parts. These increased the amount of movement in the test set-up when the pre-compression was applied. For instance, when the hydraulic jack pressed on the system of channels, the entire set-up and the specimen were subjected to small movements. These stabilised once the test was under way, but created difficulties in aligning everything in the same manner for every test. This could have caused an increase in variabilities between and during the tests. It is therefore recommended that future studies look into methods of connecting the end channels to a base for the set-up, reducing the possible movements.

In conclusion the triplet test was created for testing conventional masonry, yet the test is successful on alternative materials with sufficient compressive strength. Greater difficulty is encountered for extremely weak materials, however, by adjusting the pre-compression levels, reasonable results can still be attained.

7.2.7 Compressive Strength of Masonry Test

The compressive strength of masonry was determined through tests conducted on wallet specimens. BS EN 1052-1 (1999) was used as a guideline for the tests. Once again the test was designed for use with conventional masonry units, however it was easily applied to alternative masonry.

Section 7.1 already looked at the results from the masonry tests compared with prediction models

from literature and standards. It was found that the tests were successful for measuring the strength and modulus of elasticity of the various masonry materials.

Section 5.7 mentioned that different loading rates were applied to the wallets and that this results in the strengths not being directly comparable with each other. This is due to the higher resistance of a material under a faster loading rate. However, as this study focuses on determining whether standards for testing the mechanical properties of conventional masonry units can be successfully applied on alternative materials, a direct comparison between materials was deemed to be less important than following the standards closely.

The materials investigated did not have any major issues or concerns during the tests and it can be concluded that the test is suitable for alternative materials. Various researchers have used similar wallet or prism tests on most of the materials investigated in this study, showing its suitability as a testing method (Feng et al., 2012; De Almeida, 2012; Kaaki, 2013). One recommendation for future studies is the inclusion of measurements in the transverse direction in order to determine the Poisson ratio of the masonry specimens.

7.2.8 Concluding Remarks

Section 7.2 investigated the suitability of the tests utilised in this study for alternative masonry units. All tests conducted in this study are discussed, namely tests on the compressive strength of masonry units, modulus of elasticity, Poisson's ratio, wedge splitting, density, triplet and the compressive strength of masonry wallets.

It is found that most of the tests can be successfully conducted on the masonry materials investigated in this study. For some of these tests certain adjustments are required for the weaker materials. The only test that failed to achieve satisfactory results was the test for Poisson's ratio. It is however concluded that the fault lay with the test method employed and that the failure was not due to the testing of alternative materials. Chapter 8 discusses the final conclusions from the study.

Chapter 8

Conclusion

This study investigated the mechanical properties of alternative masonry units (AMUs). There are two main objectives to this study. The first objective is to determine if standards and test set-ups for testing the mechanical properties of conventional masonry units can be successfully applied to alternative units. To accomplish this, three alternative masonry materials (compressed stabilised earth blocks (CSEB), alkali-activated concrete blocks (AACBs) and adobe blocks) were tested and compared with the results from conventional concrete masonry units (CMUs).

The second objective is the determination of reliable mechanical properties of the masonry from the tests for future use in numerical modelling. These models can be used to determine the minimum technical specifications for low income housing (LIH) in South Africa. Due to the main objectives of this study the alternative materials were chosen according to a number of criteria. The most important being that the materials needed to exhibit a wide spectrum of mechanical properties in order to put the standards and test set-up through a range of possibilities, thereby proving or disproving whether the set-ups are applicable to a wide range of materials. The other criteria for choosing the materials relate to the block's potential use for LIH in South Africa, namely low environmental impact, cost effectiveness, producibility in South Africa and if possible social acceptability. Therefore, the CSEBs, AACBs and adobe blocks were chosen.

The test set-ups and mechanical properties tested for included the following: the compressive strength of the individual units over a range of ages, at 7, 14, 28, 56 and 91 days, including both bedface and headface strength at 28 days; modulus of elasticity tests on cylinders at 28 days; tests to determine Poisson's ratio; wedge splitting tests to determine the fracture energy and tensile strength of the material; dry density tests to determine the density of the units through the use of the constant mass method; shear tests on triplet specimens that determined the initial shear strength as well as the internal angle of friction; compressive strength tests on masonry wallets through which both the compressive strength and modulus of elasticity of the wallets were determined.

8.1 Conclusions

This study showed that the test set-ups investigated were able to successfully determine the mechanical properties of both the CMU and AMUs. However, for some materials adjustments are required to successfully determine their mechanical properties. Hereafter follows the conclusions made with regards to the mechanical properties of the materials and the test set-ups.

8.1.1 Observations Made with Regards to the Mechanical Properties

- The compressive strength of the CMUs, CSEBs and AACBs increased over time, while the adobe specimens showed very little increase over time. The CMU, AACB, CSEB and adobe units' compressive strengths at 28 days were 12.09 MPa, 17.89 MPa, 6.55 MPa and 0.80 MPa respectively. Showing that the CMU, AACB and CSEB had sufficient strength (> 4.0 MPa) for single storey buildings with solid masonry units according to SANS 10400-K (2011).
- The headface and bedface compressive strength results at 28 days were normalised with shape factors given by BS EN 772-1 (2011). The results showed that the CMU, AACB and adobe normalised headface and bedface strengths are within 20 %, proving the successfulness of the shape factors. The CSEB is only within 33 % due to unusually strong headface results.
- The modulus of elasticity results for the CMU and CSEB materials are relatable to values found in literature. The stiffness of the alkali-activated concrete (AAC) material was low for a similar concrete material, however this also corresponds with results found in literature.
- The modulus of elasticity of adobe was found to be much higher than the results from literature. This was cause for concern and a number of reasons could exist for the much higher modulus of elasticity including: the adobe material in this study could have been much stiffer than those from previous studies, the method of creating the adobe cylinders could have altered the mechanical properties, or the modulus of elasticity set-up employed on the adobe specimens could have been unsuitable for such a weak material.
- While the modulus of elasticity results fell within acceptable ranges it was found that the specimens underwent bending in what should have been a uniaxial test. It is unclear to what extent this affected the final results and it is therefore recommended that these tests be redone in future studies with an emphasis on preventing any bending of the specimens.
- Poisson's ratio results are unsatisfactory due to the fact that a material cannot have a Poisson's ratio greater than 0.5 and the results are thus discarded. This was most likely due to bending of the test specimens. It is recommended that future studies reinvestigate the test set-up used to determine Poisson's ratio.
- The fracture energy of the alternative masonry materials has not been studied often in

literature, making a direct comparison difficult. Instead a comparison was made with an equation relating the maximum aggregate size to the fracture energy, however this equation was developed for concrete and mortar. It was seen that both the CMU and CSEB fracture energies were similar to the predicted values from the equation. The AACB and adobe fracture energies were much lower than those predicted by the equation. The low AACB fracture energy may be related to the low stiffness of the material, whereas the low adobe fracture energy is expected due to the extreme weakness of the material in tension.

- The triplet tests provided the initial shear strength and the coefficient of friction. When compared to recommended design values from SANS 10164-1 (1980) it was seen that the initial shear strengths of the AACB, CSEB and adobe material were much lower than recommended, while the CMU was slightly higher. Conversely, the coefficient of friction recommended by SANS 10164-1 (1980) was lower than the CMU, CSEB and adobe specimens, and very similar to that of the AACB specimen.
- The order from greatest to lowest strength of the masonry wallets was the same as that of the individual units, namely first the AACBs with the highest strength, then the CMUs followed by the CSEBs and finally adobe. The modulus of elasticity of the wallets also followed the same pattern from highest to lowest as the individual units. First CMUs, then AACBs, then CSEBs and the lowest was adobe.
- The failure mechanism for the CMU, AACB and CSEB masonry wallets was splitting failure on the small side of the specimen. The adobe specimens had a greater amount of crushing in the top courses of the wallets, with final failure being due to large cracks down the centre of the large side of the wallets.
- The results from the compressive strength of the masonry wallets were compared with the simplified method of determining the compressive strength from EN 1996-3 (2006). It was found that the simplified method overestimated the experimental results for all materials investigated. This is expected for the CSEB and adobe specimen due to their weak nature, but is unusual for the AACBs and especially the CMUs.
- Two prediction methods for determining the modulus of elasticity of the masonry wallets were compared with the experimental results. The prediction method from EN 1996-1-1 (2005) gave results that are far lower than the actual results while the results from the prediction method from Brooks (2015) is closer to the experimental results but still lower for all materials except the AACBs. It can be concluded that the moduli of elasticity of the materials tested in this study were higher than the data used to develop these models. The exception was the AACBs, whose modulus of elasticity was slightly lower than Brooks, once more highlighting the lower stiffness of the material. The very low values from EN 1996-1-1 (2005) could be due to the standard being overly conservative.

The tests conducted in this study provided a wealth of mechanical properties for both conventional and alternative masonry units. These results can be used in future studies into numerical models of masonry for low income housing in South Africa, thereby laying the framework for

the minimum technical specifications for alternative masonry units.

8.1.2 Observations Made with Regards to the Test Set-ups

Determining the suitability of the standards and test set-ups used in this study for testing AMUs is one of the main objectives of this study. The following conclusions could be drawn from the investigation with recommendation being given for adjustments to these tests.

- The compressive strength tests on individual masonry units are found to be commonly applied to conventional and alternative masonry in literature. The tests in this study are considered to be a success on both the CMU and AMUs. However, due to the differences in size and shape between AMUs in practice and the fact that the effects of testing masonry with different geometry is not fully understood, standardised tests cannot yet be developed for the AMUs until further research is conducted.
- For the modulus of elasticity tests it is found that cylinders used in this study gave results that fell within the acceptable ranges and that the test method is successful on AMUs. The very weak adobe specimens did require adjusting of the loading rates, however their tests are also concluded to be successful. It is recommended that the results be compared to tests conducted on blocks in the headface and bedface orientation to quantify if creating the cylinders changed the mechanical properties of the specimens. It is also recommended that taking core samples from the blocks be investigated as a method that produces results with less chance of variability.
- The modulus of elasticity tests and Poisson's ratio tests were conducted on the same specimens and it was found that they underwent bending. As these were suppose to be uniaxial tests, the bending must be eliminated in future studies to ensure accurate results. Two possible methods of reducing the bending is to ensure perfect alignment of the specimens between a parallel base and load plate, and to ensure the base plate has sufficient stiffness to prevent it from influencing the tests. The issues with these tests affected both CMUs and AMUs and it is predicted that if they can be solved then the tests will be applicable to AMUs.
- The wedge splitting test is concluded to be successful in determining the fracture energy of AMUs. However, the weak adobe specimens had a high variability due to limits on the testing machine. It is therefore recommended that a more sensitive machine be used for future studies of very weak materials.
- The simplicity of the density tests are well suited for AMUs and the density values fell within expected ranges. It is concluded that the density test is suitable for AMUs.
- The triplet tests gave good results for all materials investigated. However, for the weaker adobe specimens the pre-compressive force was reduced to avoid crushing. Nonetheless, with the reduction of the pre-compressive force all materials gave adequate results and the test can be deemed appropriate for AMUs.

- The compressive strength tests on masonry samples created from alternative materials have already been conducted by various researchers and shown to be successful. This study also found the tests to be appropriate for AMUs. A recommended addition to the test would be inclusion of measurements in the transverse direction in order to determine the Poisson ratio of the masonry specimens.

The results from this study showed that with some small adjustments the standards and tests for determining the mechanical properties of conventional masonry units can be successfully applied on alternative units.

8.2 Recommendations for Future Studies

The following recommendations for future studies were identified through observations made during the course of this study.

- This study did not focus on the optimisation of the mix designs and characteristics of the AMUs investigated. It is therefore recommended that future studies conduct a more in depth study of the CSEBs, AACBs and adobe blocks, in order to optimise their ability to provide structurally viable, environmentally friendly and socially acceptable LIH.
- It is recommended that a thorough investigation be conducted on the non-structural aspects of AMUs. These include properties such as durability, thermal performance, porosity, water absorption and drying shrinkage.
- While this study tested and characterised AMUs with different test set-ups, there are still large amounts of testing and development required before the tests can be used with 100% confidence on the AMUs. While this study investigated a broad range of mechanical characteristics and tests, a thorough investigation of each individual test is needed. It is recommended that this study acts as a basis towards achieving this goal in future studies.
- Masonry relies not only on the masonry blocks but also on the mortar utilised in the masonry. This study did not conduct a detailed investigation into the effects of various mortars on AMUs or which mortars are the most appropriate for AMUs. It is therefore recommended that future studies look at different mortar strengths and types with different AMUs.
- To allow the AMUs to be used in practice minimum environmental and mechanical specifications are required. To determine these it is recommended that a typical single storey bonded masonry wall be modelled using non-linear finite elements with the necessary loading conditions. This will show the demands on a masonry wall and therefore on the masonry unit. These demands can be translated into minimum technical specifications. Modelling of individual masonry units is also recommended as it will prove beneficial to further the understanding of the AMUs. This study has provided the mechanical characteristics to model various AMUs as well as a means to validate and verify the models. To

validate and verify the models on the single storey bonded masonry wall it is recommended that a future study conduct experimental tests on full scale masonry walls as well.

References

- ASTM C1314-11A (2011). *Standard Test Method for Compressive Strength of Masonry Prisms*. ASTM International. West Conshohocken, USA.
- ASTM C1716M-16 (2016). *Standard Specification for Compression Testing Machine Requirements for Concrete Masonry Units, Related Units, and Prisms*. ASTM International. West Conshohocken, USA.
- ASTM C469/C469M (2010). *Standard Test Method for Static Modulus of Elasticity and Poisson's Ratio of Concrete in Compression*. ASTM International. West Conshohocken, USA.
- Abdullah, M.M.A., Ibrahim, W.M.W. and Tahir, M.F.M. (2015). '12 - The properties and durability of fly ash-based geopolymeric masonry bricks'. In: *Eco-Efficient Masonry Bricks and Blocks*. Ed. by F. Pacheco-Torgal, P.B. Lourenço, J.A. Labrincha, S. Kumar and P. Chindaprasirt. Oxford: Woodhead Publishing, pp. 273–287.
- Ahmari, S. and Zhang, L. (2015). 'The properties and durability of alkali-activated masonry units'. In: *Handbook of Alkali-activated Cements, Mortars and Concretes*. Ed. by F. Pacheco-Torgal, J.A. Labrincha, C. Leonelli, A. Palomo and P. Chindaprasirt. Cambridge: Woodhead Publisher, pp. 643–660.
- Alecci, V., Fagone, M., Rotunno, T. and De Stefano, M. (2013). 'Shear strength of brick masonry walls assembled with different types of mortar'. In: *Construction and Building Materials* 40, pp. 1038–1045.
- Aubert, J.E., Fabbri, A., Morel, J.C. and Maillard, P. (2013). 'An earth block with a compressive strength higher than 45 MPa!' In: *Construction and Building Materials* 47, pp. 366–369.
- Avrami, E., Guillaud, H. and Hardy, M. (2008). *Terra literature review - an overview of research in earthen architecture conservation*. Los Angeles: The Getty Conservation Institute.
- Aymerich, F., Fenu, L. and Meloni, P. (2012). 'Effect of reinforcing wool fibres on fracture and energy absorption properties of an earthen material'. In: *Construction and Building Materials* 27.1, pp. 66–72.
- BS 1377:1990 (1990). *Soils for civil engineering purposes*. British Standards Institution. London, United Kingdom.

- BS 5930:2015 (2015). *Code of practice for ground investigations*. British Standards Institution. London, United Kingdom.
- BS EN 1052-1 (1999). *Methods of tests for masonry - Part 1: Determination of compressive strength*. British Standards Organization. London, United Kingdom.
- BS EN 1052-3 (2002). *Methods of tests for masonry units - Part 3: Determination of initial shear strength*. British Standards Organization. London, United Kingdom.
- BS EN 12390-13 (2013). *Testing hardened concrete Part - 13 Determination of secant modulus of elasticity in compression*. British Standards Organization. London, United Kingdom.
- BS EN 772-1 (2011). *Methods of tests for masonry units - Part 1: Determination of compressive strength*. British Standards Organization. London, United Kingdom.
- BS EN 772-13 (2000). *Methods of tests for masonry units - Part 13: Determination of net and gross dry density of masonry units*. British Standards Organization. London, United Kingdom.
- BS EN 772-16 (2011). *Methods of tests for masonry units - Part 16: Determination of dimensions*. British Standards Organization. London, United Kingdom.
- Barnard, R. (2014). ‘Mechanical properties of fly ash/slag based geopolymer concrete with the addition of macro fibres’. MA thesis. Stellenbosch University.
- Barr, B.I.G., Abusiaf, H.F. and Sener, S. (1998). ‘Size effect and fracture energy studies using compact compression specimens’. In: *Materials and Structures* 31.1, pp. 36–41.
- Bhanumathidas, N. and Kalidas, N. (2005). ‘The FaL-G Concrete for Housing and Infrastructure’. In: *Second International Symposium on Concrete Technology for Sustainable Development*.
- Boshoff, W.P., de Klerk, M.D., Coetzee, G., de Villiers, W.I. and Tolêdo Filho, R.D. (2013). ‘Alternative Materials for Masonry Units’. In: *The Southern African Housing Foundation International Conference, Exhibition and Housing Awards*. The Southern African Housing Foundation.
- Brooks, J.J. (2015). *Concrete and Masonry Movement*. Oxford, United Kingdom: Butterworth Heinemann.
- Brown, P.W. and Clifton, J.R. (1978). ‘Adobe. I: The Properties of Adobe’. In: *Studies in Conservation* 23.4, pp. 139–146.
- Brühwiler, E. and Wittmann, F.H. (1990). ‘The wedge splitting test, a new method of performing stable fracture mechanics tests’. In: *Engineering Fracture Mechanics* 35.1-3, pp. 117–125.
- Centre for Affordable Housing Finance in Africa (2013). *Housing Finance in Africa: A Review of Some of Africa’s Housing Finance Markets*.

- Cheah, C.B., Part, W.K. and Ramli, M. (2015). ‘The hybridizations of coal fly ash and wood ash for the fabrication of low alkalinity geopolymers load bearing block cured at ambient temperature’. In: *Construction and Building Materials* 88, pp. 41–55.
- Dahmen, J. and Muñoz, J.F. (2014). ‘Earth Masonry Unit : Sustainable CMU Alternative’. In: 6.2, pp. 903–909.
- Davidovits, J. (2013). *Geopolymer Cement*. URL: <https://www.geopolymer.org/library/technical-papers/21-geopolymer-cement-review-2013/> (visited on 24/10/2016).
- De Almeida, J.A.P.P. (2012). ‘Mechanical characterization of traditional adobe masonry elements’. MA thesis. University of Minho.
- De Vasconcelos, G.F.M. (2005). ‘Experimental investigations on the mechanics of stone masonry: Characterization of granites and behavior of ancient masonry shear walls’. PhD thesis. University of Minho.
- Deboucha, S. and Hashim, R. (2011). ‘A review on bricks and stabilized compressed earth blocks’. In: *Scientific Research and Essays* 6.3, pp. 499–506.
- Domone, P. and Illston, J., eds. (2010). *Construction Materials, Their Nature and Behaviour*. 4th ed. London: Spon Press.
- EBANZ (2015). *Earth Building Standards*. Earth Building Association of New Zealand. URL: http://www.earthbuilding.org.nz/?page_id=15 (visited on 10/08/2016).
- EN 1996-1-1 (2005). *Eurocode 6 - Design of masonry structures - Part 1-1: General rules for reinforced and unreinforced masonry structures*. European Committee for Standardisation. Brussels, Belgium.
- EN 1996-3 (2006). *Eurocode 6 - Design of masonry structures - Part 3: Simplified calculation methods for unreinforced masonry structures*. European Committee for Standardisation. Brussels, Belgium.
- Evonik Industries (2010). *GPD Safety Summary, Sodium Hydroxide*.
- Feng, W., Gang, L., Hong-Nan, L. and Jin-Qing, J. (2012). ‘Strength and stress-strain characteristics of traditional adobe block and masonry’. In: *Materials and Structures* 46.9, pp. 1449–1457.
- Fernandez-Jimenez, A.M., Palomo, A. and Lopez-Hombrados (2006). ‘Engineering Properties of Alkali-Activated Fly Ash Concrete’. In: *ACI Materials Journal* 103.2.
- Galetakis, M. and Raka, S. (2004). ‘Utilization of limestone dust for artificial stone production: An experimental approach’. In: *Minerals Engineering* 17.2, pp. 355–357.
- Garcia-Lodeiro, I., Palomo, A. and Fernández-Jiménez, A. (2015). ‘An overview of the chemistry of alkali-activated cement-based binders’. In: *Handbook of Alkali-activated Cements, Mortars*

- and Concretes. Ed. by F. Pacheco-Torgal, J.A. Labrincha, C. Leonelli, A. Palomo and P. Chindaprasirt. Cambridge: Woodhead Publisher, pp. 19–47.
- Gous, M.D. (2015). ‘Characterisation of Mechanical Properties of Alternative Masonry Units’. Unpublished Research Report. Stellenbosch University.
- Hall, M.R. (2012). *Modern Earth Buildings*. 33, pp. 688–711.
- Heath, A., Maskell, D., Walker, P., Lawrence, M. and Fourie, C. (2012). ‘Modern earth masonry - Structural properties and structural design’. In: *The Structural Engineer* 90.4, pp. 38–44.
- Hillerborg, A., Modeer, M. and Petersson, P.E. (1976). ‘Analysis of Crack Formation and Crack Growth in Concrete by Means of Fracture Mechanics and Finite Elements’. In: *Cement and Concrete Research* 6, pp. 773–782.
- Horn, A. (2006). *Earth Building Soil Analysis and Adobe Brick Making*. Cape Town: Eco Design Architects and Consultants.
- INSWAREB (2011). *Case Study on Development and Dissemination of FaL-G Technology*. ECO CARBON PVT. LTD. URL: <http://www.fal-g.com/>.
- Jablonski, N. (1996). *Mix Design for Concrete Blocks*. The Aberdeen Group.
- Jayasudha, R.K., Radhakrishna and Niranjana, P.S. (2013). ‘Properties of Fal-G Masonry Blocks’. In: *IJRET: International Journal of Research in Engineering and Technology*, pp. 384–389.
- Kaaki, T. (2013). ‘Behavior and strength of masonry prisms loaded in compression’. Masters Thesis. Dalhousie University.
- Kota-Fredericks, Z. (2013). *Speaking notes by Human Settlements Deputy Minister Zou Kota-Fredericks at the South Africa Netherlands Research Programme on Alternatives in Development Conference, Durban*. URL: <http://www.gov.za/speaking-notes-human-settlements-deputy-minister-zou-kota-frederickss-south-africa-netherlands> (visited on 17/11/2015).
- Kühl, H. (1908). *Slag cement and process of making the same*. US Patent 900,939.
- Kumar, S. (2000). ‘Fly ash-lime-phosphogypsum cementitious binder: A new trend in bricks’. In: *Materials and Structures* 33.1, pp. 59–64.
- (2002). ‘A perspective study on fly ash-lime-gypsum bricks and hollow blocks for low cost housing development’. In: *Construction and Building Materials* 16.8, pp. 519–525.
- (2003). ‘Fly ash-lime-phosphogypsum hollow blocks for walls and partitions’. In: *Building and Environment* 38.2, pp. 291–295.

- Laing, H. (2011). ‘CMA House - Bringing Detail and Durability to Affordable Housing’. In: *International Conference on Housing and Construction Conference and Exhibition*. South African Housing Foundation.
- Lee, N.K. and Lee, H.K. (2013). ‘Setting and mechanical properties of alkali-activated fly ash/slag concrete manufactured at room temperature’. In: *Construction and Building Materials* 47, pp. 1201–1209.
- Lourenço, P.B. (1998). ‘Experimental and numerical issues in the modelling of the mechanical behaviour of masonry’. In: *Structural Analysis of Historical Constructions II*, pp. 57–91.
- Lourenço, P.B., Barros, J.O. and Oliveira, J.T. (2004). ‘Shear testing of stack bonded masonry’. In: *Construction and Building Materials* 18.2, pp. 125–132.
- Malherbe, D. (2016). ‘The mechanical properties of Cement-Stabilised Earth blocks containing agro-industrial residues’. MA thesis. Stellenbosch University.
- Manjunath, G. S., Radhakrishna, Giridhar, C. and Jadhav, M. (2011). ‘Compressive strength development in ambient cured geo-polymer Mortar’. In: *International Journal of Earth Sciences and Engineering* 04.06, pp. 830–834.
- Manning, D. and Vetterlein, J. (2004). *Exploitation and Use of Quarry Fines*. Tech. rep. 087/MIST2/DACM/01.
- Martins, T. and Varum, H. (2006). ‘Adobe’s mechanical characterization in ancient constructions: The case of Aveiro’s region’. In: *Materials Science Forum* 514-516.PART 2, pp. 1571–1575.
- Mindess, S., Young, J.F. and D., Darwin (2003). *Concrete*. Upper Saddle River, NJ: Pearson Education.
- Morel, J.C., Pkla, A. and Walker, P. (2007). ‘Compressive strength testing of compressed earth blocks’. In: *Construction and Building Materials* 21.2, pp. 303–309.
- Murat Algin, H. and Turgut, P. (2008). ‘Cotton and limestone powder wastes as brick material’. In: *Construction and Building Materials* 22.6, pp. 1074–1080.
- Norton, J. (1986). *Building with Earth*. Rugby, United Kingdom: IT Publications.
- Owens, G., ed. (2009). *Fulton’s Concrete Technology*. 9th ed. Midrand, South Africa: Cement and Concrete Institute.
- PCA (1993). *Masonry Information: Compressive Strength of Masonry*. Portland Cement Association. Illinois, USA.
- Pacheco-Torgal, F. (2015a). ‘1 - Introduction to eco-efficient masonry bricks and blocks’. In: *Eco-Efficient Masonry Bricks and Blocks*. Ed. by F. Pacheco-Torgal, P.B. Lourenço, J.A. Labrincha, S. Kumar and P. Chindaprasirt. Oxford: Woodhead Publishing, pp. 1 –10.

- Pacheco-Torgal, F. (2015b). ‘A Introduction to Handbook of Alkali-activated Cements, Mortars and Concretes’. In: *Handbook of Alkali-activated Cements, Mortars and Concretes*. Ed. by F. Pacheco-Torgal, J.A. Labrincha, C. Leonelli, A. Palomo and P. Chindaprasirt. Cambridge: Woodhead Publisher, pp. 1–18.
- Pacheco-Torgal, F., Lourenço, P.B., J.A., Labrincha, Kumar, S. and P., Chindaprasirt (2015). *Eco-Efficient Masonry Bricks and Blocks - Design, Properties and Durability*. Oxford: Woodhead Publishing.
- Provis, J.L. (2014). ‘Geopolymers and other alkali activated materials: why, how, and what?’ In: *Materials and Structures* 47, pp. 11–25.
- Provis, J.L. and van Deventer, J.S.J. (2009). *Geopolymers. Structures, Processing, Properties and Industrial Applications*. Woodhead Publishing.
- Quagliarini, E. and Lenci, S. (2010). ‘The influence of natural stabilizers and natural fibres on the mechanical properties of ancient Roman adobe bricks’. In: *Journal of Cultural Heritage* 11.3, pp. 309–314.
- Quagliarini, E., D’Orazio, M. and Lenci, S. (2015). ‘16 - The properties and durability of adobe earth-based masonry blocks’. In: *Eco-Efficient Masonry Bricks and Blocks*. Ed. by F. Pacheco-Torgal, P.B. Lourenço, J.A. Labrincha, S. Kumar and P. Chindaprasirt. Oxford: Woodhead Publishing, pp. 361–378.
- RILEM (1996). ‘RILEM TC 127-MS: Tests for Masonry Materials and Structures’. In: *Materials and Structures* 29.8, pp. 459–463.
- Raut, S.P., Ralegaonkar, R.V. and Mandavgane, S.A. (2011). ‘Development of sustainable construction material using industrial and agricultural solid waste: A review of waste-create bricks’. In: *Construction and Building Materials* 25.10, pp. 4037–4042.
- Rigassi, V. (1985). *Compressed Earth Blocks: Manual of production*. Vol. 1. Braunschweig, Germany: Friedr. Vieweg & Sohn Verslagsgesellschaft GmbH.
- Riza, F.V. and Rahman, I.A. (2015). ‘17 - The properties of compressed earth-based (CEB) masonry blocks’. In: *Eco-Efficient Masonry Bricks and Blocks*. Ed. by F. Pacheco-Torgal, P.B. Lourenço, J.A. Labrincha, S. Kumar and P. Chindaprasirt. Oxford: Woodhead Publishing, pp. 379–392.
- SANS 10100 (2000). *The structural use of concrete, part 1: Limit state design*. 2.2. Standards South Africa. Pretoria.
- SANS 10164-1 (1980). *The structural use of masonry Part 1: Unreinforced masonry walling*. Standards South Africa. Pretoria.
- SANS 10400-A (2010). *The application of the National Building Regulations Part A: General principles and requirements*. 3rd ed. Standards South Africa. Pretoria.

- SANS 10400-K (2011). *The application of the National Building Regulations Part K: Walls*. 3rd ed. Standards South Africa. Pretoria.
- SANS 10400 (1990). *The application of the National Building Regulations*. 1st ed. Standards South Africa. Pretoria.
- SANS 1215 (2008). *Concrete masonry units Published*. 1.4. Standards South Africa. Pretoria.
- SANS 201 (2008). *Sieve analysis, fines content and dust content of aggregates*. 2.2. Standards South Africa. Pretoria.
- SANS 5844 (2006). *Particle and Relative Density of Aggregate*. 2.2. Standards South Africa. Pretoria.
- Sassoni, E., Mazzotti, C. and Pagliai, G. (2014). ‘Comparison between experimental methods for evaluating the compressive strength of existing masonry buildings’. In: *Construction and Building Materials* 68, pp. 206–219.
- Schneemayer, A., Schranz, C., Kolbitsch, A. and Tschegg, E.K. (2014). ‘Fracture-Mechanical Properties of Mortar-to-Brick Interfaces’. In: 1997, pp. 1–8.
- Shakir, A.A. and Mohammed, A.A. (2013). ‘Manufacturing of Bricks in the Past , in the Present and in the Future : A state of the Art Review’. In: 2.3, pp. 145–156.
- Shi, C., Krivenko, P.V. and Roy, D. (2006). *Alkali-Activated Cements and Concretes*. Taylor and Francis Group.
- Silveira, D., Varum, H., Costa, A., Martins, T., Pereira, H. and Almeida, J. (2012). ‘Mechanical properties of adobe bricks in ancient constructions’. In: *Construction and Building Materials* 28.1, pp. 36–44.
- Štemberk, P. and Kohoutková, A. (2005). ‘Image-Analysis-Based Measuring of Lateral Deformation of Hardening Concrete’. In: *MATERIALS SCIENCE (MEDŽIAGOTYRA)* 11.3, pp. 292–296.
- The Clay Brick Association of SA (2016). *Top Projects - Affordable and Density Housing*. URL: <http://www.claybrick.org.za/gallery/7>.
- Theart, P.J. (2014). ‘Development of a multi-criteria assessment tool to choose between housing systems for the low cost housing market’. MA thesis. Stellenbosch University.
- Torgal, F.P. and Jalali, S. (2011). *Eco-efficient Construction and Building Materials*. London: Springer.
- Trunk, B., Schober, G., Helbling, A.K. and Wittmann, F.H. (1999). ‘Fracture mechanics parameters of autoclaved aerated concrete’. In: *Cement and Concrete Research* 29.6, pp. 855–859.

- Turgut, P. (2007). ‘Cement composites with limestone dust and different grades of wood sawdust’. In: *Building and Environment* 42.11, pp. 3801–3807.
- (2008). ‘Properties of masonry blocks produced with waste limestone sawdust and glass powder’. In: *Construction and Building Materials* 22, pp. 1422–1427.
- (2010). ‘Masonry composite material made of limestone powder and fly ash’. In: *Powder Technology* 204.1, pp. 42–47.
- (2012). ‘Manufacturing of building bricks without Portland cement’. In: *Journal of Cleaner Production* 37, pp. 361–367.
- Turgut, P. and Murat Algin, H. (2007). ‘Limestone dust and wood sawdust as brick material’. In: *Building and Environment* 42.9, pp. 3399–3403.
- UN Habitat and Ohchr (2014). ‘The Right to Adequate Housing’. In: Fact Sheet No. 21/Rev.1.
- US Energy Information Administration (EIA) (2009). *Emissions of Greenhouse Gases Report*. URL: <http://www.eia.gov/oiaf/1605/ggrpt/carbon.html> (visited on 01/12/2015).
- United Nations (2015). *The Millennium Development Goals Report*. New York: United Nations.
- Velde, B. (2008). ‘Formation of Earthen Materials’. In: *Terra Literature Overview*. Ed. by E. Avrami, H. Guillaud and M. Hardy. Los Angeles: The Getty Conservation Institute, pp. 15–20.
- Venkatarama Reddy, B. V. and Jagadish, K. S. (2003). ‘Embodied energy of common and alternative building materials and technologies’. In: *Energy and Buildings* 35, pp. 129–137.
- Venkatarama Reddy, B.V. (2012). ‘Stabilised soil blocks for structural masonry in earth construction’. In: *Modern earth buildings: Materials, engineering, construction and applications*. Ed. by M.R. Hall, R. Lindsay and M. Krayenhoff. Cambridge: Woodhead Publishing, pp. 324–363.
- Venkatarama Reddy, B.V., Lal, R. and Nanjunda Rao, K. (2007). ‘Optimum Soil Grading for the Soil-Cement Blocks’. In: *Journal of Materials in Civil Engineering* 19.2, pp. 139–148.
- Vermeltfoort, A.T., Martens, D.R.W. and van Zijl, G.P.A.G. (2007). ‘Brick-mortar interface effects on masonry under compression’. In: *Canadian Journal of Civil Engineering* 34.11, pp. 1475–1485.
- Walker, P. (2004). ‘Strength and Erosion Characteristics of Earth Blocks and Earth Block Masonry’. In: *Journal of Materials in Civil Engineering* 16.5, pp. 497–506.
- Wittmann, F. H., Rokugo, K., Brühwiler, E., Mihashi, H. and Simonin, P. (1988). ‘Fracture energy and strain softening of concrete as determined by means of compact tension specimens’. In: *Materials and Structures* 21.1, pp. 21–32.

- Wittmann, F.H. (2002). 'Crack formation and fracture energy of normal and high strength concrete'. In: *Sadhana* 27.4, pp. 413–423.
- Zhao, Z., Kwon, S.H. and Shah, S.P. (2008). 'Effect of specimen size on fracture energy and softening curve of concrete: Part I. Experiments and fracture energy'. In: *Cement and Concrete Research* 38.8-9, pp. 1049–1060.